



Karlsruhe Institute of Technology  
Department of Physics  
Institute for Theoretical Physics

# **Energy and Structure Analysis of the SU(3) Sphaleron**

Diploma thesis

by

**Pascal Nagel**

Advisor: Prof. Dr. Frans R. Klinkhamer (Karlsruhe, Germany)  
Co-Advisor: Prof. Dr. Yves Brihaye (Mons, Belgium)  
Submitted on: 21st of January 2014



---

## Abstract

We apply Simulated Annealing to approximate energy and field structure of the SU(3) sphaleron  $\hat{S}$  and obtain results, which suggest the existence of a finite, non-vanishing solution of Yang-Mills-Higgs theory. In conjunction with this, we analytically show the regularity of the obtained approximation. Additionally, we analyse the structure of the  $\hat{S}$  sphaleron energy barrier and find numerical evidence to suggest meta-stability of the solution.



## Contents

<b>1</b>	<b>Introduction</b>	<b>1</b>
<b>2</b>	<b>Chiral SU(3) gauge theory</b>	<b>7</b>
<b>3</b>	<b>Topology and <math>\hat{S}</math> sphaleron <i>Ansatz</i></b>	<b>8</b>
3.1	Topology . . . . .	8
3.2	Approximate sphaleron <i>Ansatz</i> . . . . .	9
3.3	Generalized sphaleron <i>Ansatz</i> . . . . .	10
3.4	Field configurations between vacuum and sphaleron . . . . .	12
3.4.1	Approximate <i>Ansatz</i> . . . . .	12
3.4.2	Generalized <i>Ansatz</i> . . . . .	13
<b>4</b>	<b>Simulated Annealing</b>	<b>18</b>
<b>5</b>	<b>Semi-analytical energy optimization and structure analysis</b>	<b>20</b>
5.1	Minimization of the approximate <i>Ansatz</i> . . . . .	22
5.2	Minimization of the generalized <i>Ansatz</i> . . . . .	24
5.2.1	$N = 1$ Legendre expansion . . . . .	28
5.2.2	$N = 2$ Legendre expansion . . . . .	30
5.2.3	$N = 3$ Legendre expansion . . . . .	33
5.3	Energy of configurations between vacuum and sphaleron . . . . .	34
5.4	Minimization with non-zero Higgs self-coupling . . . . .	38
<b>6</b>	<b>SU(2) sphaleron <math>S</math></b>	<b>40</b>
6.1	Topology and sphaleron <i>Ansatz</i> . . . . .	40
6.2	Generalized <i>Ansatz</i> . . . . .	42
<b>7</b>	<b>Conclusion</b>	<b>45</b>
<b>A</b>	<b>Energy density of the generalized <math>\hat{S}</math> <i>Ansatz</i></b>	<b>48</b>

---

**CONTENTS**

<b>B Structure functions and general energy density</b>	<b>49</b>
B.1 Structure functions . . . . .	49
B.2 General energy density . . . . .	53
<b>C Simulated annealing base source code (C++)</b>	<b>64</b>
<b>D Coefficients of the <math>\hat{S}_{approx}</math> <i>Ansatz</i></b>	<b>67</b>
<b>E Figures and coefficients of the generalized <math>\hat{S}</math> <i>Ansatz</i></b>	<b>68</b>
E.1 $N = 0$ Legendre expansion . . . . .	68
E.2 $N = 1$ Legendre expansion . . . . .	72
E.3 $N = 2$ Legendre expansion . . . . .	79
E.4 $N = 3$ Legendre expansion . . . . .	88
<b>F Coefficients of the regular <math>S</math> <i>Ansatz</i></b>	<b>92</b>
<b>G Figures of the generalized <math>S</math> <i>Ansatz</i></b>	<b>93</b>

## List of Figures

1.1	Sine-Gordon potential $V(\phi)$	1
1.2	Sine-Gordon kink	2
1.3	Mappings of different winding numbers $Q$	3
1.4	Non-contractible $S^n$ relevant for sphalerons $S$ and $S^*$	5
1.5	Spectral flow for a transition over the sphaleron barrier	6
5.1	Total energy density approximations for various degrees of angular dependency	21
a	$N = 0$	21
b	$N = 1$	21
c	$N = 2$	21
d	$N = 3$	21
5.2	Approximation of profile functions $f(x)$ and $h(x)$ for $\hat{S}_{approx}$ with $\lambda = 0$	23
5.3	$N = 1$ x-grid convergence of $E_{\hat{S}}$	26
5.4	$N = 1$ total energy density approximations for various $N_S$	29
a	$N_S = 1800$	29
b	$N_S = 2500$	29
c	$N_S = 4000$	29
d	$N_S = 13000$	29
5.5	Selected $N = 1$ profile function approximations for various $N_S$	30
a	$f_3(x)$	30
b	$f_{5,0}(x)$	30
c	$f_{8,0}(x)$	30
d	$h_{1,0}(x)$	30
5.6	$N = 2$ total energy density approximations for various $N_S$	31
a	$N_S = 600$	31
b	$N_S = 900$	31
c	$N_S = 1200$	31

*LIST OF FIGURES*

---

d	$N_S = 1800$	31
5.7	Selected $N = 2$ profile function approximations for various $N_S$	32
a	$f_{8,0}(x)$	32
b	$h_2(x)$	32
c	$f_3(x)$	32
d	$f_{8,1}(x)$	32
5.8	$N = 3$ total energy density approximations for various $N_S$	34
a	$N_S = 400$	34
b	$N_S = 600$	34
c	$N_S = 800$	34
d	$N_S = 1000$	34
5.9	$N = 1$ approximation of the $\hat{S}$ NCL structure	36
5.10	$N = 2$ approximation of the $\hat{S}$ NCL structure	37
5.11	Approximation of the S sphaleron NCL structure	37
6.1	SA approximation of profile functions $f(x)$ and $h(x)$ for the SU(2) sphaleron $S$ with $\lambda = 0$	41
6.2	0th order profile functions for the SU(2) sphaleron $S$	44
6.3	1st order profile functions for the SU(2) sphaleron $S$	44

**List of Tables**

1.1	Homotopy groups of unitary groups . . . . .	4
5.1	Approximations of $E_{\hat{S}}$ ( $\lambda = 0$ ) for various degrees of angular expansion, with $E_S$ defined by (6.7) . . . . .	21
5.2	$N = 1$ approximation of $E_{\hat{S}}$ ( $\lambda = 0$ ) for increasing number of steps per temperature $N_S$ , with $E_S$ defined by (6.7) . . . . .	28
5.3	$N = 2$ approximation of $E_{\hat{S}}$ ( $\lambda = 0$ ) for increasing number of steps per temperature $N_S$ , with $E_S$ defined by (6.7) . . . . .	31
5.4	$N = 3$ approximation of $E_{\hat{S}}$ ( $\lambda = 0$ ) for increasing number of steps per temperature $N_S$ , with $E_S$ defined by (6.7) . . . . .	33
5.5	$N = 2$ approximation of $E_{\hat{S}}$ for various $\lambda$ . . . . .	39

## 1 Introduction

To introduce the reader to topological aspects of quantum field theory, let us commence by taking a look at the sine-Gordon kink, which has no application in particle physics, but serves well to illustrate the basic notion of topological invariants.

We consider a scalar field in  $1 + 1$  space-time dimensions

$$\mathcal{L} = \frac{1}{2} \partial_\mu \phi \partial^\mu \phi - V(\phi), \quad (1.1)$$

with the sine-Gordon potential

$$V(\phi) = \frac{1}{b^2} [1 - \cos(b\phi)] \quad (1.2)$$

shown in fig. 1.1. In the standard way of computing the equations of motion, we obtain the sine-Gordon equation

$$\partial_t^2 \phi - \partial_x^2 \phi + \frac{1}{b} \sin(b\phi) = 0. \quad (1.3)$$

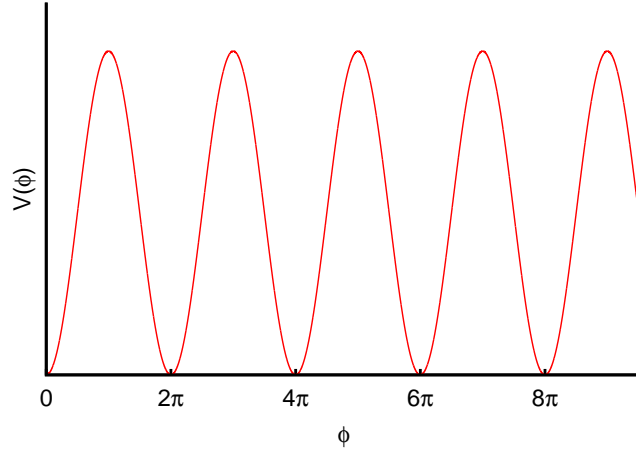


Figure 1.1: Sine-Gordon potential  $V(\phi)$

A subset of its solutions describes a wave moving with constant velocity  $v$

$$\phi(x, t) = f(x - vt) = f(\xi) \quad (1.4)$$

$$f(\xi) = \frac{4}{b} \arctan \exp \left[ \pm \frac{\xi}{\sqrt{b(1 - v^2)}} \right], \quad (1.5)$$

which is depicted in fig. 1.2. It will not have escaped the reader, that this wave does not alter its shape and therefore does not dissipate over time, wherefore it is called a *solitary wave* or a *soliton*.

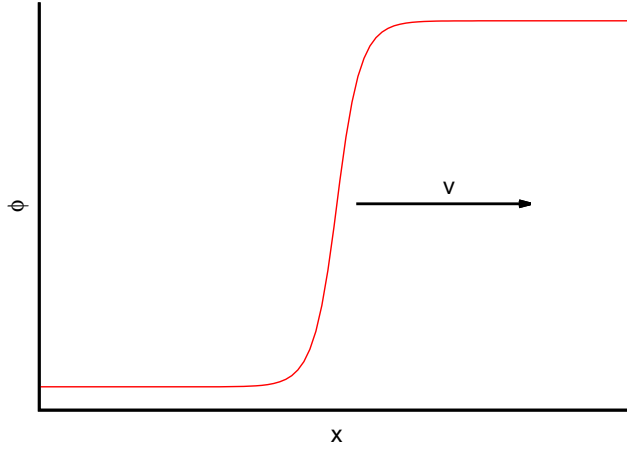


Figure 1.2: Sine-Gordon kink

The sine-Gordon equation (1.3) is also solved by an infinite number of constant solutions

$$\phi = \frac{2\pi n}{b}, \quad n \in \mathbb{Z} \quad (1.6)$$

that correspond to the degenerate vacua (minima) of the sine-Gordon potential (fig. 1.1). Hence, the kink solution (1.5) connects two constant solutions with different  $n$ , by describing the transition from one vacuum to another, over the energy barrier

$$E = \frac{8}{b^2}. \quad (1.7)$$

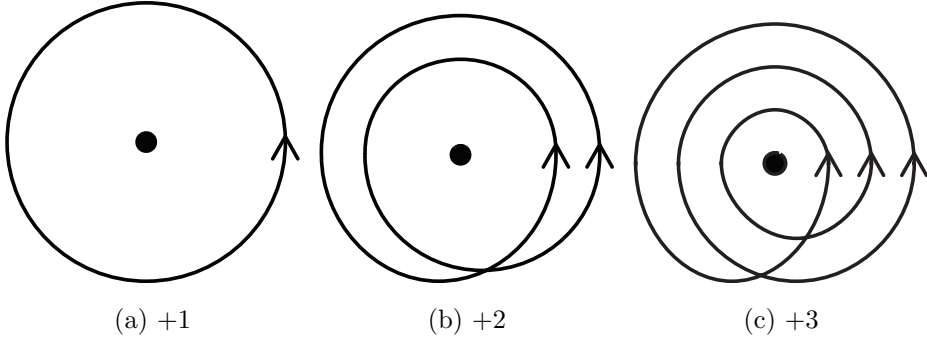
A 1-kink describing, for instance, the transition  $n = 0 \rightarrow 1$  is described by (1.5), with boundary conditions  $\phi(-\infty) = 0$  and  $\phi(\infty) = 2\pi/b$ . This solution is stable, as it cannot be continuously deformed into the ground state with  $n = 0$  at both boundaries. Since the kinks stability is tied to the topological properties of the field space at spacial infinity ( $x \rightarrow \pm\infty$ ), it is referred to as a *topological soliton*. In this particular case the field space at spacial infinity consists of a discrete set of field values, namely (1.6).

The stability of the kink indicates the existence of a conserved current

$$J^\mu = \frac{b}{2\pi} \epsilon^{\mu\nu} \partial_\nu \phi, \quad (1.8)$$

as well as a conserved charge  $Q$ , equal to the difference in  $n$  and hence an integer

$$\begin{aligned} Q &= \int_{-\infty}^{\infty} J^0 dx \\ &= \frac{b}{2\pi} \int_{-\infty}^{\infty} \partial_x \phi dx \\ &= \frac{b}{2\pi} [\phi(\infty) - \phi(-\infty)] = \Delta n. \end{aligned} \quad (1.9)$$


 Figure 1.3: Mappings of different winding numbers  $Q$ 

In general, topological objects in quantum field theory are defined by a mapping from coordinate space to group space. To illustrate this regarding the sine-Gordon model, consider the field  $\phi$  as the angle of a circle ( $S^1$ ) and the kink solution (1.5) as a map  $U : x \rightarrow \phi$  from coordinate space to group space. The topological charge  $Q$  is, in this case, simply a winding number, which indicates how often the  $S^1$  of fields is covered during a transition from  $x = -\infty \rightarrow \infty$  (see fig. 1.3).

In order to classify the topology of more complex spaces  $X$ , the notion of *homotopy groups*

$$\pi_n [X] \quad (1.10)$$

will serve to be extremely useful<sup>1</sup>. With regard to the sine-Gordon model the homotopy group

$$\pi_1 [S^1] = \mathbb{Z} \quad (1.11)$$

is simply the fundamental group, whose elements resemble the winding numbers  $Q$ .

For more details on the sine-Gordon soliton the reader is referred to [18], from which most of the sine-Gordon introduction was adopted.

Let us now proceed to a physically more relevant theory, namely gauge theories in 3+1 dimensions and sphalerons in particular. In this instance, the boundary at spacial infinity ( $r \rightarrow \infty$ ) becomes a 2-sphere ( $S^2$ ), parameterized by the well familiar angles  $\theta$  and  $\phi$ , with  $\theta \in [0, \pi]$  and  $\phi \in [0, 2\pi]$ . In order to ensure a finite field energy, the field strength  $F^{\mu\nu}$  must vanish at spacial infinity, wherefore the field  $A_\mu$  on the  $S^2_\infty$  must be in *pure gauge*

$$\lim_{r \rightarrow \infty} A_\mu(r, \theta, \phi) = g^{-1} (\partial_\mu U) U^{-1}, \quad U \in SU(N). \quad (1.12)$$

---

<sup>1</sup>To define the n-th homotopy group, the base point preserving maps from an n-dimensional sphere (with base point) into a given space (with base point) are collected into equivalence classes, called homotopy classes. Two mappings are homotopic if one can be continuously deformed into the other. These homotopy classes form a group, called the n-th homotopy group,  $\pi_n [X]$ , of the given space  $X$  with base point.

Just as before, there exist topologically distinct boundary conditions, that are linked by finite energy solutions. Consider the following toy model *Ansatz* [24] for the field

$$A_\mu[h] = \frac{1+h}{2g} (\partial_\mu U) U^{-1}, \quad h \in [-1, 1], \quad (1.13)$$

which continuously connects  $A_\mu = 0$  and  $A_\mu[h] = g^{-1} (\partial_\mu U) U^{-1}$ , as  $h$  goes from  $-1$  to  $1$ , along a path in configuration space<sup>2</sup>. The corresponding energy

$$E[h] \propto \frac{(h^2 - 1)^2}{g^2} \quad (1.14)$$

displays the desired properties. It vanishes at the boundary conditions  $h = -1, 1$  and has an energy barrier, which reaches its maximum  $E_{max}$  at  $h = 0$ . Other than (1.13), there exist an infinite number of interpolating paths, connecting the boundary conditions at hand. If we now find a non-zero minimum of  $E_{max}$  over all paths, then the corresponding field configuration is an unstable classical solution termed *sphaleron*.

In contrast to this model, the *Ansatz* we apply later on involves the path parameterizing variable(s) ( $= h$  in the previous model) to be embedded in the map  $U \in SU(N)$  in a non-trivial way<sup>3</sup>. This is done by constructing the smash product<sup>4</sup> of the  $S^2$  at spacial infinity and an n-sphere ( $S^n$ ) and mapping it onto group space

$$U : S^n \wedge S_\infty^2 \rightarrow SU(N), \quad (1.15)$$

being mindful of choosing  $n$  as to generate a topologically non-trivial map

$$\pi_{n+2}[SU(N)] \neq 0. \quad (1.16)$$

A brief list of homotopy groups of unitary groups [13] is given in table 1.1.

	$\pi_1$	$\pi_2$	$\pi_3$	$\pi_4$	$\pi_5$	$\pi_6$
$U(1)$	$\mathbb{Z}$	0	0	0	0	0
$U(2)$	0	0	$\mathbb{Z}_2$	$\mathbb{Z}_2$	$\mathbb{Z}_{12}$	
$U(3)$	0	0	$\mathbb{Z}$	0	$\mathbb{Z}$	$\mathbb{Z}_6$

Table 1.1: Homotopy groups of unitary groups

<sup>2</sup>Configuration space is a vector space defined by all finite energy field configurations, that are not excluded by imposed constraints.

<sup>3</sup>See, e.g. map (3.1) for the  $SU(3)$  sphaleron  $\hat{S}$  or (6.1) for the  $SU(2)$  sphaleron  $S$

<sup>4</sup>“The smash product  $\wedge$  topologically transforms the Cartesian product  $S^p \times S^m$  to  $S^{p+m}$  by contracting, for fixed points  $x_0 \in S^p$  and  $y_0 \in S^m$ , the set  $\{x_0\} \times S^m \cup S^p \times \{y_0\}$  to a single point” [1].

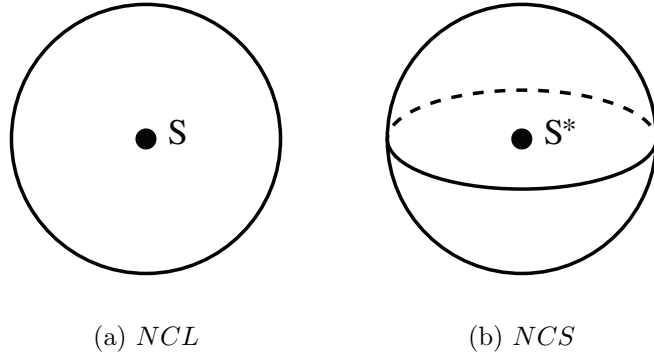


Figure 1.4: Non-contractible  $S^n$  relevant for sphalerons  $S$  and  $S^*$

The colored homotopy groups are linked to three different sphalerons, namely  $\pi_3 [SU(2)]$  (red) to the  $SU(2)$  sphaleron  $S$  [3, 10],  $\pi_4 [SU(2)]$  (blue) to the  $SU(2)$  sphaleron  $S^*$  [11] and  $\pi_5 [SU(3)]$  (green) to the  $SU(3)$  sphaleron  $\hat{S}$  [1]. Fig. 1.4 depicts the corresponding non-contractible n-spheres in configuration space, which are mapped to envelop a subspace of  $SU(N)$ , that is not simply connected.

As before, the non-trivial topology of group space leads to a conserved current

$$J^\mu = \frac{g^2}{32\pi^2} \epsilon^{\mu\nu\alpha\beta} \left( A_\nu^a \partial_\alpha A_\beta^a + \frac{1}{3} f^{abc} A_\nu^a A_\alpha^b A_\beta^c \right) \quad (1.17)$$

and charge

$$Q = \int d^3x J^0, \quad (1.18)$$

given in this particular case by the Hodge dual of the Chern-Simons 3-form. It is noteworthy, that the currents  $J^\mu$  related to each of the three sphaleron solutions  $S$ ,  $S^*$  and  $\hat{S}$  each describe chiral anomalies. The  $S$  sphaleron is connected to the Adler-Bell-Jackiw (triangle) anomaly [6, 7], resulting in B+L non-conservation within the electroweak standard model. Analogously, the  $S^*$  sphaleron is related to the Witten anomaly [8] and the  $\hat{S}$  sphaleron to the Bardeen anomaly [9].

To inspect possible fermion number non-conservation, brought about by these anomalies, one must evaluate the zero modes of the respective fermion Hamiltonian

$$H = i\vec{\sigma} \cdot (\nabla - g\vec{A}). \quad (1.19)$$

This analysis for sphalerons  $S$  and  $S^*$ , which is summarized in detail in [5], yields a violation of fermion number conservation for the  $S$  gauge fields, if they couple solely to left-handed fermions. The corresponding energy eigenvalue for the transition from one vacuum to another over the sphaleron barrier is shown in fig. 1.5a.

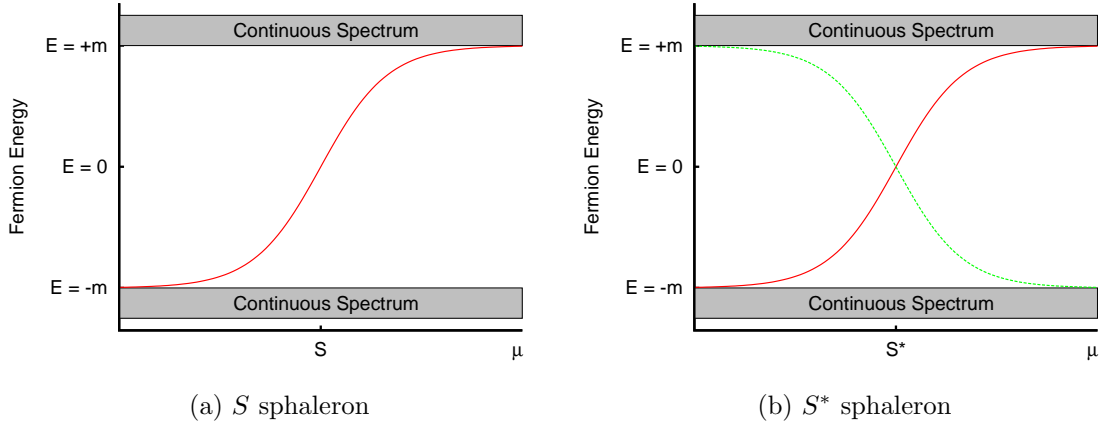


Figure 1.5: Spectral flow for a transition over the sphaleron barrier

The  $S^*$  sphaleron on the other hand has no such effect, as eigenvalues of the four-dimensional Euclidean Dirac operator  $\not{D}_4$  always cross in pairs of two, from above and below, for both chiralities [11], as depicted in fig. 1.5b.

Zero modes of the fermion Hamiltonian, coupling the SU(3) gauge fields of the  $\hat{S}$  sphaleron to left-handed fermions, although only evaluated on the symmetry axis in [1], suggest spectral flow properties similar to the  $S^*$  sphaleron and hence no fermion number violation.

## 2 Chiral $SU(3)$ gauge theory

In the following we will employ  $SU(3)$  Yang-Mills-Higgs theory with a single triplet of complex scalar fields and a single triplet of massless left-handed Weyl fermions, both in the **3** representation of  $SU(3)$ .

The theory has the following classical action

$$S = \int_{\mathbb{R}^4} d^4x \left\{ \frac{1}{2} \text{tr} F_{\mu\nu} F^{\mu\nu} + (D_\mu \Phi)^\dagger (D^\mu \Phi) - \lambda (\Phi^\dagger \Phi - \eta^2)^2 + i \bar{\Psi} \sigma^\mu D_\mu \Psi \right\}, \quad (2.1)$$

with the  $SU(3)$  Yang-Mills field strength tensor  $F_{\mu\nu} = \partial_\mu A_\nu - \partial_\nu A_\mu + g[A_\mu, A_\nu]$ , the covariant derivative  $D_\mu = \partial_\mu + gA_\mu$  and the Yang-Mills gauge field  $A_\mu(x) = A_\mu^a(x)\tau^a$ , with  $SU(3)$  generators  $\tau^a = \lambda^a/(2i)$ . The matrices  $\lambda^a$  are the eight Gell-Mann matrices

$$\begin{aligned} \lambda_1 &= \begin{pmatrix} 0 & 1 & 0 \\ 1 & 0 & 0 \\ 0 & 0 & 0 \end{pmatrix}, & \lambda_2 &= \begin{pmatrix} 0 & -i & 0 \\ i & 0 & 0 \\ 0 & 0 & 0 \end{pmatrix}, & \lambda_3 &= \begin{pmatrix} 1 & 0 & 0 \\ 0 & -1 & 0 \\ 0 & 0 & 0 \end{pmatrix}, \\ \lambda_4 &= \begin{pmatrix} 0 & 0 & 1 \\ 0 & 0 & 0 \\ 1 & 0 & 0 \end{pmatrix}, & \lambda_5 &= \begin{pmatrix} 0 & 0 & -i \\ 0 & 0 & 0 \\ i & 0 & 0 \end{pmatrix}, & \lambda_6 &= \begin{pmatrix} 0 & 0 & 0 \\ 0 & 0 & 1 \\ 0 & 1 & 0 \end{pmatrix}, \\ \lambda_7 &= \begin{pmatrix} 0 & 0 & 0 \\ 0 & 0 & -i \\ 0 & i & 0 \end{pmatrix}, & \lambda_8 &= \frac{1}{\sqrt{3}} \begin{pmatrix} 1 & 0 & 0 \\ 0 & 1 & 0 \\ 0 & 0 & -2 \end{pmatrix}. \end{aligned} \quad (2.2)$$

It is apparent from the Higgs potential in action (2.1), that the triplet of complex scalar fields  $\Phi(x)$  acquires a vacuum expectation value (vev) of  $\eta = v/\sqrt{2}$ . The triplet of two-component Weyl spinors is described by the field  $\Psi(x)$  and its complex conjugate  $\bar{\Psi}(x)$ .

Throughout this thesis we will employ the Minkowski space metric in the form of  $g_{\mu\nu}(x) = \text{diag}(+1, -1, -1, -1)$ , natural units  $\hbar = c = 1$ , as well as the convention of greek letter indices running from 0 to 3 and latin letter indices running from 1 to 3, unless otherwise specified. Additionally, in order to make the energy functionals more numerically approachable, we will regularly use dimensionless and compactified radial coordinates

$$x = \frac{\xi}{1 + \xi}, \quad \text{with } \xi = gvr. \quad (2.3)$$

Finally, the static bosonic energy of action (2.1) is given by:

$$E[A, \Phi] = \int_{\mathbb{R}^3} d^3x \left\{ \frac{1}{2} \text{tr}(F_{mn})^2 + |D_m \Phi|^2 + \lambda (|\Phi|^2 - \eta^2)^2 \right\}. \quad (2.4)$$

### 3 Topology and $\hat{S}$ sphaleron *Ansatz*

#### 3.1 Topology

Identical to [1] we introduce a topologically nontrivial map  $S^3 \wedge S_\infty^2 \rightarrow SU(3)$ , with parameters  $(\psi, \mu, \alpha)$  and coordinates  $(\theta, \phi)$  on the sphere at spacial infinity.

The following map is a generator of  $\pi_5[SU(3)] = \mathbb{Z}$ :

$$U : S^5 \rightarrow SU(3), \quad U(z_1, z_2, z_3) = \begin{pmatrix} z_1^2 & z_1 z_2 - \bar{z}_3 & z_1 z_3 + \bar{z}_2 \\ z_1 z_2 + \bar{z}_3 & z_2^2 & z_2 z_3 - \bar{z}_1 \\ z_1 z_3 - \bar{z}_2 & z_2 z_3 + \bar{z}_1 & z_3^2 \end{pmatrix}, \quad (3.1)$$

with  $z_1, z_2, z_3 \in \mathbb{C}$ ,  $|z_1|^2 + |z_2|^2 + |z_3|^2 = 1$  and parametrization

$$\begin{pmatrix} z_1 \\ z_2 \\ z_3 \end{pmatrix} = \begin{pmatrix} 1 - \cos^2 \frac{\theta}{2}(1 - \cos \psi) + i \cos \frac{\theta}{2} \sin \psi \cos \mu \\ e^{i\phi} \sin \frac{\theta}{2} \cos \frac{\theta}{2}(1 - \cos \psi) \\ \cos \frac{\theta}{2} \sin \psi \sin \mu (\sin \alpha + i \cos \alpha) \end{pmatrix}, \quad (3.2)$$

with angles  $\psi, \mu, \theta \in [0, \pi]$  and  $\alpha, \phi \in [0, 2\pi]$ <sup>1</sup>.

We now identify two special maps, corresponding to the  $\hat{S}$  located at the "top" ( $\psi = \pi$ ) and the vacuum solution  $V$  at the "bottom" ( $\psi = 0$ ) of the non-contractible manifold, respectively. The "height" corresponds to the energy of the configuration (see fig. 1.4).

At  $\psi = 0$   $U(z_1, z_2, z_3)$  becomes independent of all parameters and coordinates

$$V = U(\psi, \mu, \alpha, \theta, \phi) \Big|_{\psi=0} = \begin{pmatrix} 1 & 0 & 0 \\ 0 & 0 & -1 \\ 0 & 1 & 0 \end{pmatrix}, \quad (3.3)$$

whereas at  $\psi = \pi$   $U(z_1, z_2, z_3)$  becomes independent only of  $\mu$  and  $\alpha$ , but continues to depend on  $\theta$  and  $\phi$

$$\begin{aligned} W(\theta, \phi) &= U(\psi, \mu, \alpha, \theta, \phi) \Big|_{\psi=\pi} \\ &= \begin{pmatrix} \cos^2 \theta & -\cos \theta \sin \theta e^{i\phi} & \sin \theta e^{-i\phi} \\ -\cos \theta \sin \theta e^{i\phi} & \sin^2 \theta e^{2i\phi} & \cos \theta \\ -\sin \theta e^{-i\phi} & -\cos \theta & 0 \end{pmatrix}. \end{aligned} \quad (3.4)$$

<sup>1</sup>Expression (3.2) refers to the single point  $(z_1, z_2, z_3) = (1, 0, 0)$  if either  $\psi = 0$  or  $\theta = \pi$ . They are the two required fixed points ( $x_0 \in S^3$  and  $y_0 \in S^2$ ) needed for the smash product.

It is crucial, that the  $S^3$ , parameterized by  $\psi$ ,  $\mu$  and  $\alpha$ , does not describe a non-contractible 3-sphere (NCS)<sup>2</sup>, but merely different variations of a single non-contractible loop (NCL), parameterized by  $\psi$ . The contractibility of the  $\mu$ - and  $\alpha$ -loops becomes most apparent, when looking at  $V$  or  $W$ , which are entirely independent of  $\mu$  and  $\alpha$ .

For arbitrary  $\psi$ , away from the highly symmetric fixed points,  $U(z_1, z_2, z_3)$  becomes increasingly complex and cumbersome to work with. We will however see later on, that the action displays a number of simplifying symmetries.

### 3.2 Approximate sphaleron *Ansatz*

The approximate *Ansatz*, as employed in [1], constructs the components of the Higgs and SU(3) gauge fields identical to the well established SU(2) S sphaleron *Ansatz*

$$A_0(r, \theta, \phi) = 0, \quad g A_m(r, \theta, \phi) = -f(r) \partial_m W(\theta, \phi) W^{-1}(\theta, \phi), \quad (3.5)$$

$$\phi(r, \theta, \phi) = h(r) \eta W(\theta, \phi) \begin{pmatrix} 1 \\ 0 \\ 0 \end{pmatrix}, \quad (3.6)$$

with Dirichlet boundary conditions

$$f(0) = h(0) = 0, \quad \lim_{r \rightarrow \infty} f(r) = \lim_{r \rightarrow \infty} h(r) = 1. \quad (3.7)$$

After the transformation into dimensionless and compact coordinates (see eq. (2.3)) and setting  $g = v = 1$ , we insert the *Ansatz* at hand into the Yang-Mills-Higgs energy functional (2.4), to obtain

$$E = 4\pi \int_0^1 dx \left\{ \frac{28}{3}(x-1)^2 f'^2 + \frac{80}{3x^2} (f(1-f))^2 + \frac{1}{2} x^2 h'^2 + \frac{4}{3(x-1)^2} (h(1-f))^2 + \frac{\lambda}{4} \frac{x^2}{(x-1)^4} (h^2 - 1)^2 \right\} \quad (3.8)$$

Solving the derivable differential equations

$$\delta f = 0 : \quad 7(x-1)x^2 (2f' + (x-1)f'') = (f-1) \left( 20(2f-1)f + \frac{x^2 h^2}{(x-1)^2} \right), \quad (3.9)$$

$$\delta h = 0 : \quad (x-1)^2 x (2h' + xh'') = \frac{8}{3}(f-1)^2 h + x^2 \frac{\lambda}{g^2} \frac{h^2 - 1}{(x-1)^2} h,$$

---

<sup>2</sup>This stands in contrast to the  $S^*$  sphaleron, whose parameters  $\mu$  and  $\nu$  describe a non-contractible 2-sphere.

is equivalent to minimizing the energy functional (3.8). Due to the nature of the numerical methods used, we will however focus on minimizing the energy functional directly.

Before integrating over angles  $\theta$  and  $\phi$  to obtain the above energy functional (3.8), it becomes apparent, that the energy density is not spherically symmetric, but merely invariant under azimuthal ( $\phi$ ) transformations. Hence, in contrast to the S sphaleron, a spherically symmetric *Ansatz* is not sufficient, leading us to the generalized  $\hat{S}$  *Ansatz*.

### 3.3 Generalized sphaleron *Ansatz*

Following [1], we introduce the following set of matrices:

$$\begin{aligned} T_\phi &= -\sin \phi \frac{\lambda_1}{2i} + \cos \phi \frac{\lambda_2}{2i}, & T_\rho &= \cos \phi \frac{\lambda_1}{2i} + \sin \phi \frac{\lambda_2}{2i}, & T_3 &= \frac{\lambda_3}{2i}, \\ V_\phi &= \sin \phi \frac{\lambda_4}{2i} + \cos \phi \frac{\lambda_5}{2i}, & V_\rho &= \cos \phi \frac{\lambda_4}{2i} - \sin \phi \frac{\lambda_5}{2i}, & V_3 &= \frac{\sqrt{3}\lambda_8 + \lambda_3}{4i}, \\ U_\phi &= \sin(2\phi) \frac{\lambda_6}{2i} + \cos(2\phi) \frac{\lambda_7}{2i}, & U_\rho &= \cos(2\phi) \frac{\lambda_6}{2i} - \sin(2\phi) \frac{\lambda_7}{2i}, & U_3 &= \frac{\sqrt{3}\lambda_8 - \lambda_3}{4i}, \end{aligned} \tag{3.10}$$

with the Gell-Mann matrices  $\lambda_i$ , for  $i = 1, \dots, 8$ .

The gauge field of the approximate *Ansatz* (3.5) can be expanded using the basis  $\{T_\phi, T_\rho, V_\phi, V_\rho, U_\phi, U_\rho, \lambda_3/(2i), \lambda_8/(2i)\}$  of  $\text{su}(3)$  to give the following generalized *Ansatz*

$$\begin{aligned} g\hat{A}_0(r, \theta, \phi) &= 0, \\ g\hat{A}_\phi(r, \theta, \phi) &= \alpha_1(r, \theta) \cos \theta T_\rho + \alpha_2(r, \theta) V_\rho + \alpha_3(r, \theta) \cos \theta U_\rho + \alpha_4(r, \theta) \frac{\lambda_3}{2i} + \alpha_5(r, \theta) \frac{\lambda_8}{2i}, \\ g\hat{A}_\theta(r, \theta, \phi) &= \alpha_6(r, \theta) T_\phi + \alpha_7(r, \theta) \cos \theta V_\phi + \alpha_8(r, \theta) U_\phi, \\ g\hat{A}_r(r, \theta, \phi) &= 0, \end{aligned} \tag{3.11}$$

in the radial gauge, with real functions  $\alpha_i$ , for  $i = 1, \dots, 8$ . The following boundary conditions apply, at  $r = 0$ :

$$\alpha_i(0, \theta) = 0, \tag{3.12}$$

on the symmetry axis ( $\bar{\theta} = 0, \pi$ ):

$$\begin{aligned}
 \alpha_i(r, \bar{\theta}) &= \bar{\alpha}_i(r) \sin \theta \Big|_{\theta=\bar{\theta}}, & \text{for } i = 1, 2, \\
 \alpha_i(r, \bar{\theta}) &= \bar{\alpha}_i(r) \sin^2 \theta \Big|_{\theta=\bar{\theta}}, & \text{for } i = 3, 4, 5, \\
 \alpha_i(r, \bar{\theta}) &= (-1)^{i-5} \cos \theta \partial_\theta \alpha_{i-5}(r, \theta) \Big|_{\theta=\bar{\theta}}, & \text{for } i = 6, 7, \\
 \alpha_i(r, \bar{\theta}) &= \frac{1}{2} \cos \theta \partial_\theta \alpha_{i-5}(r, \theta) \Big|_{\theta=\bar{\theta}}, & \text{for } i = 8,
 \end{aligned} \tag{3.13}$$

and towards infinity:

$$\lim_{r \rightarrow \infty} \begin{pmatrix} \alpha_1(r, \theta) \\ \alpha_2(r, \theta) \\ \alpha_3(r, \theta) \\ \alpha_4(r, \theta) \\ \alpha_5(r, \theta) \\ \alpha_6(r, \theta) \\ \alpha_7(r, \theta) \\ \alpha_8(r, \theta) \end{pmatrix} = \begin{pmatrix} -2 \sin \theta (1 + \sin^2 \theta) \\ 2 \sin \theta \cos^2 \theta \\ -2 \sin^2 \theta \\ -\sin^2 \theta (1 + 2 \sin^2 \theta) \\ \sqrt{3} \sin^2 \theta \\ 2 \\ 2 \\ -2 \sin \theta \end{pmatrix}. \tag{3.14}$$

The Higgs field *Ansatz* (3.6) can be generalized in the same manner:

$$\begin{aligned}
 \hat{\Phi}(r, \theta, \phi) &= \eta [\beta_1(r, \theta) \lambda_3 + \beta_2(r, \theta) \cos \theta 2iT_\rho + \beta_3(r, \theta) 2iV_\rho] \begin{pmatrix} 1 \\ 0 \\ 0 \end{pmatrix}, \\
 &= \eta \begin{pmatrix} \beta_1(r, \theta) \\ \beta_2(r, \theta) \cos \theta e^{i\phi} \\ \beta_3(r, \theta) e^{-i\phi} \end{pmatrix},
 \end{aligned} \tag{3.15}$$

with real functions  $\beta_i$ , for  $i = 1, \dots, 3$ . The boundary conditions are:

At  $r = 0$ :

$$\beta_i(0, \theta) = 0, \tag{3.16}$$

on the symmetry axis ( $\bar{\theta} = 0, \pi$ ):

$$\partial_\theta \beta_1(r, \theta) \Big|_{\theta=\bar{\theta}} = 0, \quad \beta_i(r, \hat{\theta}) = \bar{\beta}_i(r) \sin \theta \Big|_{\theta=\bar{\theta}}, \quad \text{for } i = 2, 3, \tag{3.17}$$

and towards infinity:

$$\lim_{r \rightarrow \infty} \begin{pmatrix} \beta_1(r, \theta) \\ \beta_2(r, \theta) \\ \beta_3(r, \theta) \end{pmatrix} = \begin{pmatrix} \cos^2 \theta \\ -\sin \theta \\ -\sin \theta \end{pmatrix}. \quad (3.18)$$

Incorporating the generalized sphaleron *Ansatz* into energy functional (2.4) gives

$$E[A, \Phi] = 4\pi \int_0^\infty dr \int_0^{\pi/2} d\theta r^2 \sin \theta e(r, \theta), \quad (3.19)$$

with  $e(r, \theta)$  containing contributions from the Yang-Mills term, the kinetic Higgs term and the Higgs potential

$$e(r, \theta) = e_{YM}(r, \theta) + e_{Hkin}(r, \theta) + e_{Hpot}(r, \theta), \quad (3.20)$$

the explicit forms of which are contained in Appendix A.

### 3.4 Field configurations between vacuum and sphaleron

To check, if the  $\hat{S}$  configuration at  $\psi = \pi$  is in fact the field configuration of highest energy, the energies of configurations between vacuum and sphaleron will have to be evaluated. Consequently, the *Ansätze* for fields  $A_\mu$  and  $\Phi$ , as well as the energy functional (2.4) need to be generalized for all positions on the 3-sphere, parameterized by  $\psi$ ,  $\mu$  and  $\alpha$ . This requires using the most general parametrization of the hitherto used map  $U$  (see eq. (3.1)).

#### 3.4.1 Approximate *Ansatz*

We start by applying the most general map  $U$  to the approximate *Ansatz* (3.5) and (3.6) and evaluating the corresponding energy functional.

Since  $\mu$  does not parameterize a non-contractible loop (NCL), we fix it in a way, that minimizes the resulting  $\psi$  dependent energy functional, namely by setting  $\mu = n\pi$ ,  $n \in \mathbb{Z}$ . This simplifies the obtained functional to

$$\begin{aligned} E = & \frac{4\pi}{1536} \int_0^1 dx \sin^2 \left( \frac{\psi}{2} \right) \left[ \frac{(f(f-1))^2}{x^2} \sin^4 \left( \frac{\psi}{2} \right) (107 - 53 \cos \psi) + 768 \sin^{-2} \left( \frac{\psi}{2} \right) x^2 h'^2 \right. \\ & + 4(x-1)^2 (2070 + 10 \cos(2\psi) - 5 \cos(3\psi) - 1499 \cos \psi) f'^2 \\ & \left. + \frac{((f-1)h)^2}{(x-1)^2} (1762 - 689 \cos \psi - 354 \cos(2\psi) + 49 \cos(3\psi)) \right]. \end{aligned} \quad (3.21)$$

As will be shown later on, all energy functionals are independent of  $\alpha$  due to underlying symmetries.

### 3.4.2 Generalized *Ansatz*

For the generalized *Ansatz* we use the same  $\text{su}(3)$  basis as before. Aside from vacuum and sphaleron configuration however, we loose all structure and are required to use the complete basis to generate the fields. The field components, depending on all parameters and coordinates  $r, \omega = (\theta, \phi, \psi, \mu, \alpha)$ , are defined as follows

$$\begin{aligned} g\hat{A}_\phi(r, \omega) = & \alpha_9(r, \theta)a_\phi(\omega)T_\phi + \alpha_1(r, \theta)b_\phi(\omega)T_\rho + \alpha_{10}(r, \theta)c_\phi(\omega)V_\phi + \alpha_2(r, \theta)d_\phi(\omega)V_\rho \\ & + \alpha_{11}(r, \theta)e_\phi(\omega)U_\phi + \alpha_3(r, \theta)f_\phi(\omega)U_\rho + \alpha_4(r, \theta)g_\phi(\omega)\frac{\lambda_3}{2i} + \alpha_5(r, \theta)h_\phi(\omega)\frac{\lambda_8}{2i}, \end{aligned} \quad (3.22)$$

$$\begin{aligned} g\hat{A}_\theta(r, \omega) = & \alpha_6(r, \theta)a_\theta(\omega)T_\phi + \alpha_{12}(r, \theta)b_\theta(\omega)T_\rho + \alpha_7(r, \theta)c_\theta(\omega)V_\phi + \alpha_{13}(r, \theta)d_\theta(\omega)V_\rho \\ & + \alpha_8(r, \theta)e_\theta(\omega)U_\phi + \alpha_{14}(r, \theta)f_\theta(\omega)U_\rho + \alpha_{15}(r, \theta)g_\theta(\omega)\frac{\lambda_3}{2i} + \alpha_{16}(r, \theta)h_\theta(\omega)\frac{\lambda_8}{2i}, \end{aligned} \quad (3.23)$$

with real functions  $a_\phi(\omega)$  through  $h_\phi(\omega)$  and  $a_\theta(\omega)$  through  $h_\theta(\omega)$ , given in appendix B.

Additionally, the previous Higgs field *Ansatz* (3.15) is generalized to

$$\begin{aligned} \hat{\Phi}(r, \omega) = & \eta \left[ \beta_1(r, \theta) \left( a_{\Phi,1}(\omega) + ia_{\Phi,2}(\omega) \right) \lambda_3 \right. \\ & + \beta_2(r, \theta) \left( e^{i(\alpha-\phi)} b_{\Phi,1}(\omega) - ib_{\Phi,2}(\omega) + b_{\Phi,3}(\omega) \right) T_\rho \\ & \left. + \beta_3(r, \theta) \left( e^{-i(\alpha-\phi)} (c_{\Phi,1}(\omega) - ic_{\Phi,3}(\omega)) + ic_{\Phi,2}(\omega) \right) V_\rho \right] \begin{pmatrix} 1 \\ 0 \\ 0 \end{pmatrix}, \end{aligned} \quad (3.24)$$

with real functions  $a_{\Phi,i}(\omega)$  through  $c_{\Phi,i}(\omega)$  given by

$$a_{\Phi,1}(\theta, \psi, \mu) = \frac{1}{4} \left( ((\cos \psi - 1) \cos \theta + \cos \psi + 1)^2 - 4 \cos^2 \mu \sin^2 \psi \cos^2 \left( \frac{\theta}{2} \right) \right) \quad (3.25)$$

$$a_{\Phi,2}(\theta, \psi, \mu) = \cos \mu \sin \psi \cos \left( \frac{\theta}{2} \right) ((\cos \psi - 1) \cos \theta + \cos \psi + 1) \quad (3.26)$$

$$b_{\Phi,1}(\theta, \psi, \mu) = 2 \sin \mu \sin \psi \cos \left( \frac{\theta}{2} \right) \quad (3.27)$$

$$b_{\Phi,2}(\theta, \psi, \mu) = \frac{1}{2} (\cos \psi - 1) \sin \theta (\cos \psi (\cos \theta + 1) - \cos \theta + 1) \quad (3.28)$$

$$b_{\Phi,3}(\theta, \psi, \mu) = \cos \mu \sin \psi (\cos \psi - 1) \sin \theta \cos \left( \frac{\theta}{2} \right) \quad (3.29)$$

$$c_{\Phi,1}(\theta, \psi, \mu) = \sin \mu \sin \psi \cos \left( \frac{\theta}{2} \right) (-\cos \psi (\cos \theta + 1) + \cos \theta - 1) \quad (3.30)$$

$$c_{\Phi,2}(\theta, \psi, \mu) = (\cos \psi - 1) \sin \theta \quad (3.31)$$

$$c_{\Phi,3}(\theta, \psi, \mu) = 2 \sin \mu \cos \mu \sin^2 \psi \cos^2 \left( \frac{\theta}{2} \right). \quad (3.32)$$

With the *Ansatz* generalized to parameterize the entire 3-sphere, we can now calculate the most general energy density  $e(r, \theta, \phi, \psi, \mu, \alpha)$ . The explicit form of which, in dependence of the previously defined real structure functions  $a_\phi$  through  $h_\phi$ ,  $a_\theta$  through  $h_\theta$  and  $a_{\Phi,i}$  through  $c_{\Phi,i}$  is very extensive and has been moved to Appendix B.

Since evaluating the energy functional from a given *Ansatz* with Mathematica is most delicate and time consuming, having the energy density in this form has a great advantage. Whenever the *Ansatz* is changed, e.g. by introducing a more general topological map or altering boundary conditions, this merely influences the structure functions. Once the new structure functions are calculated, obtaining the energy density requires no further effort. Only by this method was it at all possible to introduce the most general topological map, without severely overstraining Mathematica.

It is essential to take into account some simplifying properties of the obtained energy functional. First, the energy functional depends on the  $S^3$  parameter  $\alpha$  only in forms such as  $\sin(\phi - \alpha)$  and  $\cos(\phi - \alpha)$  and thusly drops out entirely whilst integrating over  $\phi$ , leaving the energy completely independent of  $\alpha$ . Second, the energy functional displays a minimum at  $\mu = n\pi$ ,  $n \in \mathbb{Z}$ , for arbitrary  $\psi$ .

As done for the approximate *Ansatz*, we fix  $\mu = \pi$  to minimize the energy functional. In order to match the generalized *Ansatz* of [1], we choose the following set of structure functions

$$\begin{pmatrix} a_\phi(\omega) \\ b_\phi(\omega) \\ c_\phi(\omega) \\ d_\phi(\omega) \\ e_\phi(\omega) \\ f_\phi(\omega) \\ g_\phi(\omega) \\ h_\phi(\omega) \end{pmatrix} = \begin{pmatrix} 1 \\ \cos \theta \\ 1 \\ 1 \\ 1 \\ \cos \theta \\ 1 \\ 1 \end{pmatrix}, \quad \begin{pmatrix} a_\theta(\omega) \\ b_\theta(\omega) \\ c_\theta(\omega) \\ d_\theta(\omega) \\ e_\theta(\omega) \\ f_\theta(\omega) \\ g_\theta(\omega) \\ h_\theta(\omega) \end{pmatrix} = \begin{pmatrix} 1 \\ 1 \\ \cos \theta \\ 1 \\ 1 \\ 1 \\ 1 \\ 1 \end{pmatrix}, \quad (3.33)$$

for which the *Ansatz*, given by (3.22) and (3.23), exactly reduces to (3.11) for the limiting case of  $\psi = \pi$ . The boundary conditions of the corresponding profile functions towards spacial infinity are generalized accordingly

$$\begin{aligned} \lim_{r \rightarrow \infty} \alpha_1(r, \theta) &= \frac{1}{64 \cos \theta} \left( 16 \sin^8 \left( \frac{\psi}{2} \right) \sin(4\theta) - 4 \sin^4 \left( \frac{\psi}{2} \right) (-4 \cos \psi + \cos(2\psi) + 19) \sin(2\theta) \right. \\ &\quad \left. + \sin^2(\psi) (4(\cos(2\psi) - 4 \cos \psi) \sin^3 \theta + 41 \sin \theta - 3 \sin(3\theta)) \right) \end{aligned} \quad (3.34)$$

$$\begin{aligned} \lim_{r \rightarrow \infty} \alpha_2(r, \theta) &= \frac{1}{16} \sin^2 \left( \frac{\psi}{2} \right) \left( 8 \sin^4 \left( \frac{\psi}{2} \right) \sin(3\theta) - 16 \sin^2 \psi \sin(2\theta) \right. \\ &\quad \left. + (12 \cos \psi + 13 \cos(2\psi) + 7) \sin \theta \right) \end{aligned} \quad (3.35)$$

$$\lim_{r \rightarrow \infty} \alpha_3(r, \theta) = \sin^4 \left( \frac{\psi}{2} \right) \sin \theta \tan \theta ((\cos \psi - 1) \cos \theta + \cos \psi + 1) \quad (3.36)$$

$$\lim_{r \rightarrow \infty} \alpha_4(r, \theta) = \frac{1}{8} \sin^4 \left( \frac{\psi}{2} \right) \sin^2 \theta \left( 8 \sin^4 \left( \frac{\psi}{2} \right) \cos(2\theta) + 4 \cos \psi - \cos(2\psi) - 11 \right) \quad (3.37)$$

$$\lim_{r \rightarrow \infty} \alpha_5(r, \theta) = \sqrt{3} \sin^4 \left( \frac{\psi}{2} \right) \sin^2 \theta \quad (3.38)$$

$$\begin{aligned} \lim_{r \rightarrow \infty} \alpha_6(r, \theta) &= \frac{1}{64} \left( 8 \sin^4 \left( \frac{\psi}{2} \right) \left( 4(\cos \psi - 3) \cos^2 \left( \frac{\psi}{2} \right) \cos(2\theta) - \sin^2 \psi \cos(3\theta) + 4 \cos \psi \right. \right. \\ &\quad \left. \left. - \cos(2\psi) + 21 \right) + \sin^2 \psi (-4 \cos \psi + \cos(2\psi) - 29) \cos \theta \right) \end{aligned} \quad (3.39)$$

$$\lim_{r \rightarrow \infty} \alpha_7(r, \theta) = \frac{1}{2 \cos \theta} \sin^2 \left( \frac{\psi}{2} \right) \left( 4 \cos^2 \psi \cos \theta - \sin^2 \psi (\cos(2\theta) + 3) \right) \quad (3.40)$$

$$\lim_{r \rightarrow \infty} \alpha_8(r, \theta) = \sin^4 \left( \frac{\psi}{2} \right) \sin \theta (\cos \psi (\cos \theta + 1) + \cos \theta - 1) \quad (3.41)$$

$$\begin{aligned} \lim_{r \rightarrow \infty} \alpha_9(r, \theta) &= \frac{1}{2} \sin^3 \left( \frac{\psi}{2} \right) \cos \left( \frac{\psi}{2} \right) \sin \left( \frac{\theta}{2} \right) \cos^2 \left( \frac{\theta}{2} \right) \\ &\quad \times \left( 8 \sin^4 \left( \frac{\psi}{2} \right) \cos(2\theta) + 4 \cos \psi - \cos(2\psi) - 19 \right) \end{aligned} \quad (3.42)$$

$$\lim_{r \rightarrow \infty} \alpha_{10}(r, \theta) = -8 \sin^3\left(\frac{\psi}{2}\right) \cos\left(\frac{\psi}{2}\right) \sin\left(\frac{\theta}{2}\right) \cos^2\left(\frac{\theta}{2}\right) ((\cos \psi - 1) \cos \theta + \cos \psi + 1) \quad (3.43)$$

$$\lim_{r \rightarrow \infty} \alpha_{11}(r, \theta) = -\sin^4\left(\frac{\psi}{2}\right) \sin \psi \sin^3 \theta \csc\left(\frac{\theta}{2}\right) \quad (3.44)$$

$$\begin{aligned} \lim_{r \rightarrow \infty} \alpha_{12}(r, \theta) = & \frac{1}{64} \sin^3\left(\frac{\psi}{2}\right) \left( 5 \left( \cos\left(\frac{5\psi}{2}\right) - 3 \cos\left(\frac{3\psi}{2}\right) \right) \cos\left(\frac{\theta}{2}\right) + 2 \cos\left(\frac{\psi}{2}\right) \right. \\ & \times \left. \left( -8 \sin^4\left(\frac{\psi}{2}\right) \left( \cos\left(\frac{3\theta}{2}\right) + 3 \cos\left(\frac{5\theta}{2}\right) + \cos\left(\frac{7\theta}{2}\right) \right) - 123 \cos\left(\frac{\theta}{2}\right) \right) \right) \end{aligned} \quad (3.45)$$

$$\lim_{r \rightarrow \infty} \alpha_{13}(r, \theta) = \frac{1}{2} \sin^3\left(\frac{\psi}{2}\right) \cos\left(\frac{\psi}{2}\right) \cos\left(\frac{\theta}{2}\right) \left( 4 \cos \psi \cos^2\left(\frac{\theta}{2}\right) (\cos \theta + 3) - 8 \sin^4\left(\frac{\theta}{2}\right) \right) \quad (3.46)$$

$$\lim_{r \rightarrow \infty} \alpha_{14}(r, \theta) = \frac{1}{4} \sin^4\left(\frac{\psi}{2}\right) \sin \psi \sin^4 \theta \csc^3\left(\frac{\theta}{2}\right) \quad (3.47)$$

$$\begin{aligned} \lim_{r \rightarrow \infty} \alpha_{15}(r, \theta) = & \frac{1}{512} \left( -64 \sin \psi \sin^6\left(\frac{\psi}{2}\right) \sin\left(\frac{7\theta}{2}\right) + \left( -838 \sin \psi - 10 \sin(2\psi) + 34 \sin(3\psi) \right. \right. \\ & \left. \left. - 3 \sin(4\psi) \right) \sin\left(\frac{\theta}{2}\right) + 32 \sin^5\left(\frac{\psi}{2}\right) \left( \cos\left(\frac{3\psi}{2}\right) - 9 \cos\left(\frac{\psi}{2}\right) \right) \sin\left(\frac{5\theta}{2}\right) \right. \\ & \left. + 8 \sin^3\left(\frac{\psi}{2}\right) \left( -82 \cos\left(\frac{\psi}{2}\right) - 17 \cos\left(\frac{3\psi}{2}\right) + 3 \cos\left(\frac{5\psi}{2}\right) \right) \sin\left(\frac{3\theta}{2}\right) \right) \end{aligned} \quad (3.48)$$

$$\lim_{r \rightarrow \infty} \alpha_{16}(r, \theta) = \frac{1}{4} \sqrt{3} \sin \psi \sin\left(\frac{\theta}{2}\right) ((\cos \psi - 1) \cos \theta + \cos \psi - 3). \quad (3.49)$$

Boundary conditions of profile functions  $\alpha_1 \dots \alpha_8$  reduce to (3.14) for  $\psi = \pi$ , as required, whereas profile functions  $\alpha_9 \dots \alpha_{16}$  vanish there.

The Higgs *Ansatz* is treated similarly, by setting the respective structure functions to

$$\begin{pmatrix} a_{\Phi,1}(\omega) \\ a_{\Phi,2}(\omega) \\ b_{\Phi,1}(\omega) \\ b_{\Phi,2}(\omega) \\ b_{\Phi,3}(\omega) \\ c_{\Phi,1}(\omega) \\ c_{\Phi,2}(\omega) \\ c_{\Phi,3}(\omega) \end{pmatrix} = \begin{pmatrix} 1 \\ \frac{16 \sin \psi \cos\left(\frac{\theta}{2}\right) ((\cos \psi - 1) \cos \theta + \cos \psi + 1)}{8 \sin^4\left(\frac{\psi}{2}\right) \cos(2\theta) - 16 \sin^2 \psi \cos \theta + 4 \cos \psi + 7 \cos(2\psi) + 5} \\ 0 \\ -2 \cos \theta \\ -\frac{4 \sin \psi \cos\left(\frac{\theta}{2}\right) \cos \theta}{(\cos \psi - 1) \cos \theta + \cos \psi + 1} \\ 0 \\ 2 \\ 0 \end{pmatrix} \quad (3.50)$$

and the profile function boundary conditions to

$$\lim_{r \rightarrow \infty} \beta_1(r, \theta) = \frac{1}{16} \left( 8 \sin^4 \left( \frac{\psi}{2} \right) \cos(2\theta) - 16 \sin^2 \psi \cos \theta + 4 \cos \psi + 7 \cos(2\psi) + 5 \right) \quad (3.51)$$

$$\lim_{r \rightarrow \infty} \beta_2(r, \theta) = \frac{1}{4} \sin^2 \psi \tan \theta - \sin^4 \left( \frac{\psi}{2} \right) \sin \theta \quad (3.52)$$

$$\lim_{r \rightarrow \infty} \beta_3(r, \theta) = \frac{1}{2} (\cos \psi - 1) \sin \theta. \quad (3.53)$$

Analogously, *Ansatz* (3.24) reduces to (3.15) and boundary conditions (3.51) through (3.53) to (3.18) for  $\psi = \pi$ .

## 4 Simulated Annealing

Simulated Annealing (SA) is a randomized metaheuristic<sup>1</sup> that applies analogies of statistical mechanics (annealing of solids) to detect the minimum of a function depending on many parameters, as first described by [15]. In contrast to most optimization methods it requires few or no assumptions about the function and can search vast finite parameter spaces. Most essential however is its ability to differentiate between local minima and the global minimum. Given a multivariate function with numerous minima, methods like Newton-Raphson<sup>2</sup> are strongly dependent on choosing initial values close to the global optimum and will fail without them, whereas SA can find the global optimum to a good approximation.

Analogous to integration methods (Monte Carlo), optimization problems also require one to resort to randomized algorithms, like SA, to solve problems with parameter spaces of high dimensions  $D$  in acceptable computation times<sup>3</sup>.

The algorithm starts off at the initial point  $x$  and determines the corresponding function value  $f(x)$ . It then generates a randomized point  $x_{prop}$  in the neighbourhood of  $x$  and determines  $f(x_{prop})$ . If the new function value is lower than the old one ( $f(x_{prop}) < f(x)$ ),  $x_{prop}$  is accepted and the procedure starts anew, this time originating from the new value of  $x$ . So far however, this method will get stuck in a local minimum, as it accepts only downward steps. This is solved by accepting certain upward steps, based on the Metropolis criterion [16]:

$$p_{accept} = \exp\left(-\frac{f(x_{prop}) - f(x)}{T}\right), \quad (4.1)$$

in which  $T$  is a controlling parameter, comparable to the temperature in the annealing of solids.

Now we slowly anneal the system. At each temperature  $T$  we repeat the above steps many ( $N_S$ ) times and subsequently lower the temperature. This, in turn is done many ( $N_T$ ) times until the temperature is close to zero, at which point no more upward steps will be accepted<sup>4</sup> and the algorithm remains 'frozen' at the global minimum. There exist several prevalent cooling schedules. The most suitable can, however, due to the complexity of most SA problems only be determined by trial and error. After applying several cooling

<sup>1</sup>Computational method that iteratively tries to improve a proposed solution to optimize it.

<sup>2</sup>The Newton-Raphson method uses Newton's method for finding a root of a function to find an optimum of said function. This is done by finding a root, not of the function itself, but of its derivative ( $f'(x) = 0$ ). This can also be applied to multivariate functions, by generalizing the derivative (Jacobian matrix).

<sup>3</sup>SA runs with  $\mathcal{O}(D)$ , whereas Newton-Raphson runs with  $\mathcal{O}(D^2)$ . Brute force algorithms even run with  $\mathcal{O}(a^D)$ , with  $a$  being the number of grid points.

<sup>4</sup>Or, in practice, the step length will go to zero, in order to maintain a good step ratio.

schedules to the problems of the subsequent chapters exponential cooling proved most efficient. This means multiplying the temperature  $T$  with a factor  $\chi \in (0, 1)$  at the end of each cycle<sup>5</sup>.

A minimal source code example in C++ can be found in Appendix C. To obtain a better understanding of the algorithm and its essential components, I have chosen to write a SA program from the ground up, as an alternative to using one of many available libraries. The source code from Appendix C serves as the basis for the optimization programs, that are used in the following chapters.

SA algorithms run optimally, only when equal numbers of steps up and down are taken. A step ratio  $r$  of  $\sim 0.5$  can be maintained, by regularly adjusting the step length, i.e. the size of the neighbourhood around the current value  $x$ , in which to generate a proposal value  $x_{prop}$ . To avoid unnecessary corrections, lower ( $l$ ) and upper ( $u$ ) step ratio boundaries are introduced. Corrections to the step length are only made, once the step ratio exceeds these bounds. The step length is then adjusted in the following way:

$$\begin{aligned} r &\rightarrow r \left( 1 + c \frac{r - u}{l} \right) && \text{if } r > u, \\ r &\rightarrow r \left( 1 - c \frac{r - l}{l} \right)^{-1} && \text{if } r < l, \end{aligned} \tag{4.2}$$

rather than simply multiplying it with a constant factor  $c^6$ . This way adjustments are only as large as necessary.

---

<sup>5</sup>A typical value for  $\chi$  is 0.85.

<sup>6</sup>A typical value for  $c$  is 2.0. This can be adjusted to make step length adjustments more or less dramatic.

## 5 Semi-analytical energy optimization and structure analysis

To minimize the energy functionals in a semi-analytical manner, profile functions, as well as  $\alpha$  and  $\beta$  functions of the generalized *Ansatz* are approximated by an expansion in orthogonal functions. The expansion coefficients are then varied in a Simulated Annealing program to minimize the resulting energy. Given the boundary conditions, we require a set of functions, that has even parity and preferably even meets one or both boundary conditions innately. An optimal candidate are the even Legendre polynomials  $P_{2n}$ . The tremendous accuracy of an expansion in Legendre polynomials, in contrast to Taylor expansions has been demonstrated in [19].

The typical form of a profile function expansion is

$$f(x) = x^n \sum_{i=0}^{M-1} a_{2i} P_{2i}(x). \quad (5.1)$$

The boundary conditions dictate constraints on the expansion coefficients (here  $a_{2i}$ ), which will be discussed for the  $\hat{S}_{approx}$  and the generalized *Ansatz* separately. Depending on the *Ansatz*, the number of profile functions varies from 2 ( $\hat{S}_{approx}$  *Ansatz*<sup>1</sup>) to 41 ( $N = 3$  generalized *Ansatz*<sup>2</sup>) and beyond. The factor  $x^n$  has been added to ensure convergence of the energy functional, by cancelling any  $x$  potencies in the denominator. Yang-Mills and kinetic Higgs energy densities require different minimum values of  $n$ . The extent  $M$  of the expansion has been chosen to ensure a good fit, while keeping the computation time reasonable<sup>3</sup>. Large  $M$  lead to extremely erratic profile functions, which, in turn, require a greater grid density for numerical integration, resulting in additional computation time.

The large number of function evaluations<sup>4</sup>, that are required to compute satisfactory results would lead to intolerable computation times, if no optimization steps were taken. Only reevaluating the affected parts of the energy function on any given parameter change<sup>5</sup> and using runtime optimized compiler settings<sup>6</sup> is paramount and improves the computation time by a factor of  $\sim 20$  and  $\sim 80$ , respectively. Parallelizing the energy function evaluation into multiple threads or the incorporation of any additional measures has been considered, but not implemented, since they are very burdensome for very little gain.

---

<sup>1</sup>This results in 29 parameters to be varied in the SA procedure.

<sup>2</sup>This results in 659 parameters to be varied in the SA procedure.

<sup>3</sup>The procedure runs with  $\mathcal{O}(M)$ .

<sup>4</sup> $N_S \times N_T \times M \times \text{Number of profile functions} \approx 5.3 \times 10^7$  for  $N = 3$ .

<sup>5</sup>Information, identifying the currently varied parameter is passed to the energy function, where only the corresponding profile functions and energy densities are recalculated. The unaffected function values, saved in static arrays, remain unaltered.

<sup>6</sup>The g++ optimization options -Ofast, implementing -ffast-math and -march=native resulted in tremendous improvements. The non standard-compliance of -ffast-math did not result in any problems.

Results, obtained from various degrees of angular dependency are summarized in table 5.1. The corresponding total energy densities are depicted in fig. 5.1.

	$E_{\hat{S},YM} \left[ \frac{4\pi v}{g} \right]$	$E_{\hat{S},Hkin} \left[ \frac{4\pi v}{g} \right]$	$E_{\hat{S}} \left[ \frac{4\pi v}{g} \right]$	$E_{\hat{S}} / E_S$
$\hat{S}_{approx}$			2.617	<b>1.700</b>
$N = 0$	1.234	1.233	2.466	<b>1.600</b>
$N = 1$	0.771	0.830	1.600	<b>1.038</b>
$N = 2$	0.705	0.663	1.369	<b>0.888</b>
$N = 3$	0.716	0.681	1.396	<b>0.906</b>

Table 5.1: Approximations of  $E_{\hat{S}}$  ( $\lambda = 0$ ) for various degrees of angular expansion, with  $E_S$  defined by (6.7)

The therein used value of  $E_S = 1.541 \left[ \frac{4\pi v}{g} \right]$  is the energy of the SU(2) Sphaleron  $S$ , the evaluation of which is discussed in detail, in chapter 6.

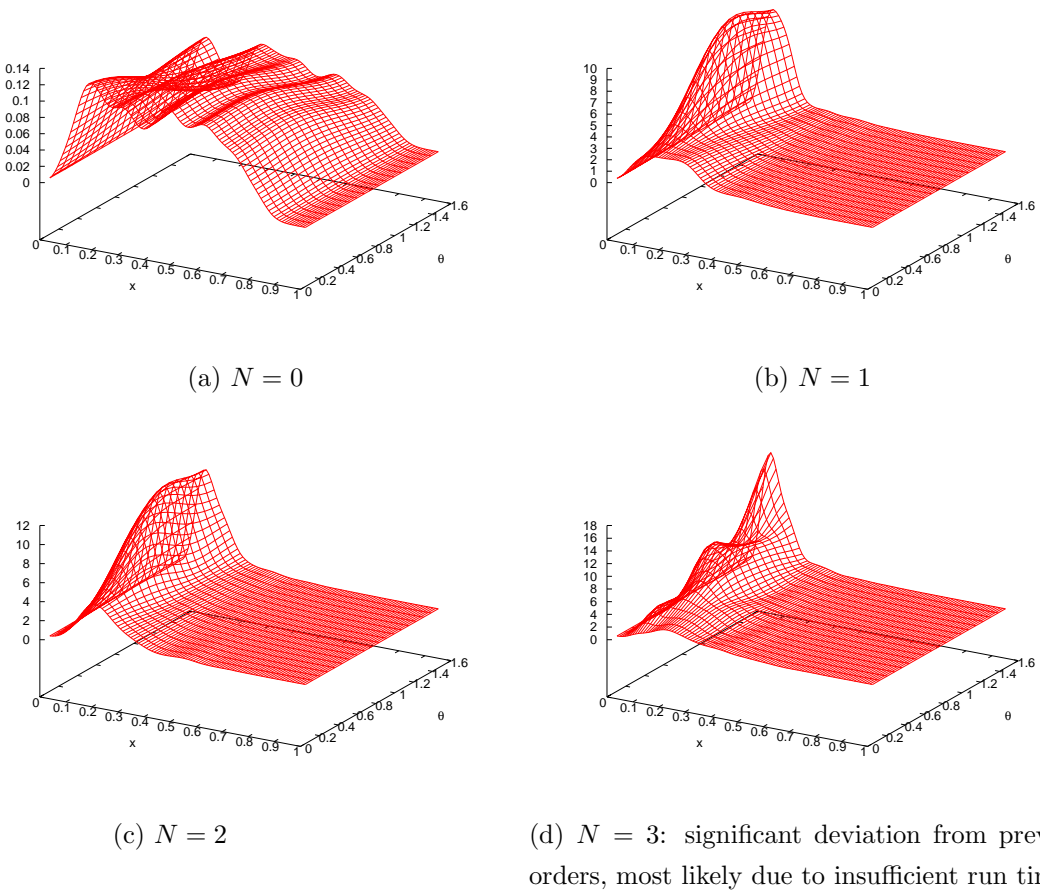


Figure 5.1: Total energy density approximations for various degrees of angular dependency

### 5.1 Minimization of the approximate *Ansatz*

The energy functional (3.8) is minimized by varying the expansion coefficients  $a_i$  and  $b_i$  of profile functions

$$f(x) = x^4 \sum_{i=0}^{17} a_{2i} P_{2i}(x) \quad (5.2)$$

and

$$h(x) = x^2 \sum_{i=0}^{12} b_{2i} P_{2i}(x), \quad (5.3)$$

with  $P_n$  denoting the Legendre polynomials, in a Simulated Annealing (SA) program.

To meet boundary conditions (3.7) and additionally achieve a vanishing gradient at the origin and towards infinity ( $f'(0) = f'(1) = h'(0) = h'(1) = 0$ ) the following constraints are enforced

$$\sum_{i=0}^{17} a_{2i} = 1, \quad \sum_{i=0}^{12} b_{2i} = 1, \quad (5.4)$$

$$\sum_{i=0}^{17} a_{2i}(4 + i + 2i^2) = 0, \quad \sum_{i=0}^{12} b_{2i}(2 + i + 2i^2) = 0. \quad (5.5)$$

In numerical practice, every time a coefficients gets randomly varied within the step length (Line 1), these boundary conditions are violated. To correct this, the first two coefficients of the respective expansion are also adjusted:

```

1 xpa[j] = a[j] + (ran1.doub() * 2.0 - 1.0) * stepa[j];
2 c1 = 0; c2 = 0;
3 for (int k=2;k<=17;k++){
4     c1+= xpa[2*k]*(4+k+2*k*k);
5     c2+= xpa[2*k];
6 }
7 xpa[0] = (7.0+c1-7.0*c2)/3.0;
8 xpa[2] = (-4.0-c1+4.0*c2)/3.0;

```

Here, the xp array contains the proposal values and the a array the current values.

The low number of varied coefficients, in combination with the compactness of the  $\hat{S}_{approx}$  energy functional, results in a very short runtime of the SA program and thusly allows for a very large number of steps per temperature  $N_S$ .

As desired, SA programs with different values of  $N_S$  converge towards one energy value, namely  $2.62 [4\pi v/g]$  and towards one set of profile functions, for large  $N_S$ . Naively this would suggest that this is the true value of  $E_{\hat{S}_{approx}}$ , however, since Simulated Annealing is a stochastic algorithm with finite  $N_S$  and because the underlying structure is entirely

unknown, lower values of  $E_{\hat{S}_{approx}}$  cannot rigorously be excluded. Hence, values acquired in this fashion, not only in this case, but throughout the entire thesis are merely upper energy bounds

$$E_{\hat{S}_{approx}} < 2.62 \left[ \frac{4\pi v}{g} \right] = 1.70 \times E_S. \quad (5.6)$$

The obtained result exactly matches the  $E_{\hat{S}_{approx}}$  boundary of [12] ( $1.70 \times E_S$ ).

The hereby obtained expansion coefficients, which generate the profile functions shown in fig. 5.2 are listed in Appendix D.

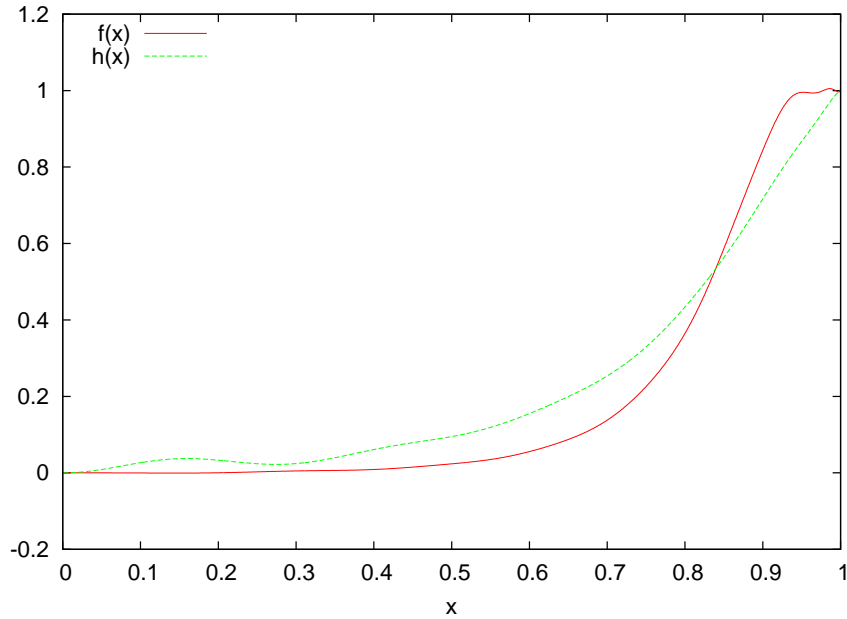


Figure 5.2: Approximation of profile functions  $f(x)$  and  $h(x)$  for  $\hat{S}_{approx}$  with  $\lambda = 0$

## 5.2 Minimization of the generalized *Ansatz*

We continue, by minimizing the energy functional of the generalized Ansatz given in appendix A. Angular dependency is introduced in yet another expansion in Legendre polynomials<sup>7</sup>:

$$\begin{aligned} i = 1, 2, 8 : \quad \alpha_i(x, \theta) &= \sin \theta \tilde{\alpha}_i(x, \theta), \\ i = 3, 4, 5 : \quad \alpha_i(x, \theta) &= \sin^2 \theta \tilde{\alpha}_i(x, \theta), \\ i = 6, 7 : \quad \alpha_i(x, \theta) &= \tilde{\alpha}_i(x, \theta), \\ j = 1 : \quad \beta_i(x, \theta) &= \tilde{\beta}_i(x, \theta), \\ j = 2, 3 : \quad \beta_i(x, \theta) &= \sin \theta \tilde{\beta}_i(x, \theta), \end{aligned} \tag{5.8}$$

$$\tilde{\alpha}_i(x, \theta) = f_i(x)[c_{i,0}P_0(\cos \theta) + c_{i,2}P_2(\cos \theta)] + \sin^2 \theta \sum_{n=0}^{N-1} f_{i,2n}(x)P_{2n}(\cos \theta), \tag{5.9}$$

$$\tilde{\beta}_j(x, \theta) = h_j(x)[g_{j,0}P_0(\cos \theta) + g_{j,2}P_2(\cos \theta)] + \sin^2 \theta \sum_{n=0}^{N-1} h_{j,2n}(x)P_{2n}(\cos \theta), \tag{5.10}$$

with an *Ansatz* very similar to (5.2) and (5.3) for profile functions  $f(x)$  and  $h(x)$ :

$$f_j(x) = x^4 \sum_{i=0}^{17} a_{j,2i}P_{2i}(x), \quad \text{for } j = 1, \dots, 5, \tag{5.11}$$

$$h_j(x) = x^2 \sum_{i=0}^{12} b_{j,2i}P_{2i}(x), \quad \text{for } j = 1, \dots, 3. \tag{5.12}$$

The final  $f_j(x)$  can be deduced from boundary conditions (3.13):

$$f_6(x) = f_1(x), \quad f_7(x) = f_2(x), \quad f_8(x) = f_3(x) \tag{5.13}$$

Furthermore, each order of angular expansion is accompanied by additional profile functions:

$$\begin{aligned} f_{k,n}(x) &= x^4(x^2 - 1) \sum_{i=0}^{19} d_{k,n,2i}P_{2i}(x), \quad \text{for } k = 1, \dots, 5, \\ f_{k,n}(x) &= x^4(x^2 - 1) \sum_{i=0}^{17} d_{k,n,2i}P_{2i}(x), \quad \text{for } k = 6, \dots, 8, \end{aligned} \tag{5.14}$$

---

<sup>7</sup>A Fourier expansion of the form

$$\alpha_i(x, \theta) = \sum_{n=0}^N \cos\left(2n\left(\theta - \frac{\pi}{2}\right)\right) f_{i,2n}(x) \tag{5.7}$$

has been tested as well, since Fourier series have proven to be most efficient (fastest convergence) in the majority of numerical problems with periodic boundary conditions. In this case however, the expansion in Legendre polynomials converges far quicker.

$$h_{k,n}(x) = x^2(x^2 - 1) \sum_{i=0}^{12} e_{k,n,2i} P_{2i}(x). \quad (5.15)$$

Coefficients  $c_{i,0}$ ,  $c_{i,2}$ ,  $g_{i,0}$ ,  $g_{i,2}$  have been chosen to satisfy boundary conditions (3.14) and (3.18)

$$\begin{pmatrix} c_{1,0} \\ c_{2,0} \\ c_{3,0} \\ c_{4,0} \\ c_{5,0} \\ c_{6,0} \\ c_{7,0} \\ c_{8,0} \\ g_{1,0} \\ g_{2,0} \\ g_{3,0} \end{pmatrix} = \begin{pmatrix} -10/3 \\ 2/3 \\ -2 \\ -7/3 \\ \sqrt{3} \\ 2 \\ 2 \\ -2 \\ 1/3 \\ -1 \\ -1 \end{pmatrix}, \quad \begin{pmatrix} c_{1,2} \\ c_{2,2} \\ c_{3,2} \\ c_{4,2} \\ c_{5,2} \\ c_{6,2} \\ c_{7,2} \\ c_{8,2} \\ g_{1,2} \\ g_{2,2} \\ g_{3,2} \end{pmatrix} = \begin{pmatrix} 4/3 \\ 4/3 \\ 0 \\ 4/3 \\ 0 \\ 0 \\ 0 \\ 0 \\ 2/3 \\ 0 \\ 0 \end{pmatrix}. \quad (5.16)$$

Similar to  $\hat{S}_{approx}$  the following conditions apply as well:

$$f_j(0) = h_j(0) = 0, \quad f_j(1) = h_j(1) = 1 \quad (5.17)$$

$$f'_j(0) = f'_j(1) = h'_j(0) = h'_j(1) = 0 \quad (5.18)$$

$$f_{k,n}(0) = f_{k,n}(1) = h_{k,n}(0) = h_{k,n}(1) = 0 \quad (5.19)$$

$$f'_{k,n}(0) = f'_{k,n}(1) = h'_{k,n}(0) = h'_{k,n}(1) = 0 \quad (5.20)$$

Conditions (5.17) and (5.18) result in constraints equivalent to those of  $\hat{S}_{approx}$  in the previous section and are, except for the additional loop over the various profile functions  $f_j$  and  $h_j$ , treated identically in practice. Since (5.19) is already fulfilled by the profile function *Ansatz* ((5.14) and (5.15)), only (5.20) causes constraints on the coefficients:

$$\sum_{i=0}^{17} a_{k,n,2i}(4 + i + 2i^2) = 0, \quad \sum_{i=0}^{12} b_{k,n,2i}(2 + i + 2i^2) = 0. \quad (5.21)$$

Considering, that there is only one constraint, only one (the first) expansion coefficient is adjusted along with the varied coefficient to ensure the boundary conditions are met.

To calculate the total energy, expansion (5.8) is plugged into the generalized Yang-Mills-Higgs energy density<sup>8</sup> and subsequently integrated analytically over  $\theta$  to shorten formula

---

<sup>8</sup>The explicit form of the energy density, with the generalized *Ansatz* incorporated can be found in Appendix A or in [1].

length and runtime, but most importantly to ensure an exact result. Analytical integration over  $x$  is not possible without fixing parameters, since the general integrand, without constraints, leads to divergencies. Hence, full analytical integration is only feasible with fixed expansion coefficients after running the SA program.

To evaluate the energy during the SA program, the partially integrated energy density  $e(x)$  is numerically integrated over  $x$ , for each function call, with the appropriate integral measure:

$$4\pi \int_0^\infty e(r) r^2 dr \rightarrow 4\pi \int_0^1 e(x) \frac{x^2}{(x-1)^4} dx, \quad (5.22)$$

with

$$e(x) = \int_0^{\pi/2} e(x, \theta) \sin \theta d\theta. \quad (5.23)$$

To determine a suitable grid size for the numerical integration over  $x$  during the SA run, the grid size has been varied to analyze the rate of convergence for both  $E_{YM}$  and  $E_{Hkin}$  (see fig. 5.3). The latter in particular converges rather slowly. To achieve acceptable computation times a grid size of 1000 intervals has been chosen, which results in an error of about  $\pm 0.005$  for the energy  $E_{Hkin}$ . However, this error only occurs during the SA run and all results presented in this thesis have been reevaluated from the profile function coefficients analytically.

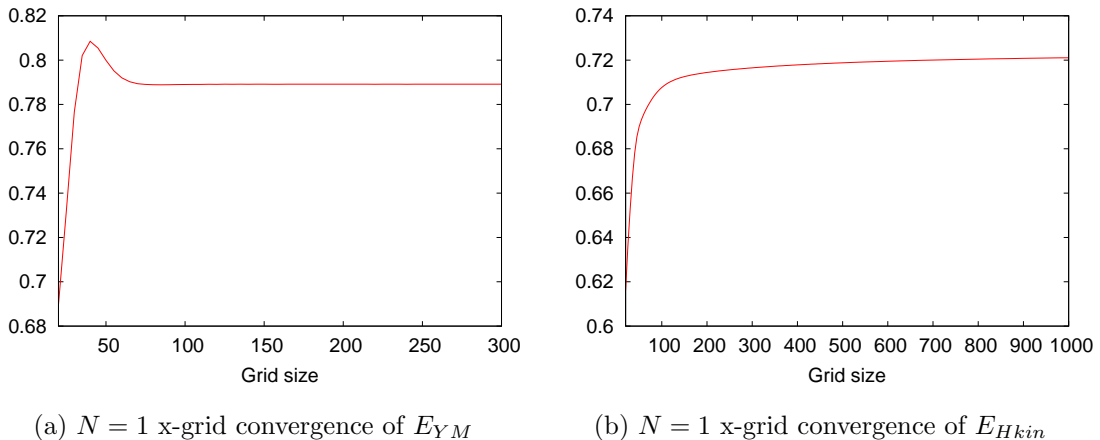


Figure 5.3:  $N = 1$  x-grid convergence of  $E_{\hat{S}}$

I hasten to add, that the discretization serves merely for the evaluation of the integral over  $x$ . All values of  $e_{YM}(x)$  and  $e_{Hkin}(x)$  are calculated analytically, including all derivatives, using recursion properties of the Legendre polynomials.

After the parameters corresponding to the minimal energy have been determined, we turn to evaluating said energy analytically. Due to the nature of floating point representation, being float type, numerical values, the obtained parameters will never meet boundary

conditions (5.17) through (5.20) exactly<sup>9</sup>. Due to this the integrand will diverge at  $x = 1$ , which is precisely why preliminary integration is not feasible. To work around this, all parameters are converted to rational numbers, i.e. 0.123456 becomes  $\frac{123456}{1000000}$ , etc. Subsequently the first (or first two) expansion coefficients are varied to meet the boundary conditions exactly. The hereby obtained, rational coefficients, in turn, lead to a vanishing integrand at  $x = 1$  and the origin for both energy densities and thusly a finite energy. All energy values, presented in sections 5.1 and 5.2, have been analytically verified in this manner. Although they are presented as numerical values, they are in fact vast fractions of integers and square roots of  $3^{10}$ , of the form:

$$E_{\hat{S}} \propto \frac{n \pm m\sqrt{3}}{r}, \quad n, m, r \in \mathbb{N}, \quad (5.24)$$

where  $n$ ,  $m$  and  $r$  are integers, several hundreds, in some cases well over a thousand digits in length.

In the following, we run SA programs for first, second and third order angular expansions and critically discuss the obtained results thereof.

---

<sup>9</sup>The error ranges from  $10^{-15}$  to  $10^{-12}$ . Small enough to ensure numerical consistency, but not for analytical integration.

<sup>10</sup>These originate from the normalization of the Gell-Mann matrix  $\lambda_8$ .

### 5.2.1 $N = 1$ Legendre expansion

Minimizing the energy functional to first order ( $N = 1$ , as in (5.9) and (5.10)) involves varying the expansion coefficients of 19 profile functions (295 coefficients in total). Results obtained from these SA programs, with the following parameters:

Grid size in x:	1000
Steps per temperature ( $N_S$ ):	200 – 13000
Initial temperature:	2.0
Final temperature:	$3.0 \times 10^{-9}$
Temperature reduction factor ( $\chi$ ):	0.85

are shown in table 5.2, their energy densities in fig. 5.4. Figures of profile functions, as well as the corresponding coefficients are available in Appendix E.2. From these results, we can further improve the upper energy bound of

$$E_{\hat{S}} < 1.600 \left[ \frac{4\pi v}{g} \right] = 1.038 \times E_S. \quad (5.25)$$

Yang-Mills and kinetic Higgs energy are of similar size, which is to be expected for a configuration of minimal energy.

The  $N = 1$  results of [12]<sup>11</sup> ( $E_{\hat{S}} < 0.923 \times E_S$ ) are lower than the ones obtained here, while still being well above the results for  $N = 2$ .

$N_S$	CPU time [h]	$E_{\hat{S},YM} \left[ \frac{4\pi v}{g} \right]$	$E_{\hat{S},Hkin} \left[ \frac{4\pi v}{g} \right]$	$E_{\hat{S}} \left[ \frac{4\pi v}{g} \right]$	$E_{\hat{S}} / E_S$
200	2.0	0.800	0.836	1.637	<b>1.062</b>
500	7.0	0.797	0.835	1.632	<b>1.059</b>
1000	9.0	0.779	0.835	1.614	<b>1.048</b>
1800	16.5	0.785	0.830	1.614	<b>1.048</b>
2500	34.5	0.788	0.833	1.620	<b>1.051</b>
4000	48.0	0.774	0.829	1.603	<b>1.040</b>
13000	116.5	0.771	0.830	1.600	<b>1.038</b>

Table 5.2:  $N = 1$  approximation of  $E_{\hat{S}}$  ( $\lambda = 0$ ) for increasing number of steps per temperature  $N_S$ , with  $E_S$  defined by (6.7)

<sup>11</sup>The Yang-Mills energy of the parameters given by [12] was verified to be  $0.75 \left[ \frac{4\pi v}{g} \right]$ , the kinetic Higgs energy however could not be reconstructed due to the lack of parameters  $b_i$  and  $e_i$  in the appendix of [12].

From table 5.2 we can identify a seemingly convergent energy value for large  $N_S$ . A rigorous proof of this convergence is however highly non-trivial, if at all possible and far beyond the scope of this thesis.

In addition to the energy minimum we are most interested in the *unique* field configuration associated with it. To check for signs of convergence towards one such configuration, we compare the energy densities of the above  $N = 1$  SA runs in fig. 5.4.

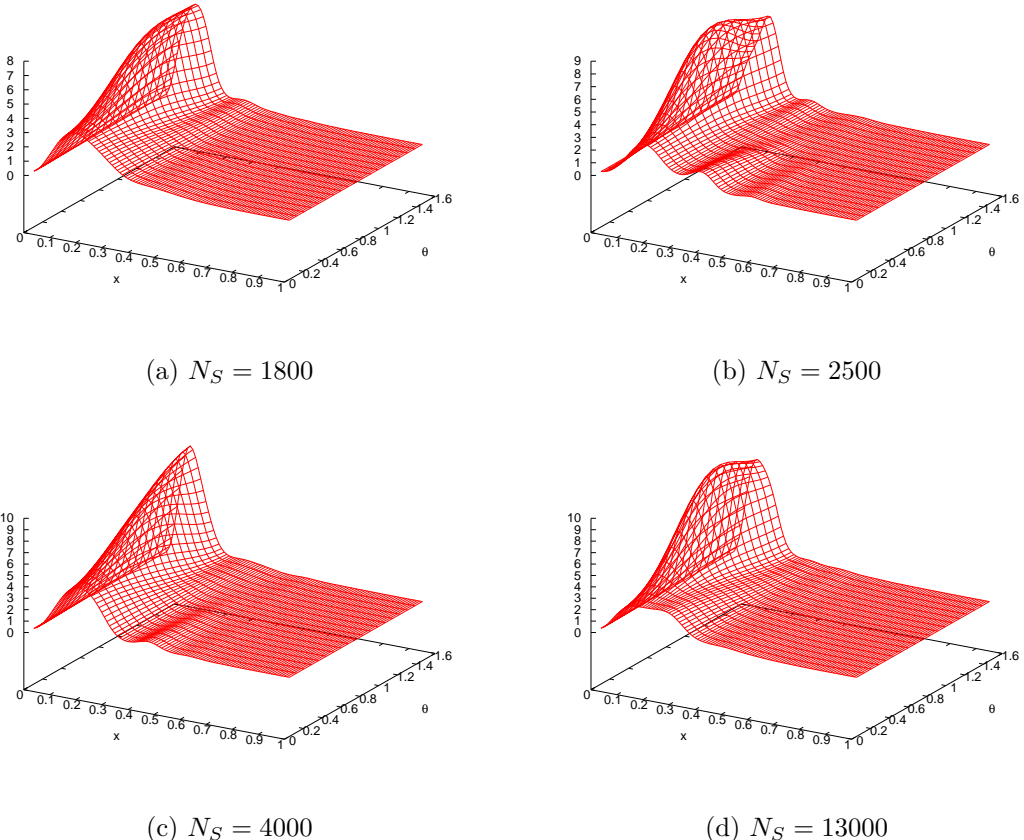
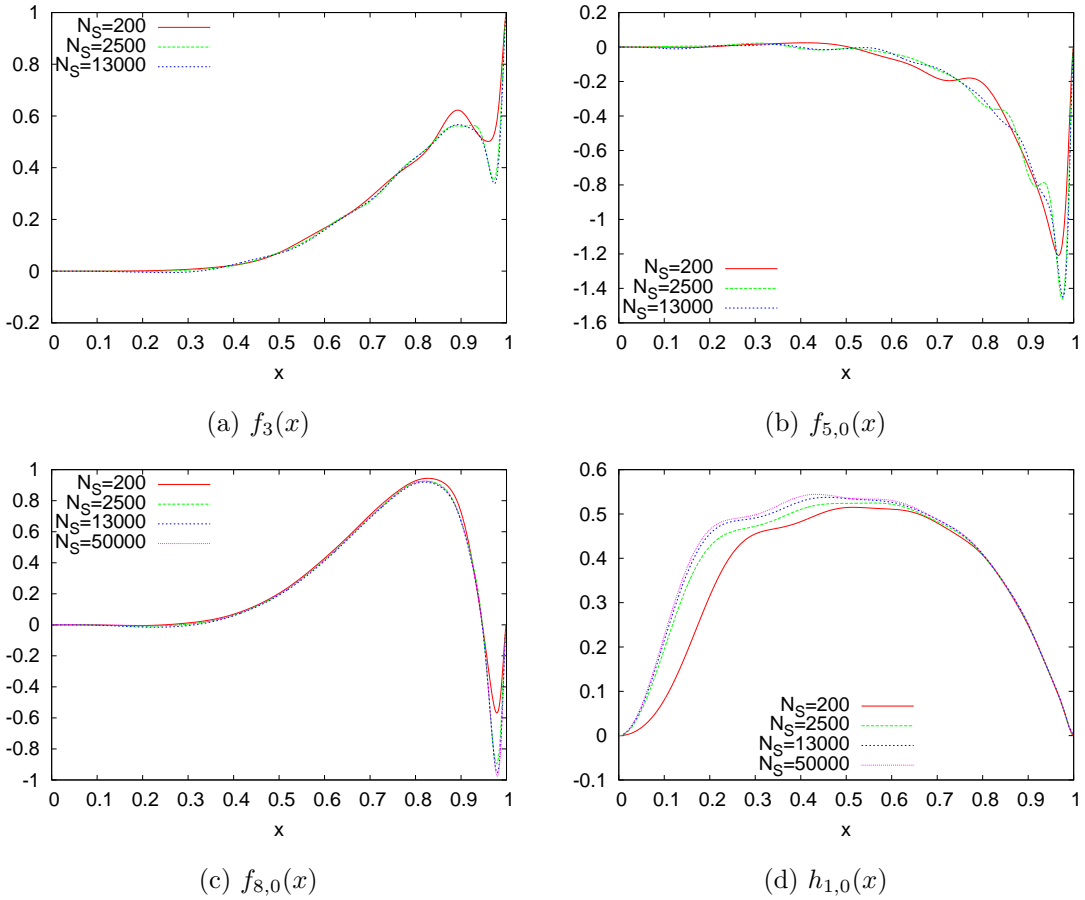


Figure 5.4:  $N = 1$  total energy density approximations for various  $N_S$

Despite their similar energy values, the energy densities of the obtained field configurations still vary noticeably<sup>12</sup>. The behavior of the corresponding profile functions however, of which a selected few are shown in fig. 5.5 for various values of  $N_S$ , clearly suggests convergent behavior for increasing  $N_S$ .

<sup>12</sup>Fig. 5.4c, for example, displays a significant deviation from the other densities


 Figure 5.5: Selected  $N = 1$  profile function approximations for various  $N_S$ 

### 5.2.2 $N = 2$ Legendre expansion

Analogous to  $N = 1$ , the expansion to second order involves varying the expansion coefficients of 30 profile functions (477 coefficients in total). SA programs, using the following parameters

Grid size in x:	1000
Steps per temperature ( $N_S$ ):	200 – 1800
Initial temperature:	1.9
Final temperature:	$3.0 \times 10^{-9}$
Temperature reduction factor ( $\chi$ ):	0.85

result in a further improvement of the upper energy bound to

$$E_{\hat{S}} < 1.369 \left[ \frac{4\pi v}{g} \right] = 0.888 \times E_S. \quad (5.26)$$

The results for varying number of steps per temperature are shown in table 5.3, their energy densities in fig. 5.6.

$N_S$	CPU time [h]	$E_{\hat{S},YM} \left[ \frac{4\pi v}{g} \right]$	$E_{\hat{S},Hkin} \left[ \frac{4\pi v}{g} \right]$	$E_{\hat{S}} \left[ \frac{4\pi v}{g} \right]$	$E_{\hat{S}} / E_S$
200	58	0.726	0.682	1.408	<b>0.914</b>
400	118.5	0.707	0.679	1.385	<b>0.899</b>
600	172	0.709	0.670	1.379	<b>0.895</b>
900	259.5	0.714	0.670	1.384	<b>0.898</b>
1200	337.5	0.705	0.663	1.369	<b>0.888</b>
1800	481.5	0.706	0.665	1.371	<b>0.890</b>

Table 5.3:  $N = 2$  approximation of  $E_{\hat{S}}$  ( $\lambda = 0$ ) for increasing number of steps per temperature  $N_S$ , with  $E_S$  defined by (6.7)

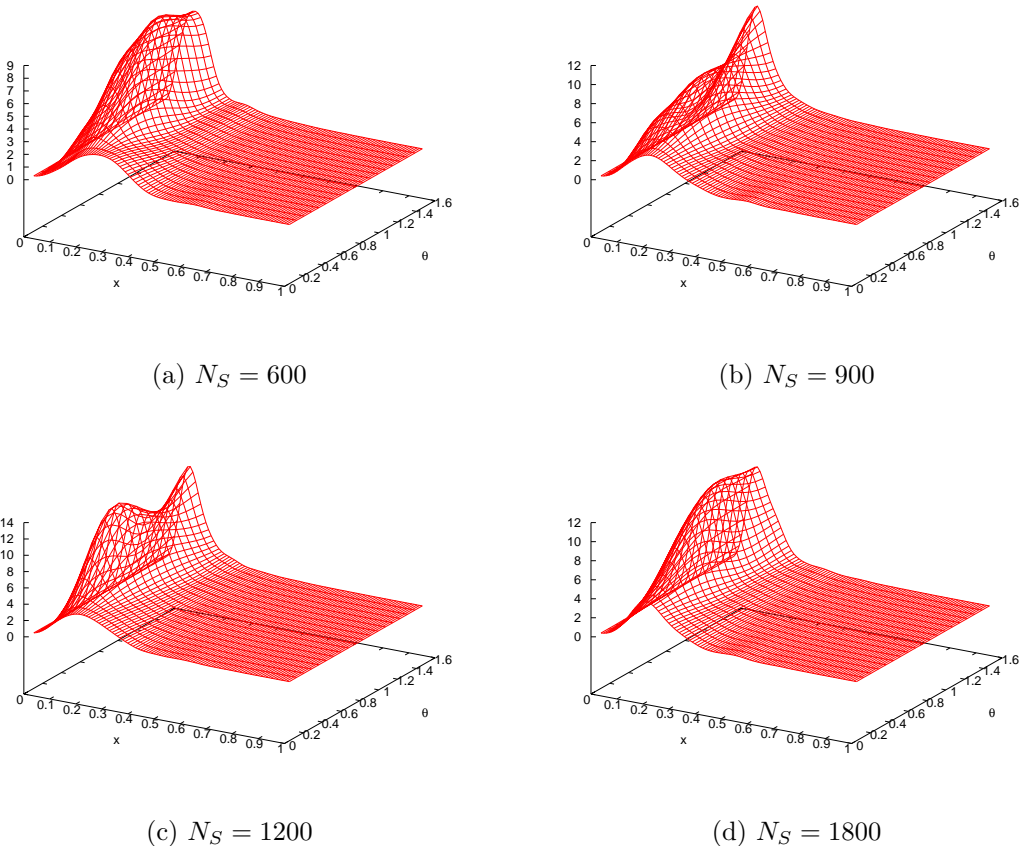
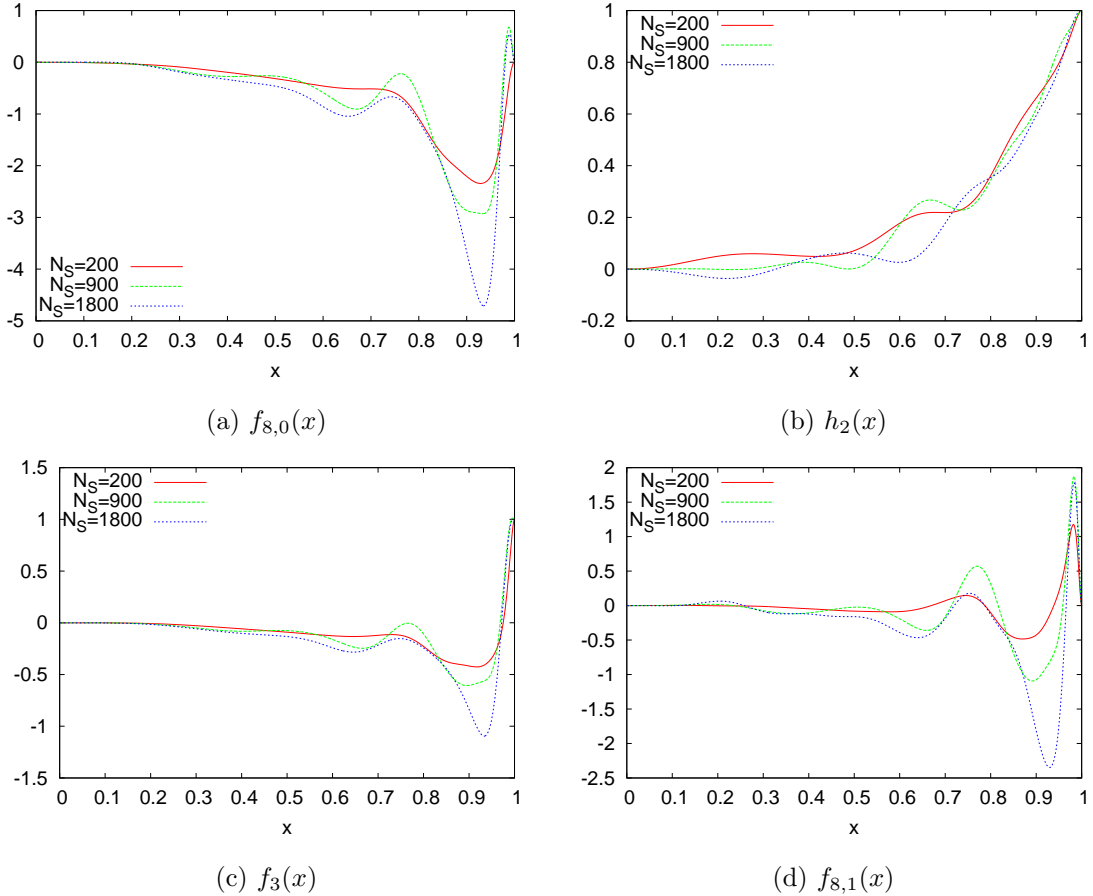


Figure 5.6:  $N = 2$  total energy density approximations for various  $N_S$

Although signs of convergence are still somewhat apparent from most profile functions (a selected few are presented in fig. 5.7), it becomes clear, that  $N_S$  is too low to obtain satisfactory approximations of the field configuration at  $N = 2$ . The lower quality of the  $N = 2$  approximation, as compared to  $N = 1$ , can also be identified by the many

Figure 5.7: Selected  $N = 2$  profile function approximations for various  $N_S$ 

polynomial wiggles, which are unlikely to be physical.

In light of the significant drop in energy from  $N = 1$  to  $N = 2$  however, the well converged configuration, obtained from  $N = 1$ , is, nevertheless, still far from the actual sphaleron configuration.

Figures of profile functions and energy densities, as well as expansion coefficients for  $N = 2$  are available in Appendix E.3.

### 5.2.3 $N = 3$ Legendre expansion

Expanding to third order involves varying the expansion coefficients of 41 profile functions (659 coefficients in total). SA programs, using the parameters

Grid size in x:	1000
Steps per temperature ( $N_S$ ):	200 – 1000
Initial temperature:	2.2
Final temperature:	$3.0 \times 10^{-9}$
Temperature reduction factor ( $\chi$ ):	0.85

have however not led to an improved energy bound (see table 5.4).

$N_S$	CPU time [h]	$E_{\hat{S},YM} \left[ \frac{4\pi v}{g} \right]$	$E_{\hat{S},Hkin} \left[ \frac{4\pi v}{g} \right]$	$E_{\hat{S}} \left[ \frac{4\pi v}{g} \right]$	$E_{\hat{S}} / E_S$
200	122	0.762	0.690	1.451	<b>0.942</b>
300	185.5	0.735	0.694	1.429	<b>0.928</b>
400	234.5	0.728	0.685	1.413	<b>0.917</b>
600	363.5	0.715	0.682	1.397	<b>0.906</b>
800	494	0.716	0.681	1.396	<b>0.906</b>
1000	609	0.722	0.680	1.402	<b>0.910</b>

Table 5.4:  $N = 3$  approximation of  $E_{\hat{S}}$  ( $\lambda = 0$ ) for increasing number of steps per temperature  $N_S$ , with  $E_S$  defined by (6.7)

Since  $N = 2$  is obtained from  $N = 3$ , for vanishing third order coefficients, it is apparent, that this is the result of insufficient run time. Clearly, the  $N = 3$  results should at least approach, if not surpass those of  $N = 2$  for large  $N_S$ . For the number of steps per temperature used here however, the rapidly growing dimension of our coefficient space, as well as the increasingly complex energy functionals of each additional order, pose a serious problem at this point.

Furthermore, the respective energy densities, shown in fig. 5.8, as well as the profile functions, have stopped showing any signs of convergence. We have therefore reached the computational limit for improving the  $E_{\hat{S}}$  energy bound, given the numerical methods used in this thesis, as well as the available computing power.

As a result, the following section employs  $N = 2$  angular expansion.

Profile functions, as well as energy densities for  $N = 3$  are available in Appendix E.4.

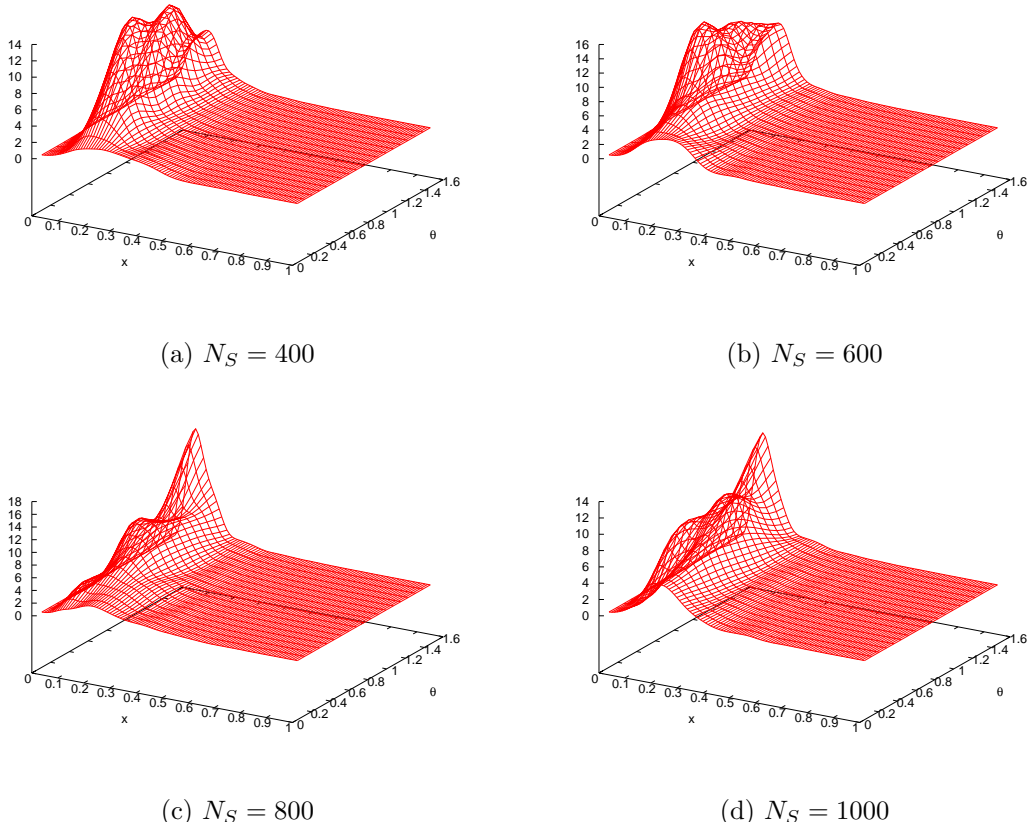


Figure 5.8:  $N = 3$  total energy density approximations for various  $N_S$

### 5.3 Energy of configurations between vacuum and sphaleron

In the following, we minimize the generalized energy functional for several values of  $\psi$ , to obtain the approximate shape of the  $\hat{S}$  energy barrier.

The energy density and profile function boundary conditions, that lead to a smooth transition from vacuum to the generalized  $\hat{S}$ , whose energy has been approximated in the previous section, have been established in chapter 3.4. They possess the required property of exactly reducing to the energy density and profile function boundary conditions of the thus far employed generalized *Ansatz* of [1], for  $\psi = \pi$ .

Minimizing for various values of  $\mu$  leads to no additional insights, as the energy is independent of  $\mu$  at  $\psi = \pi$  and  $\mu$  does not parameterize a NCL. Furthermore, minimizing over a 20x20 grid would lead to 400 programs running for several weeks, far exceeding the available computational capacities. The parameter has hence been fixed to  $\mu = \pi$ , resulting in the energy functional of lowest energy.

We now proceed to adjust the previously used profile function expansions to account for the generalization of boundary conditions and define

$$\alpha_i(x, \theta) = f_i(x) \left( \lim_{r \rightarrow \infty} \alpha_i(r, \theta) \right) + \sum_{n=0}^{N-1} f_{i,2n}(x) P_{2n}(\cos \theta) \begin{cases} \sin^2 \theta & \text{for } i = 6, 7, 9, \dots, 16, \\ \sin^3 \theta & \text{for } i = 1, 2, 8, \\ \sin^4 \theta & \text{for } i = 3, 4, 5, \end{cases} \quad (5.27)$$

$$\beta_j(x, \theta) = h_j(x) \left( \lim_{r \rightarrow \infty} \beta_j(r, \theta) \right) + \sum_{n=0}^{N-1} h_{j,2n}(x) P_{2n}(\cos \theta) \begin{cases} \sin^2 \theta & \text{for } j = 1, \\ \sin^3 \theta & \text{for } j = 2, 3, \end{cases} \quad (5.28)$$

with 0th order profile functions  $f_j(x)$  and  $h_j(x)$ :

$$f_j(x) = x^4 \sum_{i=0}^{17} a_{j,2i} P_{2i}(x), \quad \text{for } j = 1, \dots, 16, \quad (5.29)$$

$$h_j(x) = x^2 \sum_{i=0}^{12} b_{j,2i} P_{2i}(x), \quad \text{for } j = 1, 2, 3, \quad (5.30)$$

as well as n-th order profile functions  $f_{k,n}(x)$  and  $h_{k,n}(x)$  for  $n \geq 1$ :

$$f_{k,n}(x) = x^4 (x^2 - 1) \sum_{i=0}^{19} d_{k,n,2i} P_{2i}(x), \quad \text{for } k = 1, \dots, 5, \quad (5.31)$$

$$f_{k,n}(x) = x^4 (x^2 - 1) \sum_{i=0}^{17} d_{k,n,2i} P_{2i}(x), \quad \text{for } k = 6, \dots, 16, \quad (5.32)$$

$$h_{k,n}(x) = x^2 (x^2 - 1) \sum_{i=0}^{12} e_{k,n,2i} P_{2i}(x), \quad \text{for } k = 1, 2, 3. \quad (5.33)$$

The boundary conditions  $\lim_{r \rightarrow \infty} \alpha_i(r, \theta)$  are given by (3.34) through (3.49),  $\lim_{r \rightarrow \infty} \beta_j(r, \theta)$  is given by (3.51) through (3.53).

Boundary conditions of profile functions  $f$  and  $h$  coincide with those of chapter 5.2 and are handled identically in practice.

One can now easily check, that (5.27) and (5.28) reduce to (5.9) and (5.10) for  $\psi = \pi$ .

Due to the extent of the generalized energy density, the preliminary analytical integration over  $\theta$  is no longer feasible and must be done numerically on every SA function evaluation, dramatically increasing the programs run time. Nevertheless, using a 20 point  $\theta$ -grid and 300 steps per temperature for each of the 1243 parameters, acceptable results, with very little random deviation have been achieved with run times just short of 1 month. Far worse than the entailed run time issues however, is losing the option to analytically verify the obtained results in the previous manner. As a result, we can no longer rigorously exclude the possibility of slowly diverging integrals over  $x$  and  $\theta$ .

Figs. 5.9 and 5.10 show the results, obtained from 26 SA programs of various  $\psi \in [0, \pi]$ , for  $N = 1$  and  $N = 2$ , respectively, using the following SA parameters

Grid size in x:	1000
Grid size in $\theta$ :	20
Steps per temperature ( $N_S$ ):	300
Initial temperature:	2.0
Final temperature:	$3.0 \times 10^{-9}$
Temperature reduction factor ( $\chi$ ):	0.85

The results have been mirrored on  $\psi = \pi$ , utilizing the parity properties of the energy functional

$$E(\psi) = E(2\pi - \psi). \quad (5.34)$$

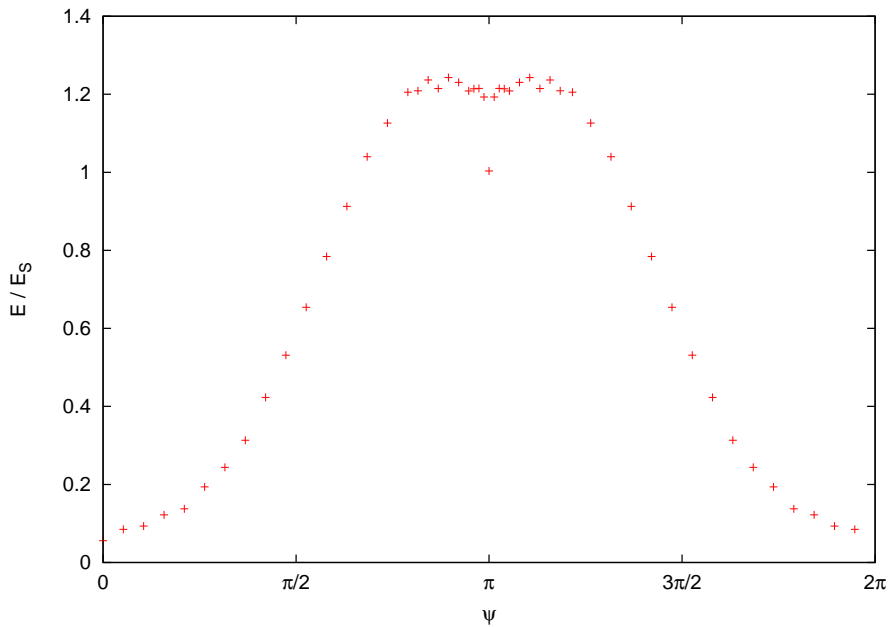


Figure 5.9:  $N = 1$  approximation of the  $\hat{S}$  NCL structure

Surprisingly, the NCL structure is not sphere-like. In fact it displays a local minimum at  $\psi = \pi$ , the possible physical implications of which are discussed in chapter 7. This contrasts with the SU(2) sphaleron S, which clearly displays a sphere-like structure (see fig. 5.11).

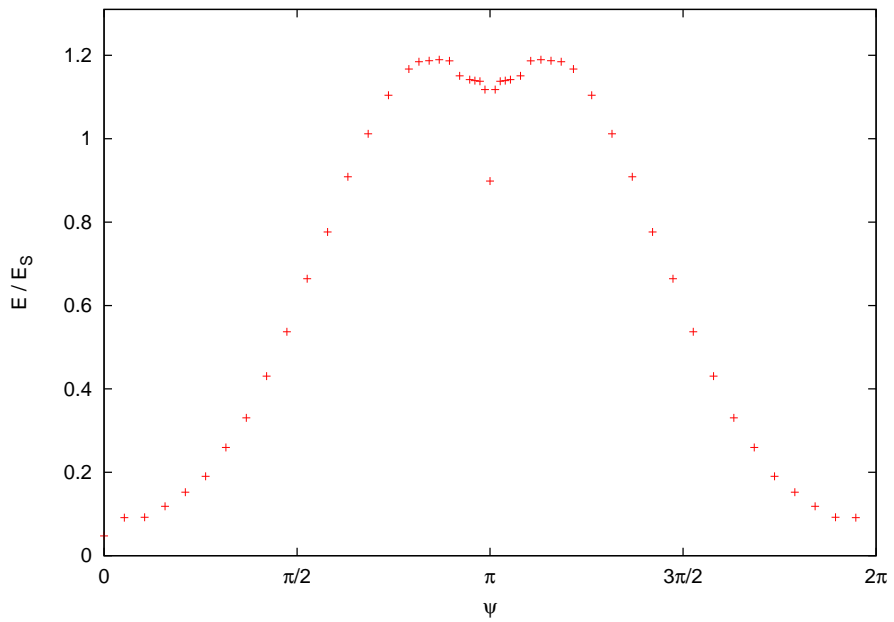
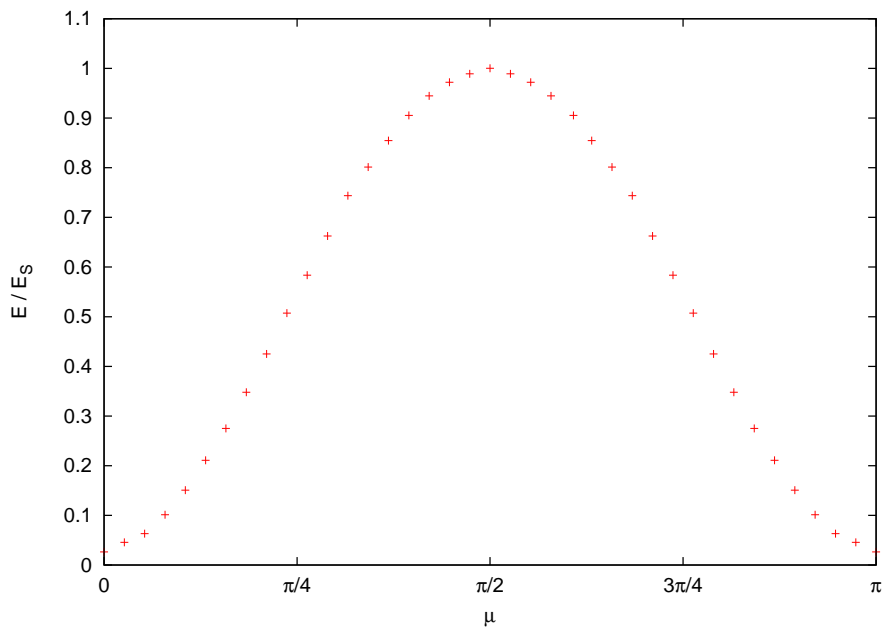
Figure 5.10:  $N = 2$  approximation of the  $\hat{S}$  NCL structure

Figure 5.11: Approximation of the S sphaleron NCL structure

## 5.4 Minimization with non-zero Higgs self-coupling

To avoid loss of generality by introducing numerical values of physical constants, the Higgs self-coupling  $\lambda$  has been set to vanish in the previous chapters. Since this is a very poor approximation, especially at low energies, it becomes essential to determine the sphaleron energy for non-zero values of  $\lambda$ .

The running Higgs self-coupling is, as of recently, well known for energies around the Higgs mass:

$$\lambda_0 = \frac{m_H^2}{2v^2} = 0.13075 \pm 0.00085, \quad (5.35)$$

with constants  $m_H = 125.9 \pm 0.4$  GeV and  $v = 246.21965$  GeV with negligible error taken from [21] and [22] respectively.

The Standard Model Higgs self-coupling  $\lambda(\mu)$  at higher energies  $\mu$ , for which all Yukawa couplings except  $y_{top}$  are negligible, has been evaluated up to three-loop in papers such as [23]. Unfortunately however, the energy range of interest for QCD sphaleron processes is far below  $m_H$ , namely of the order of 100 MeV, where perturbation theory collapses.

This being the case, we have no reliable value for  $\lambda(100$  MeV) and will therefore minimize the energy functional for several arbitrary, somewhat evenly spaced values, in order to gain a crude insight into the energy behavior for varying  $\lambda$ .

In the following, we approximate the minimum of the  $N = 2$  energy functional, with  $e_{Hpot}$  (see eq. (B.19)) incorporated, using the following SA parameters

Grid size in x:	1000
Steps per temperature ( $N_S$ ):	400
Initial temperature:	2.0
Final temperature:	$3.0 \times 10^{-9}$
Temperature reduction factor ( $\chi$ ):	0.85

Due to run time issues, we are restricted to very few values of  $\lambda$ , for which the results depicted in table 5.5 are obtained.

$\lambda$	$\hat{E}_{\hat{S}} \left[ \frac{4\pi v}{g} \right]$	$E_S \left[ \frac{4\pi v}{g} \right]$	$\hat{E}_{\hat{S}} / E_S$
0	1.369	1.541	<b>0.888</b>
0.001	1.435	1.741	<b>0.824</b>
0.01	1.466	1.852	<b>0.792</b>
0.05	1.495	2.013	<b>0.743</b>
0.131	1.515	2.160	<b>0.701</b>
0.3	1.541	2.226	<b>0.692</b>
0.5	1.548	2.305	<b>0.672</b>
1	1.582	2.389	<b>0.662</b>
10	1.683	2.696	<b>0.624</b>
100	2.503	4.631	<b>0.540</b>

Table 5.5:  $N = 2$  approximation of  $E_{\hat{S}}$  for various  $\lambda$ 

The corresponding coefficients are included on the enclosed CD, as they are too lengthly for the appendix.

## 6 $SU(2)$ sphaleron $S$

In previous chapters the energy of the  $SU(2)$  sphaleron  $S$  has served as a frame of reference. All energy values for the sphaleron  $\hat{S}$  are given as a quotient  $E_{\hat{S}}/E_S$ <sup>1</sup>, for which it is clearly necessary to evaluate  $E_S$ . This will be done in the following.

### 6.1 Topology and sphaleron *Ansatz*

As done in [3, 10] and similar to  $\hat{S}$ , we introduce a topologically nontrivial map  $S^1 \wedge S_\infty^2 \rightarrow SU(2)$ , with parameter  $\mu \in [0, \pi]$  and coordinates  $\theta \in [0, \pi]$  and  $\phi \in [0, 2\pi]$ .

The following map is a generator of  $\pi_3[SU(2)] = \mathbb{Z}$ :

$$U(\mu, \theta, \phi) = \begin{pmatrix} (\cos \mu - i \cos \theta \sin \mu)e^{i\mu} & \sin \mu \sin \theta e^{i\phi} \\ -\sin \mu \sin \theta e^{-i\phi} & (\cos \mu + i \cos \theta \sin \mu)e^{-i\mu} \end{pmatrix}. \quad (6.1)$$

As before, the sphaleron is located atop the non contractible manifold:  $\mu = \pi/2$ .

We obtain

$$\begin{aligned} W(\theta, \phi) &= U(\mu, \theta, \phi) \Big|_{\mu=\pi/2} \\ &= \begin{pmatrix} \cos \theta & \sin \theta (\cos \phi + i \sin \phi) \\ \sin \theta (-\cos \phi + i \sin \phi) & \cos \theta \end{pmatrix} \end{aligned} \quad (6.2)$$

and with it the  $SU(2)$  gauge field and Higgs field

$$gA_\mu(r, \theta, \phi) = -f(r)\partial_\mu W(\theta, \phi)W^{-1}(\theta, \phi), \quad (6.3)$$

$$\phi(r, \theta, \phi) = h(r)\eta W(\theta, \phi) \begin{pmatrix} 0 \\ 1 \end{pmatrix}, \quad (6.4)$$

with boundary conditions

$$f(0) = h(0) = 0, \quad \lim_{r \rightarrow \infty} f(r) = \lim_{r \rightarrow \infty} h(r) = 1. \quad (6.5)$$

---

<sup>1</sup>Keeping in mind, that the values of the quotients are given for equivalent couplings  $g_w$  and  $g_s$ , which is clearly not physical.

The resulting energy functional

$$E = 4\pi \int_0^1 dx \left\{ 4(x-1)^2 f'^2 + \frac{8}{x^2} (f(1-f))^2 + \frac{1}{2} x^2 h'^2 + \frac{1}{(x-1)^2} (h(1-f))^2 + \frac{\lambda}{4} \frac{x^2}{(x-1)^4} (h^2 - 1)^2 \right\}, \quad (6.6)$$

is minimized, using the semi-analytical Simulated Annealing method of chapter 5. For large numbers of steps per temperature  $N_S$ ,  $E_S$  converges to the following value:

$$E_S = 1.542 \left[ \frac{4\pi v}{g} \right]. \quad (6.7)$$

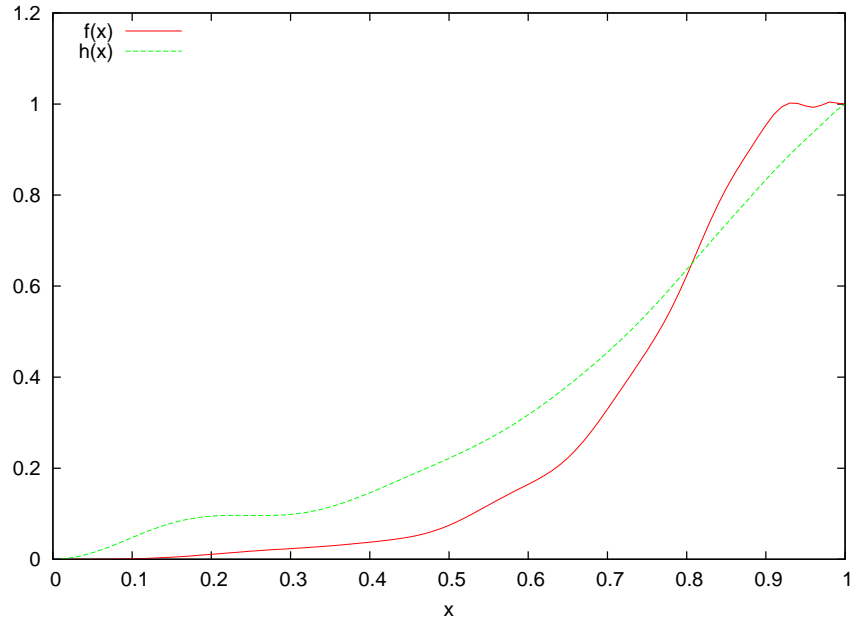


Figure 6.1: SA approximation of profile functions  $f(x)$  and  $h(x)$  for the  $SU(2)$  sphaleron  $S$  with  $\lambda = 0$

## 6.2 Generalized *Ansatz*

To obtain a better understanding of the structure of the  $SU(2)$  sphaleron  $S$ , let us generalize the preceding *Ansatz* in a fashion similar to the generalization, that [1] uses for the sphaleron  $\hat{S}$  (see chapter 3.3).

Introducing the following set of matrices:

$$\begin{aligned} S_\phi &= -\sin \phi(-i\sigma_1) + \cos \phi(-i\sigma_2), \\ S_\rho &= \cos \phi(-i\sigma_1) + \sin \phi(-i\sigma_2), \\ S_3 &= -i\sigma_3, \end{aligned} \tag{6.8}$$

with the Pauli matrices  $\sigma_i$

$$\sigma_1 = \begin{pmatrix} 0 & 1 \\ 1 & 0 \end{pmatrix}, \quad \sigma_2 = \begin{pmatrix} 0 & -i \\ i & 0 \end{pmatrix}, \quad \sigma_3 = \begin{pmatrix} 1 & 0 \\ 0 & -1 \end{pmatrix}, \tag{6.9}$$

we construct the following  $SU(2)$  gauge field *Ansatz* in the radial gauge:

$$\begin{aligned} gA_0(r, \theta, \phi) &= 0, \\ gA_\theta(r, \theta, \phi) &= -\alpha_1(r, \theta)S_\phi, \\ gA_\phi(r, \theta, \phi) &= -\alpha_2(r, \theta)\cos\theta S_\rho - \alpha_3(r, \theta)S_3, \\ gA_r(r, \theta, \phi) &= 0. \end{aligned} \tag{6.10}$$

The following boundaries towards infinity apply:

$$\lim_{r \rightarrow \infty} \begin{pmatrix} \alpha_1(r, \theta) \\ \alpha_2(r, \theta) \\ \alpha_3(r, \theta) \end{pmatrix} = \begin{pmatrix} 1 \\ -\sin\theta \\ \sin^2\theta \end{pmatrix}. \tag{6.11}$$

Similarly, we construct the Higgs field *Ansatz*:

$$\Phi(r, \theta, \phi) = \eta [\beta_1(r, \theta)\cos\theta \mathbf{I}_2 + \beta_2(r, \theta)S_\phi] \begin{pmatrix} 0 \\ 1 \end{pmatrix}, \tag{6.12}$$

with the following boundaries towards infinity:

$$\lim_{r \rightarrow \infty} \begin{pmatrix} \beta_1(r, \theta) \\ \beta_2(r, \theta) \end{pmatrix} = \begin{pmatrix} 1 \\ \sin\theta \end{pmatrix}. \tag{6.13}$$

This results in the following energy densities:

$$e_{YM} = \frac{1}{g^2 r^4 \sin^2 \theta} \left\{ \alpha_1^2 \left( 2(1 - 2\alpha_3)^2 + 8\alpha_2^2 \cos^2 \theta \right) + 2\alpha_2^2 \sin^2 \theta - 2\alpha_2 \sin(2\theta) \partial_\theta \alpha_2 \right. \\ \left. + 4\alpha_1 \left( (-1 + 2\alpha_2 \sin \theta - \cos \theta \partial_\theta \alpha_2) + 2\alpha_2 \cos \theta \partial_\theta \alpha_3 \right) \right. \\ \left. + (\partial_\theta \alpha_2)^2 + 2(\partial_\theta \alpha_3)^2 + \cos(2\theta) \partial_\theta \alpha_2 \right\} \quad (6.14)$$

$$+ \frac{1}{g^2 r^2 \sin^2 \theta} \left\{ (\partial_r \alpha_1)^2 + (\partial_r \alpha_2)^2 + 2(\partial_r \alpha_3)^2 + \cos(2\theta) \left( (\partial_r \alpha_2)^2 - (\partial_r \alpha_1)^2 \right) \right\}, \\ e_{Hkin} = \frac{\eta^2}{8r^2 \sin^2 \theta} \left\{ \beta_1^2 \left( 8(\beta_3^2 \cos^2 \theta + \alpha_2^2 \cos^4 \theta + \sin^4 \theta) + 2\alpha_1^2 \sin^2(2\theta) \right) \right. \\ \left. + 8\beta_1 \left( 2\alpha_2 \beta_2 \cos^2 \theta - 2\sin^2 \theta (\cos \theta \sin \theta \partial_\theta \beta_1 + \alpha_1 (\beta_2 \sin \theta + \cos \theta \partial_\theta \beta_2)) \right) \right. \\ \left. + 8 \left( \beta_2^2 (1 + (\alpha_3 - 2)\alpha_3 + \alpha_2^2 \cos^2 \theta + \alpha_1^2 \sin^2 \theta) + \alpha_1 \beta_2 \sin \theta \sin(2\theta) \partial_\theta \beta_1 \right. \right. \\ \left. \left. + \sin^2 \theta ((\partial_\theta \beta_2)^2 + \cos^2 \theta (\partial_\theta \beta_1)^2) \right) \right\} \\ + \eta^2 \left\{ \cos^2 \theta (\partial_r \beta_1)^2 + (\partial_r \beta_2)^2 \right\}, \quad (6.15)$$

$$e_{Hpot} = \lambda \eta^4 [\beta_2^2 + \beta_1^2 \cos^2 \theta - 1]^2. \quad (6.16)$$

We now turn to approximating the minimum of the corresponding energy functional. Angular dependency is introduced with an *Ansatz* similar to (5.8)

$$\alpha_1(x, \theta) = \tilde{\alpha}_i(x, \theta), \\ \alpha_2(x, \theta) = -\sin \theta \tilde{\alpha}_i(x, \theta), \\ \alpha_3(x, \theta) = \sin^2 \theta \tilde{\alpha}_i(x, \theta), \quad (6.17)$$

$$\beta_1(x, \theta) = \tilde{\beta}_i(x, \theta), \\ \beta_i(x, \theta) = \sin \theta \tilde{\beta}_i(x, \theta),$$

$$\tilde{\alpha}_i(x, \theta) = f_i(x) + \sin^2 \theta \sum_{n=0}^{N-1} f_{i,2n}(x) P_{2n}(\cos \theta), \quad (6.18)$$

$$\tilde{\beta}_j(x, \theta) = h_j(x) + \sin^2 \theta \sum_{n=0}^{N-1} h_{j,2n}(x) P_{2n}(\cos \theta). \quad (6.19)$$

The profile functions  $f_i(x)$ ,  $h_i(x)$ ,  $f_{i,2n}(x)$  and  $h_{i,2n}(x)$  are identical to (5.11) through (5.15).

Since  $N = 0$  introduces no angular dependency the minimum of the energy functional is evaluated for  $N = 1$  using Simulated Annealing. As expected, the introduction of angular dependency does not lower the energy bound for

$$E_S = 1.541 \left[ \frac{4\pi v}{g} \right]. \quad (6.20)$$

Fig. 6.3 shows the extremely low amplitude of the profile functions correlated to the introduction of angular dependence. This further demonstrates, that the lowest energy configuration has no angular dependence and can be constructed with (6.3) and (6.4).

Additional figures of functions  $\alpha(x, \theta)$  and  $\beta(x, \theta)$ , as well as energy densities  $e_{YM}$  and  $e_{Hkin}$  are shown in Appendix G.

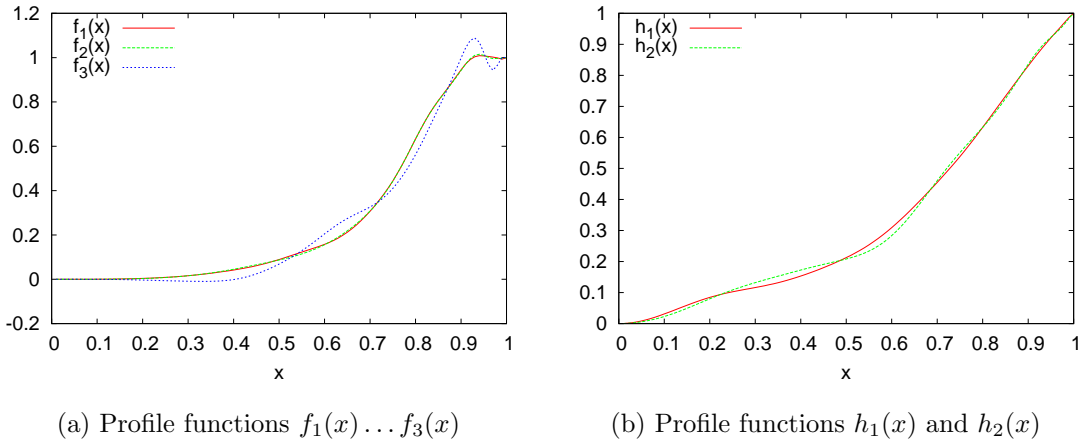


Figure 6.2: 0th order profile functions for the  $SU(2)$  sphaleron  $S$

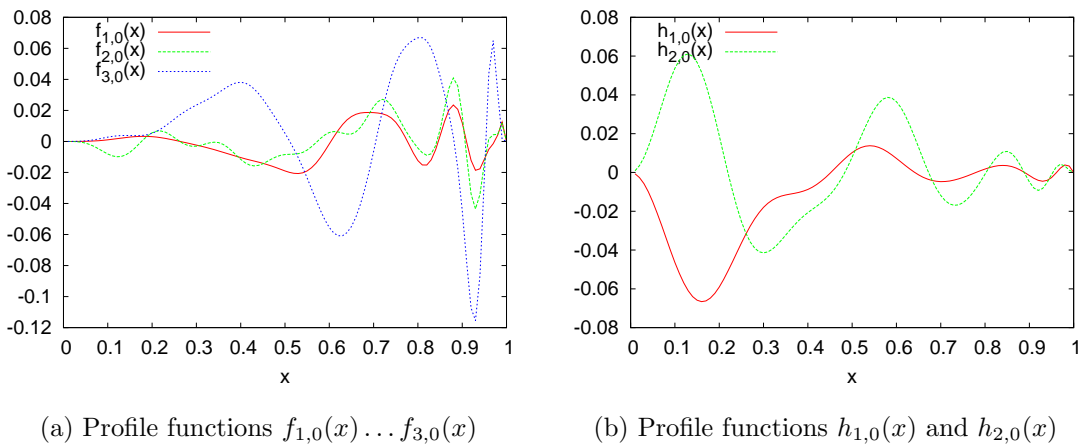


Figure 6.3: 1st order profile functions for the  $SU(2)$  sphaleron  $S$

## 7 Conclusion

We have applied Simulated Annealing to approximate energy and field structure of the  $\hat{S}$  sphaleron. In conjunction with this, it was possible to analytically show the regularity of the obtained approximating configurations. The seeming convergence of the generating profile functions suggests the existence of a finite, non-vanishing solution of Yang-Mills-Higgs theory. Nevertheless, the actual convergence and existence of a solution cannot be rigorously proven by the mere numerical analysis conducted here.

The dependability of conclusions, derived from the obtained results, is limited by several factors. First, we have absolutely no notion of the underlying structure and the local minima, to which the programs have annealed, could very well be far from the global minimum. Second, all expansions, be it to approximate radial or angular components of the fields, are only to finite order ( $N \rightarrow \infty$  might not be smooth). Third, the expansion bases are, strictly speaking, incomplete, as they have been modified to ensure convergence of the energy functional (see also remarks in chapter 5).

The quality of approximations of the sphaleron field configuration is strongly limited by computational capacities. It seems likely though, that calculations, based on third or higher order angular expansion and greatly increased run times, would lead to very good results.

Far more crucial, than determining a good value of  $E_{\hat{S}}$  however, is the conducted analysis of the energy barrier structure. By minimizing a more general *Ansatz* for various points on the NCL, it was possible to reveal a dip in the energy barrier. Naturally, the obtained NCL structure is subject to the same error sources and is by no means proven here.

Physically this opens up the possibility of a non-trivial, meta-stable solution of SU(3) Yang-Mills-Higgs theory, for which the term sphaleron (meaning “ready to fall”, reflecting on its instability) would certainly no longer be appropriate. Perhaps, the SU(3) gauge fields of the solution contribute to glueball states of QCD [25].

## References

- [1] F.R. Klinkhamer and C. Rupp, *A sphaleron for the non-Abelian anomaly*, Nucl. Phys. B709 (2005) 171 [hep-th/0410195].
- [2] M. Nakahara, *Geometry, Topology and Physics*, Institute of Physics Publishing, Bristol, 1990.
- [3] F.R. Klinkhamer and N.S. Manton, *A saddle point solution in the Weinberg-Salam theory*, Phys. Rev. D30 (1984) 2212.
- [4] M. Atiyah, I.M. Singer, *The index of elliptic operators I,III,IV*, Ann. Math. 87 (1968) 484; 87 (1968) 546; 93 (1971) 119.
- [5] F.R. Klinkhamer and C. Rupp, *Sphalerons, spectral flow and anomalies*, J. Math. Phys., 44, No. 8 (2003) [hep-th/0304167].
- [6] S.L. Adler, *Axial vector vertex in spinor electrodynamics*, Phys. Rev. 177 (1969) 2426.
- [7] J.S. Bell, R. Jackiw, *A PCAC puzzle:  $\pi^0 \rightarrow \gamma\gamma$  in the sigma model*, Nuovo Cim. A 60 (1969) 47.
- [8] E. Witten, *An  $SU(2)$  anomaly*, Phys. Lett. B 117 (1982) 324.
- [9] W.A. Bardeen, *Anomalous Ward identities in spinor field theories*, Phys. Rev. 184 (1969) 95.
- [10] N.S. Manton, *Topology in the Weinberg-Salam theory*, Phys. Rev. D28 (1983) 2019.
- [11] F.R. Klinkhamer, *Construction of a new electroweak sphaleron*, Nucl. Phys. B 410 (1993) 343 [hep-ph/9306295].
- [12] M. Haberichter, *Untersuchungen des  $SU(3)$  Sphalerons*, Dipl. thesis ITP KIT (2009).
- [13] A.G. Abanov, *Homotopy groups used in physics*, Lecture notes on topological terms in condensed matter physics (PHY 680), Stony Brook University (NY, USA), (2009).
- [14] R.S. Palais, *The principle of symmetric criticality*, Commun. Math. Phys. 69 (1979) 19.
- [15] S. Kirkpatrick, C. D. Gelatt Jr., M. P. Vecchi, *Optimization by Simulated Annealing*, Science 220 (4598): 671-680 (1983).
- [16] N. Metropolis, A. W. Rosenbluth, N. Marshall, A. H. Teller, E. Teller, *Equation of State Calculations by Fast Computing Machines*, The Journal of Chemical Physics 21 (6): 1087 (1953).

## REFERENCES

---

- [17] W.H. Press, S.A. Teukolsky, W.T. Vetterling, B.P. Flannery, *Numerical Recipes*, Cambridge University Press, Cambridge, 2007.
- [18] L.H. Ryder, *Quantum Field Theory - 2nd edition*, Cambridge University Press, Cambridge, 1996.
- [19] M.A. Cohen, C.O. Tan, *A Polynomial Approximation for Arbitrary Functions*, arXiv:1108.0608v2[math.NA], 2012.
- [20] H. Aoyama, H. Goldberg, *Anomalous Baryon Number Nonconservation in pp Collisions at 40 TeV*, Phys. Lett. B, Vol. 188, no. 4: 506, 1987.
- [21] J. Beringer et al. (Particle Data Group), *Review of Particle Physics*, Phys. Rev. D86, 010001 (2012) and 2013 partial update for the 2014 edition.
- [22] P.J. Mohr, B.N. Taylor, D.B. Newell, *CODATA Recommended Values of the Fundamental Physical Constants*, arXiv:1203.5425[physics.atom-ph], 2010.
- [23] A.V. Bednyakov, A.F. Pikelner, V.N. Velizhanin, *Three-loop Higgs self-coupling beta-function in the Standard Model with complex Yukawa matrices*, arXiv:1310.3806[hep-ph], 2013.
- [24] M.S. Volkov, *Computation of the winding number diffusion rate due to the cosmological sphaleron*, arXiv:hep-th/9604054, 1996.
- [25] F.R. Klinkhamer, *Private communication*, December 2013.

## A Energy density of the generalized $\hat{S}$ Ansatz

What follows is the energy density of the generalized *Ansatz*, given by (3.11) and (3.15), with boundary conditions (3.14) and (3.18), as in [1].

Depending on the gauge, an additional gauge fixing term may also contribute.

$$\begin{aligned}
e_{YM} = & \frac{1}{2g^2 r^2 \sin^2 \theta} \left\{ \cos^2 \theta [\partial_r \alpha_1]^2 + [\partial_r \alpha_2]^2 + \cos^2 \theta [\partial_r \alpha_3]^2 + [\partial_r \alpha_4]^2 + [\partial_r \alpha_5]^2 \right\} \\
& + \frac{1}{2g^2 r^2} \left\{ [\partial_r \alpha_6]^2 + [\cos \theta \partial_r \alpha_7]^2 + [\partial_r \alpha_8]^2 \right\} \\
& + \frac{1}{2g^2 r^4 \sin^2 \theta} \left\{ \left[ \alpha_6 - \sin \theta \alpha_1 - \frac{1}{2} \alpha_2 \alpha_8 + \alpha_4 \alpha_6 - \frac{1}{2} \cos^2 \theta \alpha_3 \alpha_7 + \cos \theta \partial_\theta \alpha_1 \right]^2 \right. \\
& + \left[ \cos \theta \alpha_7 + \frac{1}{2} \cos \theta (\alpha_3 \alpha_6 - \alpha_1 \alpha_8 - \sqrt{3} \alpha_5 \alpha_7 - \alpha_4 \alpha_7) - \partial_\theta \alpha_2 \right]^2 \\
& + \left[ 2\alpha_8 + \sin \theta \alpha_3 + \frac{1}{2} \alpha_4 \alpha_8 - \frac{1}{2} \alpha_2 \alpha_6 - \frac{1}{2} \sqrt{3} \alpha_5 \alpha_8 - \frac{1}{2} \cos^2 \theta \alpha_1 \alpha_7 - \cos \theta \partial_\theta \alpha_3 \right]^2 \\
& + \left[ \cos \theta (\alpha_1 \alpha_6 + \frac{1}{2} \alpha_2 \alpha_7 - \frac{1}{2} \alpha_3 \alpha_8) - \partial_\theta \alpha_4 \right]^2 \\
& \left. + \left[ \frac{1}{2} \sqrt{3} \cos \theta (\alpha_3 \alpha_8 + \alpha_2 \alpha_7) - \partial_\theta \alpha_5 \right]^2 \right\}, \tag{A.1}
\end{aligned}$$

$$\begin{aligned}
e_{Hkin} = & \eta^2 \left\{ [\partial_r \beta_1]^2 + \cos^2 \theta [\partial_r \beta_2]^2 + [\partial_r \beta_3]^2 \right\} \\
& + \frac{\eta^2}{r^2} \left\{ \left[ \partial_\theta \beta_1 - \frac{1}{2} \cos \theta (\alpha_7 \beta_3 + \alpha_6 \beta_2) \right]^2 + \left[ \partial_\theta \beta_3 + \frac{1}{2} \cos \theta (\alpha_8 \beta_2 + \alpha_7 \beta_1) \right]^2 \right. \\
& + \left[ \cos \theta \partial_\theta \beta_2 - \sin \theta \beta_2 + \frac{1}{2} (\alpha_6 \beta_1 - \alpha_8 \beta_3) \right]^2 \Big\} \\
& + \frac{\eta^2}{4r^2 \sin^2 \theta} \left\{ \left[ \alpha_4 \beta_1 + \alpha_5 \beta_1 / \sqrt{3} + \cos^2 \theta \alpha_1 \beta_2 + \alpha_2 \beta_3 \right]^2 \right. \\
& + \cos^2 \theta \left[ 2\beta_2 - \alpha_1 \beta_1 + \alpha_4 \beta_2 - \alpha_5 \beta_2 / \sqrt{3} - \alpha_3 \beta_3 \right]^2 \\
& \left. + \left[ 2\beta_3 + \alpha_2 \beta_1 - 2\alpha_5 \beta_3 / \sqrt{3} + \cos^2 \theta \alpha_3 \beta_2 \right]^2 \right\}, \tag{A.2}
\end{aligned}$$

$$e_{Hpot} = \lambda \eta^4 [\beta_1^2 + \cos^2 \theta \beta_2^2 + \beta_3^2 - 1]^2. \tag{A.3}$$

## B Structure functions and general energy density

### B.1 Structure functions

What follows, are the most general structure functions of the generalized *Ansatz* given by (3.22), (3.23) and (3.24).

$$a_\phi(\theta, \phi, \psi, \mu, \alpha) = \frac{1}{2} \sin^3\left(\frac{\psi}{2}\right) \cos\left(\frac{\psi}{2}\right) \sin\left(\frac{\theta}{2}\right) \cos^2\left(\frac{\theta}{2}\right) \left( \cos \mu \left( 8 \sin^4\left(\frac{\psi}{2}\right) \cos(2\theta) + 4 \cos \psi - \cos(2\psi) - 19 \right) - 16 \sin \mu \sin^2\left(\frac{\psi}{2}\right) \sin \theta \cos(\alpha - \phi) \right) \quad (\text{B.1})$$

$$b_\phi(\theta, \phi, \psi, \mu, \alpha) = \frac{1}{32} (\cos \psi - 1) \sin \theta \left( (\cos \psi - 1) \cos \theta + \cos \psi + 1 \right) \left( 8 \sin^4\left(\frac{\psi}{2}\right) \cos(2\theta) + 4 \cos \psi - \cos(2\psi) - 19 \right) - \sin \mu \sin^4\left(\frac{\psi}{2}\right) \sin \psi \sin^3 \theta \csc\left(\frac{\theta}{2}\right) \sin(\alpha - \phi) \quad (\text{B.2})$$

$$c_\phi(\theta, \phi, \psi, \mu, \alpha) = -\frac{1}{2} \sin \psi (\cos \psi - 1) \sin\left(\frac{\theta}{2}\right) \cos^2\left(\frac{\theta}{2}\right) \left( -4 \sin^2 \mu \sin \psi \cos\left(\frac{\theta}{2}\right) \times \sin(2(\alpha - \phi)) + \sin \mu \sin \theta \left( 2 \cos \mu \sin \psi (\cos \psi - 1) \cos\left(\frac{\theta}{2}\right) \sin(\alpha - \phi) + \cos(\alpha - \phi) \left( \sin^2 \psi - 4 \sin^4\left(\frac{\psi}{2}\right) \cos \theta \right) \right) - 4 \cos \mu ((\cos \psi - 1) \cos \theta) + \cos \psi + 1 \right) \quad (\text{B.3})$$

$$d_\phi(\theta, \phi, \psi, \mu, \alpha) = (1 - \cos \psi) \left( \sin\left(\frac{\theta}{2}\right) \cos^3\left(\frac{\theta}{2}\right) \left( \sin^2\left(\frac{\psi}{2}\right) \left( \sin \psi \left( 2 \sin \mu \sin\left(\frac{\theta}{2}\right) \times \sin(\alpha - \phi) ((\cos \psi - 1) \cos \theta + \cos \psi + 1) + \sin(2\mu) \sin \psi \sin \theta \cos(\alpha - \phi) \right) - \cos(2\mu - \psi) - \cos(2\mu + \psi) - 2 \cos(2\mu) - 2 \cos \psi (\cos \theta + 2) + 2 \cos \theta - 8 \right) + 2 \sin^2 \mu \sin^2 \psi \cos(2(\alpha - \phi)) \right) + \sin \theta \right) \quad (\text{B.4})$$

$$e_\phi(\theta, \phi, \psi, \mu, \alpha) = \frac{1}{8} \sin \psi (\cos \psi - 1) \sin\left(\frac{\theta}{2}\right) \cos^2\left(\frac{\theta}{2}\right) \left( \sin \mu \cos(\alpha - \phi) \left( 8 \sin^4\left(\frac{\psi}{2}\right) \cos(2\theta) \right) \right)$$

$$+ 4 \cos \psi - \cos(2\psi) - 19 \Big) + 16 \cos \mu \sin^2 \left( \frac{\psi}{2} \right) \sin \theta \Big) \quad (\text{B.5})$$

$$\begin{aligned} f_\phi(\theta, \phi, \psi, \mu, \alpha) = & \frac{1}{2} \sin \mu \sin^3 \left( \frac{\psi}{2} \right) \cos \left( \frac{\psi}{2} \right) \sin \left( \frac{\theta}{2} \right) \cos^2 \left( \frac{\theta}{2} \right) \sin(\alpha - \phi) \Big( -8 \sin^4 \left( \frac{\psi}{2} \right) \\ & \times \cos(2\theta) - 4 \cos \psi + \cos(2\psi) + 19 \Big) + \sin^4 \left( \frac{\psi}{2} \right) \sin^2 \theta ((\cos \psi - 1) \cos \theta \\ & + \cos \psi + 1) \end{aligned} \quad (\text{B.6})$$

$$\begin{aligned} g_\phi(\theta, \phi, \psi, \mu, \alpha) = & \frac{1}{64} \cos^2 \left( \frac{\theta}{2} \right) \left( 256 \sin(2\mu) \sin^4 \left( \frac{\psi}{2} \right) \cos^2 \left( \frac{\psi}{2} \right) \sin \theta \cos(\alpha - \phi) \right. \\ & - 256 \sin \mu \sin^3 \left( \frac{\psi}{2} \right) \cos \left( \frac{\psi}{2} \right) \sin \left( \frac{\theta}{2} \right) \sin(\alpha - \phi) ((\cos \psi - 1) \cos \theta \\ & + \cos \psi + 1) - \sin^2 \theta \Big( -16 \sin(4\mu) \csc(2\mu) \sin^2 \psi \sin^4 \left( \frac{\psi}{2} \right) \\ & + \cos(4\psi)(1 - 2 \cos \theta) + 4 \cos(3\psi)(4 \cos \theta - 3) \Big) + 2 \cos(\psi)(-46 \cos \theta \\ & - 29 \cos(2\theta) + 14 \cos(3\theta) + 61) + 2 \sin^2 \left( \frac{\theta}{2} \right) (4 \cos(2\psi)(\cos \theta + 7 \cos(2\theta) \\ & - 10) - 5 \cos \theta + 35 \cos(2\theta) - 88) \Big) \end{aligned} \quad (\text{B.7})$$

$$\begin{aligned} h_\phi(\theta, \phi, \psi, \mu, \alpha) = & \frac{1}{8} \sqrt{3} \sin^3 \left( \frac{\psi}{2} \right) \left( 32 \cos \left( \frac{\psi}{2} \right) \sin \left( \frac{\theta}{2} \right) \cos^2 \left( \frac{\theta}{2} \right) \left( \sin \mu \sin(\alpha - \phi) \right. \right. \\ & \times (-(\cos \psi - 1) \cos \theta - \cos \psi - 1) + \sin(2\mu) \sin(\psi) \cos \left( \frac{\theta}{2} \right) \cos(\alpha - \phi) \Big) \\ & + \sin \left( \frac{\psi}{2} \right) \sin^2 \theta (2 \sin^2 \mu (\cos(2\psi) - 2 \sin^2 \psi \cos \theta) + \cos(2\mu) + 7) \Big) \end{aligned} \quad (\text{B.8})$$

$$\begin{aligned} a_\theta(\theta, \phi, \psi, \mu, \alpha) = & \frac{1}{64} \left( \frac{1}{2} \sin \psi \left( \sin \psi (16 \sin(2\mu) \sin \theta \cos(\alpha - \phi) ((\cos \psi - 1) \cos \theta + \cos \psi - 3) \right. \right. \\ & + (-4 \cos \psi + \cos(2\psi) - 61) \cos \theta) + 128 \sin \mu \sin \left( \frac{\theta}{2} \right) \sin(\alpha - \phi) \Big) \\ & + 4 \sin^4 \left( \frac{\psi}{2} \right) \left( 2 \cos^2 \mu \left( 4(\cos \psi - 3) \cos^2 \left( \frac{\psi}{2} \right) \cos(2\theta) - \sin^2 \psi \cos(3\theta) \right. \right. \end{aligned}$$

$$+ 4 \cos \psi - \cos(2\psi) \Big) + \cos(2\mu) (\sin^2 \psi \cos \theta + 5) + 37 \Big) \Big) \quad (B.9)$$

$$\begin{aligned} b_\theta(\theta, \phi, \psi, \mu, \alpha) = & \frac{1}{32} \left( 4 \left( 4 \sin \mu \cos \left( \frac{\psi}{2} \right) \cos(\alpha - \phi) \left( - 2 \sin^5 \left( \frac{\psi}{2} \right) \left( 3 \sin \left( \frac{3\theta}{2} \right) + \sin \left( \frac{5\theta}{2} \right) \right) \right. \right. \right. \\ & - \left( \sin \left( \frac{3\psi}{2} \right) - 7 \sin \left( \frac{\psi}{2} \right) \right) \cos^2 \left( \frac{\psi}{2} \right) \sin \left( \frac{\theta}{2} \right) \Big) + \sin(2\mu) \sin^2 \psi \sin(\alpha - \phi) \\ & \times \left( \sin^2 \left( \frac{\psi}{2} \right) \sin(2\theta) + (3 - \cos \psi) \sin \theta \right) \Big) + \cos \mu \sin^3 \left( \frac{\psi}{2} \right) \cos \left( \frac{\psi}{2} \right) \\ & \times \left( (-20 \cos \psi + 5 \cos(2\psi) - 113) \cos \left( \frac{\theta}{2} \right) - 8 \sin^4 \left( \frac{\psi}{2} \right) \left( \cos \left( \frac{3\theta}{2} \right) \right. \right. \\ & \left. \left. + 3 \cos \left( \frac{5\theta}{2} \right) + \cos \left( \frac{7\theta}{2} \right) \right) \right) \Big) \end{aligned} \quad (B.10)$$

$$\begin{aligned} c_\theta(\theta, \phi, \psi, \mu, \alpha) = & \frac{1}{128} \left( - 16 \sin(3\mu) \sin^3 \psi \sin \left( \frac{\theta}{2} \right) \cos^2 \left( \frac{\theta}{2} \right) \sin(\alpha - \phi) ((\cos \psi - 1) \cos \theta \right. \\ & + \cos \psi - 3) - 1024 \cos(2\mu) \sin^4 \left( \frac{\psi}{2} \right) \cos^2 \left( \frac{\psi}{2} \right) \cos^4 \left( \frac{\theta}{2} \right) \sin^2(\alpha - \phi) \\ & + 2 \sin(2\mu) \sin^2 \psi \sin \theta \cos(\alpha - \phi) \left( 8 \sin^4 \left( \frac{\psi}{2} \right) (4 \cos \theta + \cos(2\theta)) - 12 \cos \psi \right. \\ & \left. + 3 \cos(2\psi) - 7 \right) - \sin \mu \sin \psi \sin \left( \frac{\theta}{2} \right) \sin(\alpha - \phi) \left( 32 \sin^2 \left( \frac{\psi}{2} \right) (\cos \psi - 3) \right. \\ & \times (\cos \psi + 2) \cos \theta - 4 \sin^2 \psi \sin^2 \left( \frac{\psi}{2} \right) \sin(4\theta) \csc(2\theta) + 67 \cos \psi + 14 \cos(2\psi) \\ & \left. - 3 \cos(3\psi) - 206 \right) - 32 \sin^2 \left( \frac{\psi}{2} \right) \left( \frac{1}{2} \sin^2 \psi \left( 8 \cos^4 \left( \frac{\theta}{2} \right) \cos(2(\alpha - \phi)) \right. \right. \\ & \left. \left. + 3 \cos(2\theta) + 9 \right) + (-3 \cos(2\psi) - 5) \cos \theta \right) \Big) \end{aligned} \quad (B.11)$$

$$\begin{aligned} d_\theta(\theta, \phi, \psi, \mu, \alpha) = & \frac{1}{128} \left( - 256 \sin^2 \mu \sin^2 \left( \frac{\psi}{2} \right) \sin^2 \psi \cos^4 \left( \frac{\theta}{2} \right) \sin(2(\alpha - \phi)) + \sin \psi \right. \\ & \times \left( 4 \sin \mu \sin \left( \frac{\theta}{2} \right) \cos(\alpha - \phi) ((\cos \psi - 1) \cos \theta + \cos \psi - 3) (8 \cos^2 \mu \right. \\ & \times \sin^2 \psi \cos \theta - \cos(2(\mu - \psi)) - \cos(2(\mu + \psi)) + 2 \cos(2\mu) - 2 \cos(2\psi) + 18) \\ & \left. + \sin(2\mu) \sin(\alpha - \phi) \left( 8 \sin \psi \sin^4 \left( \frac{\psi}{2} \right) \sin(3\theta) + \sin \theta \left( \sin(\psi) \left( 64 \sin^4 \left( \frac{\psi}{2} \right) \right. \right. \right. \right. \right. \\ & \left. \left. \left. \left. \left. \left. + 12 \cos \psi - 12 \cos(2\psi) - 12 \cos(3\psi) - 206 \right) \cos \theta \right) \right) \right) \end{aligned}$$

$$\begin{aligned}
 & \times \cos \theta + 5 \cos(2\psi) - 17 \Big) - 10 \sin(2\psi) \Big) \Big) - 128 \cos \mu \sin^2 \left( \frac{\psi}{2} \right) \sin \theta \sin^3 \left( \frac{\theta}{2} \right) \Big) \\
 & + 64 \cos \mu \sin^2 \left( \frac{\psi}{2} \right) \sin(2\psi) (\cos \theta + 3) \cos^3 \left( \frac{\theta}{2} \right) \Big) \tag{B.12}
 \end{aligned}$$

$$\begin{aligned}
 e_\theta(\theta, \phi, \psi, \mu, \alpha) = & \frac{1}{4} \left( 8 \sin \mu \sin^2 \left( \frac{\psi}{2} \right) \sin \psi \cos^3 \left( \frac{\theta}{2} \right) \sin(\alpha - \phi) + \sin \theta \left( \sin(2\mu) \sin \psi \right. \right. \\
 & \times \sin^3 \left( \frac{\psi}{2} \right) \cos \left( \frac{\psi}{2} \right) \sin \theta \cos(\alpha - \phi) ((\cos \psi - 1) \cos \theta + \cos \psi - 3) \\
 & + \sin^2 \mu \sin^2 \psi \cos(2(\alpha - \phi)) (-\cos \psi (\cos \theta + 1) + \cos \theta + 3) \\
 & \left. \left. + 4 \sin^4 \left( \frac{\psi}{2} \right) (\cos \psi \cos \theta + \cos \psi + \cos \theta - 1) \right) \right) \tag{B.13}
 \end{aligned}$$

$$\begin{aligned}
 f_\theta(\theta, \phi, \psi, \mu, \alpha) = & \frac{1}{8} \sin \theta \left( 32 \cos \mu \sin^5 \left( \frac{\psi}{2} \right) \cos \left( \frac{\psi}{2} \right) \cos^3 \left( \frac{\theta}{2} \right) - \sin^2 \psi ((\cos \psi - 1) \cos \theta \right. \\
 & + \cos \psi - 3) \left( 2 \sin^2 \mu \sin(2(\alpha - \phi)) - \sin(2\mu) \sin^2 \left( \frac{\psi}{2} \right) \sin \theta \sin(\alpha - \phi) \right) \Big) \\
 & - 4 \sin \mu \sin^3 \left( \frac{\psi}{2} \right) \cos \left( \frac{\psi}{2} \right) \cos^3 \left( \frac{\theta}{2} \right) \cos(\alpha - \phi) \tag{B.14}
 \end{aligned}$$

$$\begin{aligned}
 g_\theta(\theta, \phi, \psi, \mu, \alpha) = & \frac{1}{64} \left( \sin \psi \left( \cos \mu \sin \left( \frac{\theta}{2} \right) ((\cos \psi - 1) \cos \theta + \cos \psi - 3) \left( -8 \sin^2 \mu \sin^2 \psi \cos \theta \right. \right. \right. \\
 & - \cos(2(\mu - \psi)) - \cos(2(\mu + \psi)) + 2 \cos(2\mu) + 16 \sin^4 \left( \frac{\psi}{2} \right) \cos(2\theta) + 8 \cos \psi \\
 & \left. \left. \left. + 40 \right) - 64 \sin(2\mu) \sin^2 \left( \frac{\psi}{2} \right) \sin \psi \cos^4 \left( \frac{\theta}{2} \right) \sin(\alpha - \phi) \right) + 32 \sin \mu \cos(\alpha - \phi) \right. \\
 & \left( 2 \sin^5 \left( \frac{\psi}{2} \right) \cos \left( \frac{\psi}{2} \right) \left( 3 \cos \left( \frac{3\theta}{2} \right) + \cos \left( \frac{5\theta}{2} \right) \right) - \sin^3 \psi \cos \left( \frac{\theta}{2} \right) \right) \Big) \tag{B.15}
 \end{aligned}$$

$$\begin{aligned}
 h_\theta(\theta, \phi, \psi, \mu, \alpha) = & \frac{1}{32} \sqrt{3} \left( \sin \psi \left( -32 \sin(2\mu) \sin^2 \left( \frac{\psi}{2} \right) \sin \psi \cos^4 \left( \frac{\theta}{2} \right) \sin(\alpha - \phi) \right. \right. \\
 & + \sin \mu \sin(2\mu) \sin^2 \left( \frac{\psi}{2} \right) \sin^2(\psi) \sin \left( \frac{5\theta}{2} \right) + \cos \mu \left( 2 \sin \left( \frac{\theta}{2} \right) \left( \cos^2 \mu \right. \right. \\
 & \times \sin^2 \psi (\cos \psi - 3) + \cos^3 \psi - 3 \cos^2 \psi + \cos \psi - 7 \Big) + \sin \left( \frac{3\theta}{2} \right) \left( \cos^2 \mu \right. \Big) \Big) \Big)
 \end{aligned}$$

$$\begin{aligned}
 & \times \sin^2 \psi (3 \cos \psi - 7) + 3 \cos^3 \psi - 7 \cos^2 \psi + \cos \psi + 3 \Big) \Big) \Big) + 8 \sin \mu \cos(\alpha - \phi) \\
 & \times \left( -2 \sin^3 \left( \frac{\psi}{2} \right) \left( \cos \left( \frac{\psi}{2} \right) + 3 \cos \left( \frac{3\psi}{2} \right) \right) \cos \left( \frac{\theta}{2} \right) - \sin^3 \psi \cos \left( \frac{3\theta}{2} \right) \right) \Big) \tag{B.16}
 \end{aligned}$$

## B.2 General energy density

The following is the energy density in its most general form. It can describe any configuration on the non-contractible 3-sphere, parameterized by  $\psi$ ,  $\mu$  and  $\alpha$  and accommodates any profile function boundary conditions. Changes in generality of the topological map or in boundary conditions can be incorporated by adjusting the real structure functions  $a_\phi(\phi, \theta, \psi, \mu, \alpha)$  through  $h_\phi(\phi, \theta, \psi, \mu, \alpha)$ ,  $a_\theta(\phi, \theta, \psi, \mu, \alpha)$  through  $h_\theta(\phi, \theta, \psi, \mu, \alpha)$  and  $a_{\Phi,i}(\theta, \psi, \mu)$  through  $c_{\Phi,i}(\theta, \psi, \mu)$  accordingly. Their most general form, with unit boundary conditions for all profile functions is given by eqs. (B.1) through (B.16) and (3.25) through (3.32).

$$\begin{aligned}
 \hat{e}_{YM} = & \frac{1}{2g^2 r^2} \left\{ (a_\theta \partial_r \alpha_9)^2 + (b_\theta \partial_r \alpha_{10})^2 + (c_\theta \partial_r \alpha_{11})^2 + (d_\theta \partial_r \alpha_{12})^2 + (e_\theta \partial_r \alpha_{13})^2 + (f_\theta \partial_r \alpha_{14})^2 \right. \\
 & \left. + (g_\theta \partial_r \alpha_{15})^2 + (h_\theta \partial_r \alpha_{16})^2 \right\} \\
 & + \frac{1}{2g^2 r^2 \sin^2 \theta} \left\{ (a_\phi \partial_r \alpha_1)^2 + (b_\phi \partial_r \alpha_2)^2 + (c_\phi \partial_r \alpha_3)^2 + (d_\phi \partial_r \alpha_4)^2 + (e_\phi \partial_r \alpha_5)^2 \right. \\
 & \left. + (f_\phi \partial_r \alpha_6)^2 + (g_\phi \partial_r \alpha_7)^2 + (h_\phi \partial_r \alpha_8)^2 \right\} \\
 & + \frac{1}{8g^2 r^4 \sin^2 \theta} \left\{ 4d_\theta^2 c_\phi^2 \alpha_{12}^2 \alpha_3^2 + e_\theta^2 c_\phi^2 \alpha_{13}^2 \alpha_3^2 + f_\theta^2 c_\phi^2 \alpha_{14}^2 \alpha_3^2 + g_\theta^2 c_\phi^2 \alpha_{15}^2 \alpha_3^2 + 3h_\theta^2 c_\phi^2 \alpha_{16}^2 \alpha_3^2 \right. \\
 & + 2\sqrt{3}g_\theta h_\theta c_\phi^2 \alpha_{15} \alpha_{16} \alpha_3^2 - 6f_\phi d_\theta e_\theta c_\phi \alpha_6 \alpha_{12} \alpha_{13} \alpha_3 + 6e_\phi d_\theta f_\theta c_\phi \alpha_5 \alpha_{12} \alpha_{14} \alpha_3 \\
 & - 6b_\phi e_\theta g_\theta c_\phi \alpha_2 \alpha_{13} \alpha_{15} \alpha_3 - 6a_\phi f_\theta g_\theta c_\phi \alpha_1 \alpha_{14} \alpha_{15} \alpha_3 - 2\sqrt{3}b_\phi e_\theta h_\theta c_\phi \alpha_2 \alpha_{13} \alpha_{16} \alpha_3 \\
 & - 2\sqrt{3}a_\phi f_\theta h_\theta c_\phi \alpha_1 \alpha_{14} \alpha_{16} \alpha_3 + 4e_\phi c_\phi \alpha_{13} \alpha_3 \alpha_9 \partial_\phi a_\theta - 4f_\theta c_\phi \alpha_{14} \alpha_{10} \alpha_3 \partial_\phi b_\theta \\
 & + 4g_\theta c_\phi \alpha_{15} \alpha_{12} \alpha_3 \partial_\phi d_\theta + 4\sqrt{3}h_\theta c_\phi \alpha_{16} \alpha_{12} \alpha_3 \partial_\phi d_\theta - 4d_\theta c_\phi \alpha_{12} \alpha_{15} \alpha_3 \partial_\phi g_\theta \\
 & - 4\sqrt{3}d_\theta c_\phi \alpha_{12} \alpha_{16} \alpha_3 \partial_\phi h_\theta - 4e_\theta c_\phi \alpha_{13} \alpha_3 \partial_\theta (a_\phi \alpha_1) + 4f_\theta c_\phi \alpha_{14} \alpha_3 \partial_\theta (b_\phi \alpha_2) \\
 & - 4g_\theta c_\phi \alpha_{15} \alpha_3 \partial_\theta (d_\phi \alpha_4) - 4\sqrt{3}h_\theta c_\phi \alpha_{16} \alpha_3 \partial_\theta (d_\phi \alpha_4) + 4d_\theta c_\phi \alpha_{12} \alpha_3 \partial_\theta (g_\phi \alpha_7) \\
 & + 4\sqrt{3}d_\theta c_\phi \partial_\theta (h_\phi \alpha_8) + (4b_\phi^2 \alpha_2^2 + c_\phi^2 \alpha_3^2 + d_\phi^2 \alpha_4^2 + e_\phi^2 \alpha_5^2 + f_\phi^2 \alpha_6^2 + 4(g_\phi \alpha_7 + 1)^2) a_\theta^2 \alpha_9^2 \\
 & + (4a_\phi^2 \alpha_1^2 + c_\phi^2 \alpha_3^2 + d_\phi^2 \alpha_4^2 + e_\phi^2 \alpha_5^2 + f_\phi^2 \alpha_6^2 + 4(g_\phi \alpha_7 + 1)^2) b_\theta^2 \alpha_{10}^2
 \end{aligned}$$

$$\begin{aligned}
 & + \left( a_\phi^2 \alpha_1^2 + b_\phi^2 \alpha_2^2 + 4d_\phi^2 \alpha_4^2 + e_\phi^2 \alpha_5^2 + f_\phi^2 \alpha_6^2 + g_\phi^2 \alpha_7^2 + 3h_\phi^2 \alpha_8^2 - 4\sqrt{3}h_\phi \alpha_8 \right. \\
 & + 2g_\phi \alpha_7 \left( \sqrt{3}h_\phi \alpha_8^2 - 2 \right) + 4 \Big) c_\theta^2 \alpha_{11}^2 + a_\phi^2 d_\theta^2 \alpha_1^2 \alpha_{12}^2 + b_\phi^2 \alpha_2^2 d_\theta^2 \alpha_{12}^2 + e_\phi^2 \alpha_5^2 d_\theta^2 \alpha_{12}^2 \\
 & + f_\phi^2 \alpha_6^2 d_\theta^2 \alpha_{12}^2 + g_\phi^2 \alpha_7^2 d_\theta^2 \alpha_{12}^2 + 3h_\phi^2 \alpha_8^2 d_\theta^2 \alpha_{12}^2 - 4g_\phi \alpha_7 d_\theta^2 \alpha_{12}^2 + 2\sqrt{3}g_\phi \alpha_7 h_\phi \alpha_8 d_\theta^2 \alpha_{12}^2 \\
 & - 4\sqrt{3}h_\phi \alpha_8 d_\theta^2 \alpha_{12}^2 + 4d_\theta^2 \alpha_{12}^2 + a_\phi^2 \alpha_1^2 e_\theta^2 \alpha_{13}^2 + b_\phi^2 \alpha_2^2 e_\theta^2 \alpha_{13}^2 + d_\phi^2 \alpha_4^2 e_\theta^2 \alpha_{13}^2 + 4f_\phi^2 \alpha_6^2 e_\theta^2 \alpha_{13}^2 \\
 & + g_\phi^2 \alpha_7^2 e_\theta^2 \alpha_{13}^2 + 3h_\phi^2 \alpha_8^2 e_\theta^2 \alpha_{13}^2 + 8g_\phi \alpha_7 e_\theta^2 \alpha_{13}^2 - 2\sqrt{3}g_\phi \alpha_7 h_\phi \alpha_8 e_\theta^2 \alpha_{13}^2 - 8\sqrt{3}h_\phi \alpha_8 e_\theta^2 \alpha_{13}^2 \\
 & + 16e_\theta^2 \alpha_{13}^2 + a_\phi^2 \alpha_1^2 f_\theta^2 \alpha_{14}^2 + b_\phi^2 \alpha_2^2 f_\theta^2 \alpha_{14}^2 + d_\phi^2 \alpha_4^2 f_\theta^2 \alpha_{14}^2 + 4e_\phi^2 \alpha_5^2 f_\theta^2 \alpha_{14}^2 + g_\phi^2 \alpha_7^2 f_\theta^2 \alpha_{14}^2 \\
 & + 3h_\phi^2 \alpha_8^2 f_\theta^2 \alpha_{14}^2 + 8g_\phi \alpha_7 f_\theta^2 \alpha_{14}^2 - 2\sqrt{3}g_\phi \alpha_7 h_\phi \alpha_8 f_\theta^2 \alpha_{14}^2 - 8\sqrt{3}h_\phi \alpha_8 f_\theta^2 \alpha_{14}^2 + 16f_\theta^2 \alpha_{14}^2 \\
 & + 4a_\phi^2 \alpha_1^2 g_\theta^2 \alpha_{15}^2 + 4b_\phi^2 \alpha_2^2 g_\theta^2 \alpha_{15}^2 + d_\phi^2 \alpha_4^2 g_\theta^2 \alpha_{15}^2 + e_\phi^2 \alpha_5^2 g_\theta^2 \alpha_{15}^2 + f_\phi^2 \alpha_6^2 g_\theta^2 \alpha_{15}^2 + 3d_\phi^2 \alpha_4^2 h_\theta^2 \alpha_{15}^2 \\
 & + 3e_\phi^2 \alpha_5^2 h_\theta^2 \alpha_{16}^2 + 3f_\phi^2 \alpha_6^2 h_\theta^2 \alpha_{16}^2 + 4\alpha_9^2 (\partial_\phi a_\theta)^2 + 4\alpha_{10}^2 (\partial_\phi b_\theta)^2 + 4\alpha_{11}^2 (\partial_\phi c_\theta)^2 + 4\alpha_{12}^2 (\partial_\phi d_\theta)^2 \\
 & + 4\alpha_{13}^2 (\partial_\phi e_\theta)^2 + 4\alpha_{14}^2 (\partial_\phi f_\theta)^2 + 4\alpha_{15}^2 (\partial_\phi g_\theta)^2 + 4\alpha_{16}^2 (\partial_\phi h_\theta)^2 + 4(\partial_\theta (a_\phi \alpha_1))^2 \\
 & + 4(\partial_\theta (b_\phi \alpha_2))^2 + 4(\partial_\theta (c_\phi \alpha_3))^2 + 4(\partial_\theta (d_\phi \alpha_4))^2 + 4(\partial_\theta (e_\phi \alpha_5))^2 + 4(\partial_\theta (f_\phi \alpha_6))^2 \\
 & + 4(\partial_\theta (g_\phi \alpha_7))^2 + 4(\partial_\theta (h_\phi \alpha_8))^2 + 12a_\phi \alpha_1 d_\theta \alpha_{12} e_\theta \alpha_{13} - 2d_\phi \alpha_4 e_\phi \alpha_5 d_\theta \alpha_{12} e_\theta \alpha_{13} \\
 & - 4\sqrt{3}a_\phi \alpha_1 h_\phi \alpha_8 d_\theta \alpha_{12} e_\theta \alpha_{13} - 12b_\phi \alpha_2 d_\theta \alpha_{12} f_\theta \alpha_{14} - 2d_\phi \alpha_4 f_\phi \alpha_6 d_\theta \alpha_{12} f_\theta \alpha_{14} \\
 & + 4\sqrt{3}b_\phi \alpha_2 h_\phi \alpha_8 d_\theta \alpha_{12} f_\theta \alpha_{14} - 8e_\phi \alpha_5 f_\phi \alpha_6 e_\theta \alpha_{13} f_\theta \alpha_{14} + 4d_\phi \alpha_4 d_\theta \alpha_{12} g_\theta \alpha_{15} \\
 & - 6a_\phi \alpha_1 e_\phi \alpha_5 d_\theta \alpha_{12} g_\theta \alpha_{15} + 6b_\phi \alpha_2 f_\phi \alpha_6 d_\theta \alpha_{12} g_\theta \alpha_{15} - 2d_\phi \alpha_4 g_\phi \alpha_7 d_\theta \alpha_{12} g_\theta \alpha_{15} \\
 & - 2\sqrt{3}d_\phi \alpha_4 h_\phi \alpha_8 d_\theta \alpha_{12} g_\theta \alpha_{15} + 6a_\phi \alpha_1 d_\phi \alpha_4 e_\theta \alpha_{13} g_\theta \alpha_{15} - 8e_\phi \alpha_5 e_\theta \alpha_{13} g_\theta \alpha_{15} \\
 & - 2e_\phi \alpha_5 g_\phi \alpha_7 e_\theta \alpha_{13} g_\theta \alpha_{15} + 2\sqrt{3}e_\phi \alpha_5 h_\phi \alpha_8 e_\theta \alpha_{13} g_\theta \alpha_{15} - 6b_\phi \alpha_2 d_\phi \alpha_4 f_\theta \alpha_{14} g_\theta \alpha_{15} \\
 & - 8f_\phi \alpha_6 f_\theta \alpha_{14} g_\theta \alpha_{15} - 2f_\phi \alpha_6 g_\phi \alpha_7 f_\theta \alpha_{14} g_\theta \alpha_{15} + 2\sqrt{3}f_\phi \alpha_6 h_\phi \alpha_8 f_\theta \alpha_{14} g_\theta \alpha_{15} \\
 & + 4\sqrt{3}d_\phi \alpha_4 d_\theta \alpha_{12} h_\theta \alpha_{16} + 2\sqrt{3}a_\phi \alpha_1 e_\phi \alpha_5 d_\theta \alpha_{12} h_\theta \alpha_{16} - 2\sqrt{3}b_\phi \alpha_2 f_\phi \alpha_6 d_\theta \alpha_{12} h_\theta \alpha_{16} \\
 & - 2\sqrt{3}d_\phi \alpha_4 g_\phi \alpha_7 d_\theta \alpha_{12} h_\theta \alpha_{16} - 6d_\phi \alpha_4 h_\phi \alpha_8 d_\theta \alpha_{12} h_\theta \alpha_{16} + 2\sqrt{3}a_\phi \alpha_1 d_\phi \alpha_4 e_\theta \alpha_{13} h_\theta \alpha_{16} \\
 & + 8\sqrt{3}e_\phi \alpha_5 e_\theta \alpha_{13} h_\theta \alpha_{16} + 2\sqrt{3}e_\phi \alpha_5 g_\phi \alpha_7 e_\theta \alpha_{13} h_\theta \alpha_{16} - 6e_\phi \alpha_5 h_\phi \alpha_8 e_\theta \alpha_{13} h_\theta \alpha_{16} \\
 & - 2\sqrt{3}b_\phi \alpha_2 d_\phi \alpha_4 f_\theta \alpha_{14} h_\theta \alpha_{16} + 8\sqrt{3}f_\phi \alpha_6 f_\theta \alpha_{14} h_\theta \alpha_{16} + 2\sqrt{3}f_\phi \alpha_6 g_\phi \alpha_7 f_\theta \alpha_{14} h_\theta \alpha_{16} \\
 & - 6f_\phi \alpha_6 h_\phi \alpha_8 f_\theta \alpha_{14} h_\theta \alpha_{16} + 2\sqrt{3}d_\phi^2 \alpha_4^2 g_\theta \alpha_{15} h_\theta \alpha_{16} - 2\sqrt{3}e_\phi^2 \alpha_5^2 g_\theta \alpha_{15} h_\theta \alpha_{16} \\
 & - 2\sqrt{3}f_\phi^2 \alpha_6^2 g_\theta \alpha_{15} h_\theta \alpha_{16} - 4f_\phi \alpha_6 d_\theta \alpha_{12} \alpha_9 \partial_\phi a_\theta + 4d_\phi \alpha_4 f_\theta \alpha_{14} \alpha_9 \partial_\phi a_\theta - 8b_\phi \alpha_2 g_\theta \alpha_{15} \alpha_9 \partial_\phi a_\theta \\
 & - 4e_\phi \alpha_5 d_\theta \alpha_{12} \alpha_{10} \partial_\phi b_\theta + 4d_\phi \alpha_4 e_\theta \alpha_{13} \alpha_{10} \partial_\phi b_\theta + 8a_\phi \alpha_1 g_\theta \alpha_{15} \alpha_{10} \partial_\phi b_\theta + 4d_\phi \alpha_4 e_\theta \alpha_{13} \alpha_{10} \partial_\phi b_\theta
 \end{aligned}$$

$$\begin{aligned}
 & + 8a_\phi\alpha_1g_\theta\alpha_{15}\alpha_{10}\partial_\phi b_\theta + 4g_\phi\alpha_7d_\theta\alpha_{12}\alpha_{11}\partial_\phi c_\theta + 4\sqrt{3}h_\phi\alpha_8d_\theta\alpha_{12}\alpha_{11}\partial_\phi c_\theta - 8d_\theta\alpha_4\alpha_{11}\partial_\phi c_\theta \\
 & - 4a_\phi\alpha_1e_\theta\alpha_{13}\alpha_{11}\partial_\phi c_\theta + 4b_\phi\alpha_2f_\theta\alpha_{14}\alpha_{11}\partial_\phi c_\theta - 4d_\phi\alpha_4g_\theta\alpha_{15}\alpha_{11}\partial_\phi c_\theta \\
 & - 4\sqrt{3}d_\phi\alpha_4h_\theta\alpha_{16}\alpha_{11}\partial_\phi c_\theta - 4b_\phi\alpha_2e_\theta\alpha_{13}\alpha_{12}\partial_\phi d_\theta - 4a_\phi\alpha_1f_\theta\alpha_{14}\alpha_{12}\partial_\phi d_\theta \\
 & + 4b_\phi\alpha_2d_\theta\alpha_{12}\alpha_{13}\partial_\phi e_\theta - 4g_\phi\alpha_7f_\theta\alpha_{14}\alpha_{13}\partial_\phi e_\theta + 4\sqrt{3}h_\phi\alpha_8f_\theta\alpha_{14}\alpha_{13}\partial_\phi e_\theta \\
 & - 16f_\theta\alpha_{14}\alpha_{13}\partial_\phi e_\theta + 4f_\phi\alpha_6g_\theta\alpha_{15}\alpha_{13}\partial_\phi e_\theta - 4\sqrt{3}f_\phi\alpha_6h_\theta\alpha_{16}\alpha_{13}\partial_\phi e_\theta + 4a_\phi\alpha_1d_\theta\alpha_{12}\alpha_{14}\partial_\phi f_\theta \\
 & + 4g_\phi\alpha_7e_\theta\alpha_{13}\alpha_{14}\partial_\phi f_\theta - 4\sqrt{3}h_\phi\alpha_8e_\theta\alpha_{13}\alpha_{14}\partial_\phi f_\theta + 16e_\theta\alpha_{13}\alpha_{14}\partial_\phi f_\theta - 4e_\phi\alpha_5g_\theta\alpha_{15}\alpha_{14}\partial_\phi f_\theta \\
 & + 4\sqrt{3}e_\phi\alpha_5h_\theta\alpha_{16}\alpha_{14}\partial_\phi f_\theta - 4f_\phi\alpha_6e_\theta\alpha_{13}\alpha_{15}\partial_\phi g_\theta + 4e_\phi\alpha_5f_\theta\alpha_{14}\alpha_{15}\partial_\phi g_\theta \\
 & + 4\sqrt{3}f_\phi\alpha_6e_\theta\alpha_{13}\alpha_{16}\partial_\phi h_\theta - 4\sqrt{3}e_\phi\alpha_5f_\theta\alpha_{14}\alpha_{16}\partial_\phi h_\theta + 4f_\phi\alpha_6d_\theta\alpha_{12}\partial_\theta(a_\phi\alpha_1) \\
 & - 4d_\phi\alpha_4f_\theta\alpha_{14}\partial_\theta(a_\phi\alpha_1) + 8b_\phi\alpha_2g_\theta\alpha_{15}\partial_\theta(a_\phi\alpha_1) - 8\alpha_9\partial_\phi a_\theta\partial_\theta(a_\phi\alpha_1) \\
 & + 4e_\phi\alpha_5d_\theta\alpha_{12}\partial_\theta(b_\phi\alpha_2) - 4d_\phi\alpha_4e_\theta\alpha_{13}\partial_\theta(b_\phi\alpha_2) - 8a_\phi\alpha_1g_\theta\alpha_{15}\partial_\theta(b_\phi\alpha_2) \\
 & - 8\alpha_{10}\partial_\phi b_\theta\partial_\theta(b_\phi\alpha_2) - 4g_\phi\alpha_7d_\theta\alpha_{12}\partial_\theta(c_\phi\alpha_3) - 4\sqrt{3}h_\phi\alpha_8d_\theta\alpha_{12}\partial_\theta(c_\phi\alpha_3) \\
 & + 8d_\theta\alpha_{12}\partial_\theta(c_\phi\alpha_3) + 4a_\phi\alpha_1e_\theta\alpha_{13}\partial_\theta(c_\phi\alpha_3) - 4b_\phi\alpha_2f_\theta\alpha_{14}\partial_\theta(c_\phi\alpha_3) + 4d_\phi\alpha_4g_\theta\alpha_{15}\partial_\theta(c_\phi\alpha_3) \\
 & + 4\sqrt{3}d_\phi\alpha_4h_\theta\alpha_{16}\partial_\theta(c_\phi\alpha_3) - 8\alpha_{11}\partial_\phi c_\theta\partial_\theta(c_\phi\alpha_3) + 4b_\phi\alpha_2e_\theta\alpha_{13}\partial_\theta(d_\phi\alpha_4) \\
 & + 4a_\phi\alpha_1f_\theta\alpha_{14}\partial_\theta(d_\phi\alpha_4) - 8\alpha_{12}\partial_\phi d_\theta\partial_\theta(d_\phi\alpha_4) - 4b_\phi d_\theta\alpha_{12}\partial_\theta(e_\phi\alpha_5) + 4g_\phi\alpha_7f_\theta\alpha_{14}\partial_\theta(e_\phi\alpha_5) \\
 & - 4\sqrt{3}h_\phi\alpha_8f_\theta\alpha_{14}\partial_\theta(e_\phi\alpha_5) + 16f_\theta\alpha_{14}\partial_\theta(e_\phi\alpha_5) - 4f_\phi\alpha_6g_\theta\alpha_{15}\partial_\theta(e_\phi\alpha_5) \\
 & + 4\sqrt{3}f_\phi\alpha_6h_\theta\alpha_{16}\partial_\theta(e_\phi\alpha_5) - 8\alpha_{13}\partial_\phi e_\theta\partial_\theta(e_\phi\alpha_5) - 4a_\phi\alpha_1d_\theta\alpha_{12}\partial_\theta(f_\phi\alpha_6) \\
 & - 4g_\phi\alpha_7e_\theta\alpha_{13}\partial_\theta(f_\phi\alpha_6) + 4\sqrt{3}h_\phi\alpha_8e_\theta\alpha_{13}\partial_\theta(f_\phi\alpha_6) - 16e_\theta\alpha_{13}\partial_\theta(f_\phi\alpha_6) \\
 & + 4e_\phi\alpha_5g_\theta\alpha_{15}\partial_\theta(f_\phi\alpha_6) - 4\sqrt{3}e_\phi\alpha_5h_\theta\alpha_{16}\partial_\theta(f_\phi\alpha_6) - 8\alpha_{14}\partial_\phi f_\theta\partial_\theta(f_\phi\alpha_6) \\
 & - 2b_\theta\alpha_{10}\left(\sqrt{3}e_\phi\alpha_5h_\phi\alpha_8c_\theta\alpha_{11} + \sqrt{3}f_\phi\alpha_6h_\phi\alpha_8d_\theta\alpha_{12} - 6c_\phi\alpha_3e_\theta\alpha_{13} + \sqrt{3}c_\phi\alpha_3h_\phi\alpha_8e_\theta\alpha_{13}\right. \\
 & \left.- 6d_\phi\alpha_4f_\theta\alpha_{14} + \sqrt{3}d_\phi\alpha_4h_\phi\alpha_8f_\theta\alpha_{14} + b_\phi\alpha_2\left(c_\phi\alpha_3c_\theta\alpha_{11} + d_\phi\alpha_4d_\theta\alpha_{12} + e_\phi\alpha_5e_\theta\alpha_{13}\right.\right. \\
 & \left.\left.+ f_\phi\alpha_6f_\theta\alpha_{14} + 4(g_\phi\alpha_7 + 1)g_\theta\alpha_{15}\right) - 2\sqrt{3}c_\phi\alpha_3e_\phi\alpha_5h_\theta\alpha_{16} - 2\sqrt{3}d_\phi\alpha_4f_\phi\alpha_6h_\theta\alpha_{16}\right. \\
 & \left.- 4\alpha_9\partial_\phi a_\theta + 2f_\phi\alpha_6\alpha_{11}\partial_\phi c_\theta - 2e_\phi\alpha_5\alpha_{12}\partial_\phi d_\theta + 2d_\phi\alpha_4\alpha_{13}\partial_\phi e_\theta - 2c_\phi\alpha_3\alpha_{14}\partial_\phi f_\theta\right. \\
 & \left.+ 4\partial_\theta(a_\phi\alpha_1) + g_\phi\alpha_7\left(3e_\phi\alpha_5c_\theta\alpha_{11} + 3f_\phi\alpha_6d_\theta\alpha_{12} - 3c_\phi\alpha_3e_\theta\alpha_{13} - 3d_\phi\alpha_4f_\theta\alpha_{14}\right.\right. \\
 & \left.\left.- 4\alpha_9\partial_\phi a_\theta + 4\partial_\theta(a_\phi\alpha_1)\right) - 2f_\phi\alpha_6\partial_\theta(c_\phi\alpha_3) + 2e_\phi\alpha_5\partial_\theta(d_\phi\alpha_4) - 2d_\phi\alpha_4\partial_\theta(e_\phi\alpha_5)\right)
 \end{aligned}$$

$$\begin{aligned}
 & + 2c_\phi\alpha_3\partial_\theta(f_\phi\alpha_6) + a_\phi\alpha_1 \left( 3d_\phi\alpha_4c_\theta\alpha_{11} - 3c_\phi\alpha_3d_\theta\alpha_{12} - 3f_\phi\alpha_6e_\theta\alpha_{13} + 3e_\phi\alpha_5f_\theta\alpha_{14} \right. \\
 & \left. + 4\alpha_{15}\partial_\phi g_\theta - 4\partial_\theta(g_\phi\alpha_7) \right) + 4f_\phi\alpha_6e_\theta\alpha_{13}\partial_\theta(g_\phi\alpha_7) - 4e_\phi\alpha_5f_\theta\alpha_{14}\partial_\theta(g_\phi\alpha_7) \\
 & - 8\alpha_{15}\partial_\phi g_\theta\partial_\theta(g_\phi\alpha_7) - 2a_\theta\alpha_9 \left( \sqrt{3}f_\phi\alpha_6h_\phi\alpha_8c_\theta\alpha_{11} - \sqrt{3}e_\phi\alpha_5h_\phi\alpha_8d_\theta\alpha_{12} + 6d_\phi\alpha_4e_\theta\alpha_{13} \right. \\
 & \left. - \sqrt{3}d_\phi\alpha_4h_\phi\alpha_8e_\theta\alpha_{13} - 6c_\phi\alpha_3f_\theta\alpha_{14} + \sqrt{3}c_\phi\alpha_3h_\phi\alpha_8f_\theta\alpha_{14} + a_\phi\alpha_1 \left( 4b_\phi\alpha_2b_\theta\alpha_{10} \right. \right. \\
 & \left. \left. + c_\phi\alpha_3c_\theta\alpha_{11} + d_\phi\alpha_4d_\theta\alpha_{12} + e_\phi\alpha_5e_\theta\alpha_{13} + f_\phi\alpha_6f_\theta\alpha_{14} + 4(g_\phi\alpha_7 + 1)g_\theta\alpha_{15} \right) \right) \\
 & + 2\sqrt{3}d_\phi\alpha_4e_\phi\alpha_5h_\theta\alpha_{16} - 2\sqrt{3}c_\phi\alpha_3f_\phi\alpha_6h_\theta\alpha_{16} + 4\alpha_{10}\partial_\phi b_\theta - 2e_\phi\alpha_5\alpha_{11}\partial_\phi c_\theta \\
 & - 2f_\phi\alpha_6\alpha_{12}\partial_\phi d_\theta + 2c_\phi\alpha_3\alpha_{13}\partial_\phi e_\theta + 2d_\phi\alpha_4\alpha_{14}\partial_\phi f_\theta + g_\phi\alpha_7 \left( 3f_\phi\alpha_6c_\theta\alpha_{11} - 3e_\phi\alpha_5d_\theta\alpha_{12} \right. \\
 & \left. + 3d_\phi\alpha_4e_\theta\alpha_{13} - 3c_\phi\alpha_3f_\theta\alpha_{14} + 4\alpha_{10}\partial_\phi b_\theta - 4\partial_\theta(b_\phi\alpha_2) \right) - 4\partial_\theta(b_\phi\alpha_2) + 2e_\phi\alpha_5\partial_\theta(c_\phi\alpha_3) \\
 & + 2f_\phi\alpha_6\partial_\theta(d_\phi\alpha_4) - 2c_\phi\alpha_3\partial_\theta(e_\phi\alpha_5) - 2d_\phi\alpha_4\partial_\theta(f_\phi\alpha_6) + b_\phi\alpha_2 \left( - 3d_\phi\alpha_4c_\theta\alpha_{11} \right. \\
 & \left. + 3c_\phi\alpha_3d_\theta\alpha_{12} + 3f_\phi\alpha_6e_\theta\alpha_{13} - 3e_\phi\alpha_5f_\theta\alpha_{14} - 4\alpha_{15}\partial_\phi g_\theta + 4\partial_\theta(g_\phi\alpha_7) \right) \\
 & - 4\sqrt{3}f_\phi\alpha_6e_\theta\alpha_{13}\partial_\theta(h_\phi\alpha_8) + 4\sqrt{3}e_\phi\alpha_5f_\theta\alpha_{14}\partial_\theta(h_\phi\alpha_8) - 8\alpha_{16}\partial_\phi h_\theta\partial_\theta(h_\phi\alpha_8) \\
 & - 2c_\theta\alpha_{11} \left( - 3d_\phi\alpha_4f_\phi\alpha_6e_\theta\alpha_{13} + \left( 3d_\phi\alpha_4e_\phi\alpha_5 - 2\sqrt{3}a_\phi\alpha_1h_\phi\alpha_8 \right) f_\theta\alpha_{14} - 3a_\phi\alpha_1f_\phi\alpha_6g_\theta\alpha_{15} \right. \\
 & \left. + \sqrt{3}a_\phi\alpha_1f_\phi\alpha_6h_\theta\alpha_{16} + c_\phi\alpha_3 \left( 4d_\phi\alpha_4d_\theta\alpha_{12} + e_\phi\alpha_5e_\theta\alpha_{13} + f_\phi\alpha_6f_\theta\alpha_{14} \right. \right. \\
 & \left. \left. + \left( g_\phi\alpha_7 + \sqrt{3}h_\phi\alpha_8 - 2 \right) g_\theta\alpha_{15} + \left( \sqrt{3}g_\phi\alpha_7 + 3h_\phi\alpha_8 - 2\sqrt{3} \right) h_\theta\alpha_{16} \right) + 2e_\phi\alpha_5\alpha_9\partial_\phi a_\theta \right. \\
 & \left. - 2f_\phi\alpha_6\alpha_{10}\partial_\phi b_\theta + 2\sqrt{3}h_\phi\alpha_8\alpha_{12}\partial_\phi d_\theta - 2a_\phi\alpha_1\alpha_{13}\partial_\phi e_\theta - 2d_\phi\alpha_4\alpha_{15}\partial_\phi g_\theta \right. \\
 & \left. - 2\sqrt{3}d_\phi\alpha_4\alpha_{16}\partial_\phi h_\theta - 2e_\phi\alpha_5\partial_\theta(a_\phi\alpha_1) + 2f_\phi\alpha_6\partial_\theta(b_\phi\alpha_2) + 2 \left( 3a_\phi\alpha_1f_\theta\alpha_{14} \right. \right. \\
 & \left. \left. + (g_\phi\alpha_7 - 2)(\alpha_{12}\partial_\phi d_\theta - \partial_\theta(d_\phi\alpha_4)) \right) - 2\sqrt{3}h_\phi\alpha_8\partial_\theta(d_{phi}\alpha_4) + 2a_\phi\alpha_1\partial_\theta(e_\phi\alpha_5) \right. \\
 & \left. + b_\phi\alpha_2 \left( \left( 6 - 2\sqrt{3}h_\phi\alpha_8 \right) e_\theta\alpha_{13} + e_\phi\alpha_5 \left( \sqrt{3}h_\theta\alpha_{16} - 3g_\theta\alpha_{15} \right) + 2 \left( \alpha_{14}\partial_\phi f_\theta - \partial_\theta(f_\phi\alpha_6) \right) \right) \right. \\
 & \left. + 2d_\phi\alpha_4\partial_\theta(g_\phi\alpha_7) + 2\sqrt{3}d_\phi\alpha_4\partial_\theta(h_\phi\alpha_8) \right) \} \tag{B.17}
 \end{aligned}$$

$$\begin{aligned}
 \hat{\epsilon}_{Hkin} = & \frac{v^2}{8} \left\{ 2b_{\Phi,1} \left( \cos(\alpha - \phi)b_{\Phi,3} - \sin(\alpha - \phi)b_{\Phi,2} \right) (\partial_r\beta_2)^2 \right. \\
 & \left. - 2 \left( \sin(\alpha - \phi)c_{\Phi,1}c_{\Phi,2} + \cos(\alpha - \phi)c_{\Phi,2}c_{\Phi,3} \right) (\partial_r\beta_3)^2 + 4 \left( a_{\Phi,1}^2 + a_{\Phi,2}^2 \right) (\partial_r\beta_1)^2 \right\}
 \end{aligned}$$

$$\begin{aligned}
 & + \left( b_{\Phi,1}^2 + b_{\Phi,2}^2 + b_{\Phi,3}^2 \right) (\partial_r \beta_2)^2 + \left( c_{\Phi,1}^2 + c_{\Phi,2}^2 + c_{\Phi,3}^2 \right) (\partial_r \beta_3)^2 \Big\} \\
 & + \frac{v^2}{96r^2} \left\{ 12a_\theta^2 \alpha_9^2 a_{\Phi,1}^2 \beta_1^2 + 12b_\theta^2 \alpha_{10}^2 a_{\Phi,1}^2 \beta_1^2 + 12c_\theta^2 \alpha_{11}^2 a_{\Phi,1}^2 \beta_1^2 + 12d_\theta^2 \alpha_{12}^2 a_{\Phi,1}^2 \beta_1^2 \right. \\
 & + 12g_\theta^2 \alpha_{15}^2 a_{\Phi,1}^2 \beta_1^2 + 4h_\theta^2 \alpha_{16}^2 a_{\Phi,1}^2 \beta_1^2 + 8\sqrt{3}g_\theta \alpha_{15} h_\theta \alpha_{16} a_{\Phi,1}^2 \beta_1^2 - 12c_{\Phi,2} \beta_3 a_\theta \alpha_9 e_\theta \alpha_{13} a_{\Phi,1} \beta_1 \\
 & - 12b_{\Phi,2} \beta_2 c_\theta \alpha_{11} e_\theta \alpha_{13} a_{\Phi,1} \beta_1 + 12b_{\Phi,3} \beta_2 d_\theta \alpha_{12} e_\theta \alpha_{13} a_{\Phi,1} \beta_1 + 12c_{\Phi,2} \beta_3 b_\theta \alpha_{10} f_\theta \alpha_{14} a_{\Phi,1} \beta_1 \\
 & - 12b_{\Phi,3} \beta_2 c_\theta \alpha_{11} f_\theta \alpha_{14} a_{\Phi,1} \beta_1 - 12b_{\Phi,2} \beta_2 d_\theta \alpha_{12} f_\theta \alpha_{14} a_{\Phi,1} \beta_1 + 12c_{\Phi,2} \beta_3 d_\theta \alpha_{12} g_\theta \alpha_{15} a_{\Phi,1} \beta_1 \\
 & - 8\sqrt{3}b_{\Phi,3} \beta_2 a_\theta \alpha_9 h_\theta \alpha_{16} a_{\Phi,1} \beta_1 - 8\sqrt{3}b_{\Phi,2} \beta_2 b_\theta \alpha_{10} h_\theta \alpha_{16} a_{\Phi,1} \beta_1 - 4\sqrt{3}c_{\Phi,2} \beta_3 d_\theta \alpha_{12} h_\theta \alpha_{16} a_{\Phi,1} \beta_1 \\
 & - 48g_\theta \alpha_{15} \partial_\theta (a_{\Phi,2} \beta_1) a_{\Phi,1} \beta_1 - 16\sqrt{3}h_\theta \alpha_{16} \partial_\theta (a_{\Phi,2} \beta_1) a_{\Phi,1} \beta_1 - 24a_\theta \alpha_9 \partial_\theta (b_{\Phi,2} \beta_2) a_{\Phi,1} \beta_1 \\
 & + 24b_\theta \alpha_{10} \partial_\theta (b_{\Phi,3} \beta_2) a_{\Phi,1} \beta_1 + 24c_\theta \alpha_{11} \partial_\theta (c_{\Phi,2} \beta_3) a_{\Phi,1} \beta_1 + 12a_{\Phi,2}^2 \beta_1^2 a_\theta^2 \alpha_9^2 + 3b_{\Phi,1}^2 \beta_2^2 a_\theta^2 \alpha_9^2 \\
 & + 3b_{\Phi,2}^2 \beta_2^2 a_\theta^2 \alpha_9^2 + 3b_{\Phi,3}^2 \beta_2^2 a_\theta^2 \alpha_9^2 + 12a_{\Phi,2}^2 \beta_1^2 b_\theta^2 \alpha_{10}^2 + 3b_{\Phi,1}^2 \beta_2^2 b_\theta^2 \alpha_{10}^2 + 3b_{\Phi,2}^2 \beta_2^2 b_\theta^2 \alpha_{10}^2 \\
 & + 3b_{\Phi,3}^2 \beta_2^2 b_\theta^2 \alpha_{10}^2 + 12a_{\Phi,2}^2 \beta_1^2 c_\theta^2 \alpha_{11}^2 + 3c_{\Phi,1}^2 \beta_3^2 c_\theta^2 \alpha_{11}^2 + 3c_{\Phi,2}^2 \beta_3^2 c_\theta^2 \alpha_{11}^2 + 3c_{\Phi,3}^2 \beta_3^2 c_\theta^2 \alpha_{11}^2 \\
 & + 12a_{\Phi,2}^2 \beta_1^2 d_\theta^2 \alpha_{12}^2 + 3c_{\Phi,1}^2 \beta_3^2 d_\theta^2 \alpha_{12}^2 + 3c_{\Phi,2}^2 \beta_3^2 d_\theta^2 \alpha_{12}^2 + 3c_{\Phi,3}^2 \beta_3^2 d_\theta^2 \alpha_{12}^2 + 3b_{\Phi,1}^2 \beta_2^2 e_\theta^2 \alpha_{13}^2 \\
 & + 3b_{\Phi,2}^2 \beta_2^2 e_\theta^2 \alpha_{13}^2 + 3b_{\Phi,3}^2 \beta_2^2 e_\theta^2 \alpha_{13}^2 + 3c_{\Phi,1}^2 \beta_3^2 e_\theta^2 \alpha_{13}^2 + 3c_{\Phi,2}^2 \beta_3^2 e_\theta^2 \alpha_{13}^2 + 3c_{\Phi,3}^2 \beta_3^2 e_\theta^2 \alpha_{13}^2 \\
 & + 3b_{\Phi,1}^2 \beta_2^2 f_\theta^2 \alpha_{14}^2 + 3b_{\Phi,2}^2 \beta_2^2 f_\theta^2 \alpha_{14}^2 + 3b_{\Phi,3}^2 \beta_2^2 f_\theta^2 \alpha_{14}^2 + 3c_{\Phi,1}^2 \beta_3^2 f_\theta^2 \alpha_{14}^2 + 3c_{\Phi,2}^2 \beta_3^2 f_\theta^2 \alpha_{14}^2 \\
 & + 3c_{\Phi,3}^2 \beta_3^2 f_\theta^2 \alpha_{14}^2 + 12a_{\Phi,2}^2 \beta_1^2 g_\theta^2 \alpha_{15}^2 + 3b_{\Phi,1}^2 \beta_2^2 g_\theta^2 \alpha_{15}^2 + 3b_{\Phi,2}^2 \beta_2^2 g_\theta^2 \alpha_{15}^2 + 3b_{\Phi,3}^2 \beta_2^2 g_\theta^2 \alpha_{15}^2 \\
 & + 4a_{\Phi,2}^2 \beta_1^2 h_\theta^2 \alpha_{16}^2 + b_{\Phi,1}^2 \beta_2^2 h_\theta^2 \alpha_{16}^2 + b_{\Phi,2}^2 \beta_2^2 h_\theta^2 \alpha_{16}^2 + b_{\Phi,3}^2 \beta_2^2 h_\theta^2 \alpha_{16}^2 + 4c_{\Phi,1}^2 \beta_3^2 h_\theta^2 \alpha_{16}^2 \\
 & + 4c_{\Phi,2}^2 \beta_3^2 h_\theta^2 \alpha_{16}^2 + 4c_{\Phi,3}^2 \beta_3^2 h_\theta^2 \alpha_{16}^2 + 48(\partial_\theta(a_{\Phi,1} \beta_1))^2 + 48(\partial_\theta(a_{\Phi,2} \beta_1))^2 \\
 & + 12(\partial_\theta(b_{\Phi,1} \beta_2))^2 + 12(\partial_\theta(b_{\Phi,2} \beta_2))^2 + 12(\partial_\theta(b_{\Phi,3} \beta_2))^2 + 12(\partial_\theta(c_{\Phi,1} \beta_3))^2 \\
 & + 12(\partial_\theta(c_{\Phi,2} \beta_3))^2 + 12(\partial_\theta(c_{\Phi,3} \beta_3))^2 - 6b_{\Phi,2} \beta_2 c_{\Phi,2} \beta_3 a_\theta \alpha_9 c_\theta \alpha_{11} + 6b_{\Phi,3} \beta_2 c_{\Phi,2} \beta_3 b_\theta \alpha_{10} c_\theta \alpha_{11} \\
 & - 6b_{\Phi,3} \beta_2 c_{\Phi,2} \beta_3 a_\theta \alpha_9 d_\theta \alpha_{12} - 6b_{\Phi,2} \beta_2 c_{\Phi,2} \beta_3 b_\theta \alpha_{10} d_\theta \alpha_{12} - 12a_{\Phi,2} \beta_1 c_{\Phi,2} \beta_3 b_\theta \alpha_{10} e_\theta \alpha_{13} \\
 & - 12a_{\Phi,2} \beta_1 b_{\Phi,3} \beta_2 c_\theta \alpha_{11} e_\theta \alpha_{13} - 12a_{\Phi,2} \beta_1 b_{\Phi,2} \beta_2 d_\theta \alpha_{12} e_\theta \alpha_{13} - 12a_{\Phi,2} \beta_1 c_{\Phi,2} \beta_3 a_\theta \alpha_9 f_\theta \alpha_{14} \\
 & + 12a_{\Phi,2} \beta_1 b_{\Phi,2} \beta_2 c_\theta \alpha_{11} f_\theta \alpha_{14} - 12a_{\Phi,2} \beta_1 b_{\Phi,3} \beta_2 d_\theta \alpha_{12} f_\theta \alpha_{14} - 12a_{\Phi,2} \beta_1 c_{\Phi,2} \beta_3 c_\theta \alpha_{11} g_\theta \alpha_{15} \\
 & - 6b_{\Phi,3} \beta_2 c_{\Phi,2} \beta_3 e_\theta \alpha_{13} g_\theta \alpha_{15} + 6b_{\Phi,2} \beta_2 c_{\Phi,2} \beta_3 f_\theta \alpha_{14} g_\theta \alpha_{15} + 8\sqrt{3}a_{\Phi,2} \beta_1 b_{\Phi,2} \beta_2 a_\theta \alpha_9 h_\theta \alpha_{16} \\
 & - 8\sqrt{3}a_{\Phi,2} \beta_1 b_{\Phi,3} \beta_2 b_\theta \alpha_{10} h_\theta \alpha_{16} + 4\sqrt{3}a_{\Phi,2} \beta_1 c_{\Phi,2} \beta_3 c_\theta \alpha_{11} h_\theta \alpha_{16} \\
 & - 2\sqrt{3}b_{\Phi,3} \beta_2 c_{\Phi,2} \beta_3 e_\theta \alpha_{13} h_\theta \alpha_{16} + 2\sqrt{3}b_{\Phi,2} \beta_2 c_{\Phi,2} \beta_3 f_\theta \alpha_{14} h_\theta \alpha_{16} + 8\sqrt{3}a_{\Phi,2}^2 \beta_1^2 g_\theta \alpha_{15} h_\theta \alpha_{16}
 \end{aligned}$$

$$\begin{aligned}
 & - 2\sqrt{3}b_{\Phi,1}^2\beta_2^2g_\theta\alpha_{15}h_\theta\alpha_{16} - 2\sqrt{3}b_{\Phi,2}^2\beta_2^2g_\theta\alpha_{15}h_\theta\alpha_{16} - 2\sqrt{3}b_{\Phi,3}^2\beta_2^2g_\theta\alpha_{15}h_\theta\alpha_{16} \\
 & + 24b_{\Phi,2}\beta_2a_\theta\alpha_9\partial_\theta(a_{\Phi,1}\beta_1) - 24b_{\Phi,3}\beta_2b_\theta\alpha_{10}\partial_\theta(a_{\Phi,1}\beta_1) - 24c_{\Phi,2}\beta_3c_\theta\alpha_{11}\partial_\theta(a_{\Phi,1}\beta_1) \\
 & + 48a_{\Phi,2}\beta_1g_\theta\alpha_{15}\partial_\theta(a_{\Phi,1}\beta_1) + 16\sqrt{3}a_{\Phi,2}\beta_1h_\theta\alpha_{16}\partial_\theta(a_{\Phi,1}\beta_1) + 24b_{\Phi,3}\beta_2a_\theta\alpha_9\partial_\theta(a_{\Phi,2}\beta_1) \\
 & + 24b_{\Phi,2}\beta_2b_\theta\alpha_{10}\partial_\theta(a_{\Phi,2}\beta_1) - 24c_{\Phi,2}\beta_3d_\theta\alpha_{12}\partial_\theta(a_{\Phi,2}\beta_1) - 24a_{\Phi,2}\beta_1b_\theta\alpha_{10}\partial_\theta(b_{\Phi,2}\beta_2) \\
 & + 12c_{\Phi,2}\beta_3e_\theta\alpha_{13}\partial_\theta(b_{\Phi,2}\beta_2) - 12b_{\Phi,3}\beta_2g_\theta\alpha_{15}\partial_\theta(b_{\Phi,2}\beta_2) + 4\sqrt{3}b_{\Phi,3}\beta_2h_\theta\alpha_{16}\partial_\theta(b_{\Phi,2}\beta_2) \\
 & - 24a_{\Phi,2}\beta_1a_\theta\alpha_9\partial_\theta(b_{\Phi,3}\beta_2) + 12c_{\Phi,2}\beta_3f_\theta\alpha_{14}\partial_\theta(b_{\Phi,3}\beta_2) + 12b_{\Phi,2}\beta_2g_\theta\alpha_{15}\partial_\theta(b_{\Phi,3}\beta_2) \\
 & - 4\sqrt{3}b_{\Phi,2}\beta_2h_\theta\alpha_{16}\partial_\theta(b_{\Phi,3}\beta_2) + 8\sqrt{3}c_{\Phi,3}\beta_3h_\theta\alpha_{16}\partial_\theta(c_{\Phi,1}\beta_3) + 24a_{\Phi,2}\beta_1d_\theta\alpha_{12}\partial_\theta(c_{\Phi,2}\beta_3) \\
 & - 12b_{\Phi,2}\beta_2e_\theta\alpha_{13}\partial_\theta(c_{\Phi,2}\beta_3) - 12b_{\Phi,3}\beta_2f_\theta\alpha_{14}\partial_\theta(c_{\Phi,2}\beta_3) - 8\sqrt{3}c_{\Phi,1}\beta_3h_\theta\alpha_{16}\partial_\theta(c_{\Phi,3}\beta_3) \\
 & - 2\sin(2(\alpha - \phi)) \left( 6(c_{\Phi,1}\beta_3f_\theta\alpha_{14} - c_{\Phi,3}\beta_3e_\theta\alpha_{13})\partial_\theta(b_{\Phi,1}\beta_2) + b_{\Phi,1}\beta_2 \left( c_{\Phi,1}\beta_3 \left( 3b_\theta\alpha_{10}c_\theta\alpha_{11} \right. \right. \right. \\
 & \left. \left. \left. - 3a_\theta\alpha_9d_\theta\alpha_{12} - e_\theta\alpha_{13} \left( 3g_\theta\alpha_{15} + \sqrt{3}h_\theta\alpha_{16} \right) \right) + c_{\Phi,3}\beta_3 \left( 3a_\theta\alpha_9c_\theta\alpha_{11} + 3b_\theta\alpha_{10}d_\theta\alpha_{12} \right. \right. \\
 & \left. \left. - f_\theta\alpha_{14} \left( 3g_\theta\alpha_{15} + \sqrt{3}h_\theta\alpha_{16} \right) \right) - 6f_\theta\alpha_{14}\partial_\theta(c_{\Phi,1}\beta_3) + 6e_\theta\alpha_{13}\partial_\theta(c_{\Phi,3}\beta_3) \right) \right) \\
 & + 2\cos(2(\alpha - \phi)) \left( b_{\Phi,1}\beta_2 \left( c_{\Phi,3}\beta_3 \left( - 3b_\theta\alpha_{10}c_\theta\alpha_{11} + 3a_\theta\alpha_9d_\theta\alpha_{12} + e_\theta\alpha_{13} \left( 3g_\theta\alpha_{15} \right. \right. \right. \right. \\
 & \left. \left. \left. + \sqrt{3}h_\theta\alpha_{16} \right) \right) + c_{\Phi,1}\beta_3 \left( 3a_\theta\alpha_9c_\theta\alpha_{11} + 3b_\theta\alpha_{10}d_\theta\alpha_{12} - f_\theta\alpha_{14} \left( 3g_\theta\alpha_{15} + \sqrt{3}h_\theta\alpha_{16} \right) \right) \right. \\
 & \left. + 6e_\theta\alpha_{13}\partial_\theta(c_{\Phi,1}\beta_3) + 6f_\theta\alpha_{14}\partial_\theta(c_{\Phi,3}\beta_3) \right) - 6(c_{\Phi,1}\beta_3e_\theta\alpha_{13} + c_{\Phi,3}\beta_3f_\theta\alpha_{14})\partial_\theta(b_{\Phi,1}\beta_2) \\
 & - 2\sin(\alpha - \phi) \left( 3c_{\Phi,1}\beta_3c_{\Phi,2}\beta_3c_\theta^2\alpha_{11}^2 + 3b_{\Phi,3}\beta_2c_{\Phi,3}\beta_3a_\theta\alpha_9c_\theta\alpha_{11} + 3b_{\Phi,3}\beta_2c_{\Phi,1}\beta_3b_\theta\alpha_{10}c_\theta\alpha_{11} \right. \\
 & \left. - 6a_{\Phi,2}\beta_1c_{\Phi,1}\beta_3g_\theta\alpha_{15}c_\theta\alpha_{11} - 6a_{\Phi,1}\beta_1c_{\Phi,3}\beta_3g_\theta\alpha_{15}c_\theta\alpha_{11} + 2\sqrt{3}a_{\Phi,2}\beta_1c_{\Phi,1}\beta_3h_\theta\alpha_{16}c_\theta\alpha_{11} \right. \\
 & \left. + 2\sqrt{3}a_{\Phi,1}\beta_1c_{\Phi,3}\beta_3h_\theta\alpha_{16}c_\theta\alpha_{11} - 12c_{\Phi,1}\beta_3\partial_\theta(a_{\Phi,1}\beta_1)c_\theta\alpha_{11} + 12c_{\Phi,3}\beta_3\partial_\theta(a_{\Phi,2}\beta_1)c_\theta\alpha_{11} \right. \\
 & \left. + 12a_{\Phi,1}\beta_1\partial_\theta(c_{\Phi,1}\beta_3)c_\theta\alpha_{11} - 12a_{\Phi,2}\beta_1\partial_\theta(c_{\Phi,3}\beta_3)c_\theta\alpha_{11} + 3c_{\Phi,1}\beta_3c_{\Phi,2}\beta_3d_\theta^2\alpha_{12}^2 \right. \\
 & \left. + 3c_{\Phi,1}\beta_3c_{\Phi,2}\beta_3e_\theta^2\alpha_{13}^2 + 3c_{\Phi,1}\beta_3c_{\Phi,2}\beta_3f_\theta^2\alpha_{14}^2 + 4c_{\Phi,1}\beta_3c_{\Phi,2}\beta_3h_\theta^2\alpha_{16}^2 \right. \\
 & \left. - 3b_{\Phi,3}\beta_2c_{\Phi,1}\beta_3a_\theta\alpha_9d_\theta\alpha_{12} + 3b_{\Phi,3}\beta_2c_{\Phi,3}\beta_3b_\theta\alpha_{10}d_\theta\alpha_{12} - 6a_{\Phi,1}\beta_1c_{\Phi,1}\beta_3a_\theta\alpha_9e_\theta\alpha_{13} \right. \\
 & \left. + 6a_{\Phi,2}\beta_1c_{\Phi,3}\beta_3a_\theta\alpha_9e_\theta\alpha_{13} - 6a_{\Phi,2}\beta_1c_{\Phi,1}\beta_3b_\theta\alpha_{10}e_\theta\alpha_{13} - 6a_{\Phi,1}\beta_1c_{\Phi,3}\beta_3b_\theta\alpha_{10}e_\theta\alpha_{13} \right. \\
 & \left. + 6a_{\Phi,1}\beta_1c_{\Phi,1}\beta_3d_\theta\alpha_{12}g_\theta\alpha_{15} - 6a_{\Phi,2}\beta_1c_{\Phi,3}\beta_3d_\theta\alpha_{12}g_\theta\alpha_{15} - 3b_{\Phi,3}\beta_2c_{\Phi,1}\beta_3e_\theta\alpha_{13}g_\theta\alpha_{15} \right. \\
 & \left. - 2\sqrt{3}a_{\Phi,1}\beta_1c_{\Phi,1}\beta_3d_\theta\alpha_{12}h_\theta\alpha_{16} + 2\sqrt{3}a_{\Phi,2}\beta_1c_{\Phi,3}\beta_3d_\theta\alpha_{12}h_\theta\alpha_{16} - \sqrt{3}b_{\Phi,3}\beta_2c_{\Phi,1}\beta_3e_\theta\alpha_{13}h_\theta\alpha_{16} \right. \\
 & \left. - 12c_{\Phi,3}\beta_3d_\theta\alpha_{12}\partial_\theta(a_{\Phi,1}\beta_1) - 12c_{\Phi,1}\beta_3d_\theta\alpha_{12}\partial_\theta(a_{\Phi,2}\beta_1) - 12a_{\Phi,1}\beta_1a_\theta\alpha_9\partial_\theta(b_{\Phi,1}\beta_2) \right)
 \end{aligned}$$

$$\begin{aligned}
 & - 12a_{\Phi,2}\beta_1\theta\alpha_{10}\partial_\theta(b_{\Phi,1}\beta_2) + 6c_{\Phi,2}\beta_3e_\theta\alpha_{13}\partial_\theta(b_{\Phi,1}\beta_2) - 6b_{\Phi,3}\beta_2g_\theta\alpha_{15}\partial_\theta(b_{\Phi,1}\beta_2) \\
 & + 2\sqrt{3}b_{\Phi,3}\beta_2h_\theta\alpha_{16}\partial_\theta(b_{\Phi,1}\beta_2) + 6c_{\Phi,1}\beta_3e_\theta\alpha_{13}\partial_\theta(b_{\Phi,2}\beta_2) + 12\partial_\theta(b_{\Phi,1}\beta_2)\partial_\theta(b_{\Phi,2}\beta_2) \\
 & - 6c_{\Phi,3}\beta_3e_\theta\alpha_{13}\partial_\theta(b_{\Phi,3}\beta_2) + 12a_{\Phi,2}\beta_1d_\theta\alpha_{12}\partial_\theta(c_{\Phi,1}\beta_3) - f_\theta\alpha_{14}\left(6a_{\Phi,1}\beta_1(c_{\Phi,3}\beta_3a_\theta\alpha_9\right. \\
 & \left.- c_{\Phi,1}\beta_3b_\theta\alpha_{10}) + 6a_{\Phi,2}\beta_1(c_{\Phi,1}\beta_3a_\theta\alpha_9 + c_{\Phi,3}\beta_3b_\theta\alpha_{10}) + 3b_{\Phi,3}\beta_2c_{\Phi,3}\beta_3g_\theta\alpha_{15}\right. \\
 & \left.+ \sqrt{3}b_{\Phi,3}\beta_2c_{\Phi,3}\beta_3h_\theta\alpha_{16} - 6c_{\Phi,3}\beta_3\partial_\theta(b_{\Phi,2}\beta_2) - 6c_{\Phi,1}\beta_3\partial_\theta(b_{\Phi,3}\beta_2) + 6b_{\Phi,3}\beta_2\partial_\theta(c_{\Phi,1}\beta_3)\right) \\
 & + 4\sqrt{3}c_{\Phi,3}\beta_3h_\theta\alpha_{16}\partial_\theta(c_{\Phi,2}\beta_3) + 12\partial_\theta(c_{\Phi,1}\beta_3)\partial_\theta(c_{\Phi,2}\beta_3) + b_{\Phi,1}\beta_2\left(b_{\Phi,2}\beta_2\left(3a_\theta^2\alpha_9^2\right.\right. \\
 & \left.+ 3b_\theta^2\alpha_{10}^2 + 3e_\theta^2\alpha_{13}^2 + 3f_\theta^2\alpha_{14}^2 + 3g_\theta^2\alpha_{15}^2 + h_\theta^2\alpha_{16}^2 - 2\sqrt{3}g_\theta\alpha_{15}h_\theta\alpha_{16}\right) + c_{\Phi,2}\beta_3\left(-3a_\theta\alpha_9c_\theta\alpha_{11}\right. \\
 & \left.- 3b_\theta\alpha_{10}d_\theta\alpha_{12} + f_\theta\alpha_{14}\left(3g_\theta\alpha_{15} + \sqrt{3}h_\theta\alpha_{16}\right)\right) + 2\left(3(a_{\Phi,2}\beta_1c_\theta\alpha_{11} - a_{\Phi,1}\beta_1d_\theta\alpha_{12})f_\theta\alpha_{14}\right. \\
 & \left.+ 2\sqrt{3}a_{\Phi,2}\beta_1a_\theta\alpha_9h_\theta\alpha_{16} - 2\sqrt{3}a_{\Phi,1}\beta_1b_\theta\alpha_{10}h_\theta\alpha_{16} + 6a_\theta\alpha_9\partial_\theta(a_{\Phi,1}\beta_1) + 6b_\theta\alpha_{10}\partial_\theta(a_{\Phi,2}\beta_1)\right. \\
 & \left.+ 3g_\theta\alpha_{15}\partial_\theta(b_{\Phi,3}\beta_2) - \sqrt{3}h_\theta\alpha_{16}\partial_\theta(b_{\Phi,3}\beta_2) - 3e_\theta\alpha_{13}\left(a_{\Phi,1}\beta_1c_\theta\alpha_{11} + a_{\Phi,2}\beta_1d_\theta\alpha_{12}\right.\right. \\
 & \left.\left.+ \partial_\theta(c_{\Phi,2}\beta_3)\right)\right) + 12a_{\Phi,1}\beta_1d_\theta\alpha_{12}\partial_\theta(c_{\Phi,3}\beta_3) + 6b_{\Phi,3}\beta_2e_\theta\alpha_{13}\partial_\theta(c_{\Phi,3}\beta_3) \\
 & - 4\sqrt{3}c_{\Phi,2}\beta_3h_\theta\alpha_{16}\partial_\theta(c_{\Phi,3}\beta_3) - b_{\Phi,2}\beta_2\left(c_{\Phi,3}\beta_3\left(-3b_\theta\alpha_{10}c_\theta\alpha_{11} + 3a_\theta\alpha_9d_\theta\alpha_{12}\right.\right. \\
 & \left.\left.+ e_\theta\alpha_{13}\left(3g_\theta\alpha_{15} + \sqrt{3}h_\theta\alpha_{16}\right)\right) + c_{\Phi,1}\beta_3\left(3a_\theta\alpha_9c_\theta\alpha_{11} + 3b_\theta\alpha_{10}d_\theta\alpha_{12} - f_\theta\alpha_{14}\left(3g_\theta\alpha_{15}\right.\right.\right. \\
 & \left.\left.\left.+ \sqrt{3}h_\theta\alpha_{16}\right)\right) + 6e_\theta\alpha_{13}\partial_\theta(c_{\Phi,1}\beta_3) + 6f_\theta\alpha_{14}\partial_\theta(c_{\Phi,3}\beta_3)\right)\right) \\
 & + 2\cos(\alpha - \phi)\left(-3c_{\Phi,2}\beta_3c_{\Phi,3}\beta_3c_\theta^2\alpha_{11}^2 + 3b_{\Phi,2}\beta_2c_{\Phi,3}\beta_3a_\theta\alpha_9c_\theta\alpha_{11} + 3b_{\Phi,2}\beta_2c_{\Phi,1}\beta_3b_\theta\alpha_{10}c_\theta\alpha_{11}\right. \\
 & \left.- 6a_{\Phi,1}\beta_1c_{\Phi,1}\beta_3g_\theta\alpha_{15}c_\theta\alpha_{11} + 6a_{\Phi,2}\beta_1c_{\Phi,3}\beta_3g_\theta\alpha_{15}c_\theta\alpha_{11} + 2\sqrt{3}a_{\Phi,1}\beta_1c_{\Phi,1}\beta_3h_\theta\alpha_{16}c_\theta\alpha_{11}\right. \\
 & \left.- 2\sqrt{3}a_{\Phi,2}\beta_1c_{\Phi,3}\beta_3h_\theta\alpha_{16}c_\theta\alpha_{11} + 12c_{\Phi,3}\beta_3\partial_\theta(a_{\Phi,1}\beta_1)c_\theta\alpha_{11} + 12c_{\Phi,1}\beta_3\partial_\theta(a_{\Phi,2}\beta_1)c_\theta\alpha_{11}\right. \\
 & \left.- 12a_{\Phi,2}\beta_1\partial_\theta(c_{\Phi,1}\beta_3)c_\theta\alpha_{11} - 12a_{\Phi,1}\beta_1\partial_\theta(c_{\Phi,3}\beta_3)c_\theta\alpha_{11} - 3c_{\Phi,2}\beta_3c_{\Phi,3}\beta_3d_\theta^2\alpha_{12}^2\right. \\
 & \left.- 3c_{\Phi,2}\beta_3c_{\Phi,3}\beta_3e_\theta^2\alpha_{13}^2 - 3c_{\Phi,2}\beta_3c_{\Phi,3}\beta_3f_\theta^2\alpha_{14}^2 - 4c_{\Phi,2}\beta_3c_{\Phi,3}\beta_3h_\theta^2\alpha_{16}^2 - 3b_{\Phi,2}\beta_2c_{\Phi,1}\beta_3a_\theta\alpha_9d_\theta\alpha_{12}\right. \\
 & \left.+ 3b_{\Phi,2}\beta_2c_{\Phi,3}\beta_3b_\theta\alpha_{10}d_\theta\alpha_{12} + 6a_{\Phi,2}\beta_1c_{\Phi,1}\beta_3a_\theta\alpha_9e_\theta\alpha_{13} + 6a_{\Phi,1}\beta_1c_{\Phi,3}\beta_3a_\theta\alpha_9e_\theta\alpha_{13}\right. \\
 & \left.- 6a_{\Phi,1}\beta_1c_{\Phi,1}\beta_3b_\theta\alpha_{10}e_\theta\alpha_{13} + 6a_{\Phi,2}\beta_1c_{\Phi,3}\beta_3b_\theta\alpha_{10}e_\theta\alpha_{13} - 6a_{\Phi,2}\beta_1c_{\Phi,1}\beta_3d_\theta\alpha_{12}g_\theta\alpha_{15}\right. \\
 & \left.- 6a_{\Phi,1}\beta_1c_{\Phi,3}\beta_3d_\theta\alpha_{12}g_\theta\alpha_{15} - 3b_{\Phi,2}\beta_2c_{\Phi,1}\beta_3e_\theta\alpha_{13}g_\theta\alpha_{15} + 2\sqrt{3}a_{\Phi,2}\beta_1c_{\Phi,1}\beta_3d_\theta\alpha_{12}h_\theta\alpha_{16}\right. \\
 & \left.+ 2\sqrt{3}a_{\Phi,1}\beta_1c_{\Phi,3}\beta_3d_\theta\alpha_{12}h_\theta\alpha_{16} - \sqrt{3}b_{\Phi,2}\beta_2c_{\Phi,1}\beta_3e_\theta\alpha_{13}h_\theta\alpha_{16} - 12c_{\Phi,1}\beta_3d_\theta\alpha_{12}\partial_\theta(a_{\Phi,1}\beta_1)\right. \\
 & \left.+ 12c_{\Phi,3}\beta_3d_\theta\alpha_{12}\partial_\theta(a_{\Phi,2}\beta_1) - 12a_{\Phi,2}\beta_1a_\theta\alpha_9\partial_\theta(b_{\Phi,1}\beta_2) + 12a_{\Phi,1}\beta_1b_\theta\alpha_{10}\partial_\theta(b_{\Phi,1}\beta_2)\right)
 \end{aligned}$$

$$\begin{aligned}
 & + 6b_{\Phi,2}\beta_2g_\theta\alpha_{15}\partial_\theta(b_{\Phi,1}\beta_2) - 2\sqrt{3}b_{\Phi,2}\beta_2h_\theta\alpha_{16}\partial_\theta(b_{\Phi,1}\beta_2) - 6c_{\Phi,3}\beta_3e_\theta\alpha_{13}\partial_\theta(b_{\Phi,2}\beta_2) \\
 & - 6c_{\Phi,1}\beta_3e_\theta\alpha_{13}\partial_\theta(b_{\Phi,3}\beta_2) + 12\partial_\theta(b_{\Phi,1}\beta_2)\partial_\theta(b_{\Phi,3}\beta_2) + 12a_{\Phi,1}\beta_1d_\theta\alpha_{12}\partial_\theta(c_{\Phi,1}\beta_3) \\
 & - 4\sqrt{3}c_{\Phi,2}\beta_3h_\theta\alpha_{16}\partial_\theta(c_{\Phi,1}\beta_3) - f_\theta\alpha_{14}\left(a_{\Phi,2}\beta_1(6c_{\Phi,1}\beta_3b_\theta\alpha_{10} - 6c_{\Phi,3}\beta_3a_\theta\alpha_9)\right. \\
 & + 6a_{\Phi,1}\beta_1(c_{\Phi,1}\beta_3a_\theta\alpha_9 + c_{\Phi,3}\beta_3b_\theta\alpha_{10}) + 3b_{\Phi,2}\beta_2c_{\Phi,3}\beta_3g_\theta\alpha_{15} + \sqrt{3}b_{\Phi,2}\beta_2c_{\Phi,3}\beta_3h_\theta\alpha_{16} \\
 & - 6c_{\Phi,2}\beta_3\partial_\theta(b_{\Phi,1}\beta_2) - 6c_{\Phi,1}\beta_3\partial_\theta(b_{\Phi,2}\beta_2) + 6c_{\Phi,3}\beta_3\partial_\theta(b_{\Phi,3}\beta_2) + 6b_{\Phi,2}\beta_2\partial_\theta(c_{\Phi,1}\beta_3)\Big) \\
 & + 4\sqrt{3}c_{\Phi,1}\beta_3h_\theta\alpha_{16}\partial_\theta(c_{\Phi,2}\beta_3) + b_{\Phi,1}\beta_2\left(b_{\Phi,3}\beta_2\left(3a_\theta^2\alpha_9^2 + 3b_\theta^2\alpha_{10}^2 + 3e_\theta^2\alpha_{13}^2 + 3f_\theta^2\alpha_{14}^2\right.\right. \\
 & \left.\left.+ 3g_\theta^2\alpha_{15}^2 + h_\theta^2\alpha_{16}^2 - 2\sqrt{3}g_\theta\alpha_{15}h_\theta\alpha_{16}\right) + c_{\Phi,2}\beta_3\left(3b_\theta\alpha_{10}c_\theta\alpha_{11} - 3a_\theta\alpha_9d_\theta\alpha_{12}\right.\right. \\
 & \left.\left.- e_\theta\alpha_{13}(3g_\theta\alpha_{15} + \sqrt{3}h_\theta\alpha_{16})\right) + 2\left(a_{\Phi,1}\beta_1\left(3d_\theta\alpha_{12}e_\theta\alpha_{13} - 3c_\theta\alpha_{11}f_\theta\alpha_{14} - 2\sqrt{3}a_\theta\alpha_9h_\theta\alpha_{16}\right)\right.\right. \\
 & \left.\left.- a_{\Phi,2}\beta_1\left(3c_\theta\alpha_{11}e_\theta\alpha_{13} + 3d_\theta\alpha_{12}f_\theta\alpha_{14} + 2\sqrt{3}b_\theta\alpha_{10}h_\theta\alpha_{16}\right) - 6b_\theta\alpha_{10}\partial_\theta(a_{\Phi,1}\beta_1)\right.\right. \\
 & \left.\left.+ 6a_\theta\alpha_9\partial_\theta(a_{\Phi,2}\beta_1) + (\sqrt{3}h_\theta\alpha_{16} - 3g_\theta\alpha_{15})\partial_\theta(b_{\Phi,2}\beta_2) - 3f_\theta\alpha_{14}\partial_\theta(c_{\Phi,2}\beta_3)\right)\right) \\
 & - 12a_{\Phi,2}\beta_1d_\theta\alpha_{12}\partial_\theta(c_{\Phi,3}\beta_3) + 6b_{\Phi,2}\beta_2e_\theta\alpha_{13}\partial_\theta(c_{\Phi,3}\beta_3) - 12\partial_\theta(c_{\Phi,2}\beta_3)\partial_\theta(c_{\Phi,3}\beta_3) \\
 & + b_{\Phi,3}\beta_2\left(c_{\Phi,3}\beta_3\left(-3b_\theta\alpha_{10}c_\theta\alpha_{11} + 3a_\theta\alpha_9d_\theta\alpha_{12} + e_\theta\alpha_{13}(3g_\theta\alpha_{15} + \sqrt{3}h_\theta\alpha_{16})\right)\right. \\
 & \left.+ c_{\Phi,1}\beta_3\left(3a_\theta\alpha_9c_\theta\alpha_{11} + 3b_\theta\alpha_{10}d_\theta\alpha_{12} - f_\theta\alpha_{14}(3g_\theta\alpha_{15} + \sqrt{3}h_\theta\alpha_{16})\right) + 6e_\theta\alpha_{13}\partial_\theta(c_{\Phi,1}\beta_3)\right. \\
 & \left.+ 6f_\theta\alpha_{14}\partial_\theta(c_{\Phi,3}\beta_3)\right)\Big) \\
 & + \frac{v^2}{96r^2\sin^2\theta}\left\{12a_\phi^2\alpha_1^2a_{\Phi,1}^2\beta_1^2 + 12b_\phi^2\alpha_2^2a_{\Phi,1}^2\beta_1^2 + 12c_\phi^2\alpha_3^2a_{\Phi,1}^2\beta_1^2 + 12d_\phi^2\alpha_4^2a_{\Phi,1}^2\beta_1^2\right. \\
 & + 12g_\phi^2\alpha_7^2a_{\Phi,1}^2\beta_1^2 + 4h_\phi^2\alpha_8^2a_{\Phi,1}^2\beta_1^2 + 8\sqrt{3}g_\phi\alpha_7h_\phi\alpha_8a_{\Phi,1}^2\beta_1^2 + 24b_{\Phi,3}\beta_2a_\phi\alpha_1a_{\Phi,1}\beta_1 \\
 & + 24b_{\Phi,2}\beta_2b_\phi\alpha_2a_{\Phi,1}\beta_1 + 24c_{\Phi,2}\beta_3d_\phi\alpha_4a_{\Phi,1}\beta_1 - 12c_{\Phi,2}\beta_3a_\phi\alpha_1e_\phi\alpha_5a_{\Phi,1}\beta_1 \\
 & - 12b_{\Phi,2}\beta_2c_\phi\alpha_3e_\phi\alpha_5a_{\Phi,1}\beta_1 + 12b_{\Phi,3}\beta_2d_\phi\alpha_4e_\phi\alpha_5a_{\Phi,1}\beta_1 + 12c_{\Phi,2}\beta_3b_\phi\alpha_2f_\phi\alpha_6a_{\Phi,1}\beta_1 \\
 & - 12b_{\Phi,3}\beta_2c_\phi\alpha_3f_\phi\alpha_6a_{\Phi,1}\beta_1 - 12b_{\Phi,2}\beta_2d_\phi\alpha_4f_\phi\alpha_6a_{\Phi,1}\beta_1 + 12c_{\Phi,2}\beta_3d_\phi\alpha_4g_\phi\alpha_7a_{\Phi,1}\beta_1 \\
 & - 8\sqrt{3}b_{\Phi,3}\beta_2a_\phi\alpha_1h_\phi\alpha_8a_{\Phi,1}\beta_1 - 8\sqrt{3}b_{\Phi,2}\beta_2b_\phi\alpha_2h_\phi\alpha_8a_{\Phi,1}\beta_1 - 4\sqrt{3}c_{\Phi,2}\beta_3d_\phi\alpha_4h_\phi\alpha_8a_{\Phi,1}\beta_1 \\
 & + 12b_{\Phi,2}^2\beta_2^2 + 12b_{\Phi,3}^2\beta_2^2 + 12c_{\Phi,2}^2\beta_3^2 + 12a_{\Phi,2}^2\beta_1^2a_\phi^2\alpha_1^2 + 3b_{\Phi,1}^2\beta_2^2a_\phi^2\alpha_1^2 + 3b_{\Phi,2}^2\beta_2^2a_\phi^2\alpha_1^2 \\
 & + 3b_{\Phi,3}^2\beta_2^2a_\phi^2\alpha_1^2 + 12a_{\Phi,2}^2\beta_1^2b_\phi^2\alpha_2^2 + 3b_{\Phi,1}^2\beta_2^2b_\phi^2\alpha_2^2 + 3b_{\Phi,2}^2\beta_2^2b_\phi^2\alpha_2^2 + 3b_{\Phi,3}^2\beta_2^2b_\phi^2\alpha_2^2 \\
 & + 12a_{\Phi,2}^2\beta_1^2c_\phi^2\alpha_3^2 + 3c_{\Phi,1}^2\beta_3^2c_\phi^2\alpha_3^2 + 3c_{\Phi,2}^2\beta_3^2c_\phi^2\alpha_3^2 + 3c_{\Phi,3}^2\beta_3^2c_\phi^2\alpha_3^2 + 12a_{\Phi,2}^2\beta_1^2d_\phi^2\alpha_4^2
 \end{aligned}$$

$$\begin{aligned}
 & + 3c_{\Phi,1}^2\beta_3^2d_\phi^2\alpha_4^2 + 3c_{\Phi,2}^2\beta_3^2d_\phi^2\alpha_4^2 + 3c_{\Phi,3}^2\beta_3^2d_\phi^2\alpha_4^2 + 3b_{\Phi,1}^2\beta_2^2e_\phi^2\alpha_5^2 + 3b_{\Phi,2}^2\beta_2^2e_\phi^2\alpha_5^2 \\
 & + 3b_{\Phi,3}^2\beta_2^2e_\phi^2\alpha_5^2 + 3c_{\Phi,1}^2\beta_3^2e_\phi^2\alpha_5^2 + 3c_{\Phi,2}^2\beta_3^2e_\phi^2\alpha_5^2 + 3c_{\Phi,3}^2\beta_3^2e_\phi^2\alpha_5^2 + 3b_{\Phi,1}^2\beta_2^2f_\phi^2\alpha_6^2 \\
 & + 3b_{\Phi,2}^2\beta_2^2f_\phi^2\alpha_6^2 + 3b_{\Phi,3}^2\beta_2^2f_\phi^2\alpha_6^2 + 3c_{\Phi,1}^2\beta_3^2f_\phi^2\alpha_6^2 + 3c_{\Phi,2}^2\beta_3^2f_\phi^2\alpha_6^2 + 3c_{\Phi,3}^2\beta_3^2f_\phi^2\alpha_6^2 \\
 & + 12a_{\Phi,2}^2\beta_1^2g_\phi^2\alpha_7^2 + 3b_{\Phi,1}^2\beta_2^2g_\phi^2\alpha_7^2 + 3b_{\Phi,2}^2\beta_2^2g_\phi^2\alpha_7^2 + 3b_{\Phi,3}^2\beta_2^2g_\phi^2\alpha_7^2 + 4a_{\Phi,2}^2\beta_1^2h_\phi^2\alpha_8^2 \\
 & + b_{\Phi,1}^2\beta_2^2h_\phi^2\alpha_8^2 + b_{\Phi,2}^2\beta_2^2h_\phi^2\alpha_8^2 + b_{\Phi,3}^2\beta_2^2h_\phi^2\alpha_8^2 + 4c_{\Phi,1}^2\beta_3^2h_\phi^2\alpha_8^2 + 4c_{\Phi,2}^2\beta_3^2h_\phi^2\alpha_8^2 + 4c_{\Phi,3}^2\beta_3^2h_\phi^2\alpha_8^2 \\
 & - 24a_{\Phi,2}\beta_1b_{\Phi,2}\beta_2a_\phi\alpha_1 + 24a_{\Phi,2}\beta_1b_{\Phi,3}\beta_2b_\phi\alpha_2 - 24a_{\Phi,2}\beta_1c_{\Phi,2}\beta_3c_\phi\alpha_3 \\
 & - 6b_{\Phi,2}\beta_2c_{\Phi,2}\beta_3a_\phi\alpha_1c_\phi\alpha_3 + 6b_{\Phi,3}\beta_2c_{\Phi,2}\beta_3b_\phi\alpha_2c_\phi\alpha_3 - 6b_{\Phi,3}\beta_2c_{\Phi,2}\beta_3a_\phi\alpha_1d_\phi\alpha_4 \\
 & - 6b_{\Phi,2}\beta_2c_{\Phi,2}\beta_3b_\phi\alpha_2d_\phi\alpha_4 - 12a_{\Phi,2}\beta_1c_{\Phi,2}\beta_3b_\phi\alpha_2e_\phi\alpha_5 - 12a_{\Phi,2}\beta_1b_{\Phi,3}\beta_2c_\phi\alpha_3e_\phi\alpha_5 \\
 & - 12a_{\Phi,2}\beta_1b_{\Phi,2}\beta_2d_\phi\alpha_4e_\phi\alpha_5 - 12a_{\Phi,2}\beta_1c_{\Phi,2}\beta_3a_\phi\alpha_1f_\phi\alpha_6 \\
 & + 12a_{\Phi,2}\beta_1b_{\Phi,2}\beta_2c_\phi\alpha_3f_\phi\alpha_6 - 12a_{\Phi,2}\beta_1b_{\Phi,3}\beta_2d_\phi\alpha_4f_\phi\alpha_6 + 12b_{\Phi,2}^2\beta_2^2g_\phi\alpha_7 + 12b_{\Phi,3}^2\beta_2^2g_\phi\alpha_7 \\
 & - 12a_{\Phi,2}\beta_1c_{\Phi,2}\beta_3c_\phi\alpha_3g_\phi\alpha_7 - 6b_{\Phi,3}\beta_2c_{\Phi,2}\beta_3e_\phi\alpha_5g_\phi\alpha_7 + 6b_{\Phi,2}\beta_2c_{\Phi,2}\beta_3f_\phi\alpha_6g_\phi\alpha_7 \\
 & - 4\sqrt{3}b_{\Phi,2}^2\beta_2^2h_\phi\alpha_8 - 4\sqrt{3}b_{\Phi,3}^2\beta_2^2h_\phi\alpha_8 - 8\sqrt{3}c_{\Phi,2}^2\beta_3^2h_\phi\alpha_8 + 8\sqrt{3}a_{\Phi,2}\beta_1b_{\Phi,2}\beta_2a_\phi\alpha_1h_\phi\alpha_8 \\
 & - 8\sqrt{3}a_{\Phi,2}\beta_1b_{\Phi,3}\beta_2b_\phi\alpha_2h_\phi\alpha_8 + 4\sqrt{3}a_{\Phi,2}\beta_1c_{\Phi,2}\beta_3c_\phi\alpha_3h_\phi\alpha_8 - 2\sqrt{3}b_{\Phi,3}\beta_2c_{\Phi,2}\beta_3e_\phi\alpha_5h_\phi\alpha_8 \\
 & + 2\sqrt{3}b_{\Phi,2}\beta_2c_{\Phi,2}\beta_3f_\phi\alpha_6h_\phi\alpha_8 + 8\sqrt{3}a_{\Phi,2}^2\beta_1^2g_\phi\alpha_7h_\phi\alpha_8 - 2\sqrt{3}b_{\Phi,1}^2\beta_2^2g_\phi\alpha_7h_\phi\alpha_8 \\
 & - 2\sqrt{3}b_{\Phi,2}^2\beta_2^2g_\phi\alpha_7h_\phi\alpha_8 - 2\sqrt{3}b_{\Phi,3}^2\beta_2^2g_\phi\alpha_7h_\phi\alpha_8 + 2\cos(2(\alpha - \phi))b_{\Phi,1}\beta_2\left(c_{\Phi,3}\beta_3\left(-3b_\phi\alpha_2c_\phi\alpha_3\right.\right. \\
 & \left.\left.+ 3a_\phi\alpha_1d_\phi\alpha_4 + e_\phi\alpha_5\left(3g_\phi\alpha_7 + \sqrt{3}h_\phi\alpha_8\right)\right) + c_{\Phi,1}\beta_3\left(3a_\phi\alpha_1c_\phi\alpha_3 + 3b_\phi\alpha_2d_\phi\alpha_4 - f_\phi\alpha_6\left(3g_\phi\alpha_7\right.\right. \\
 & \left.\left.+\sqrt{3}h_\phi\alpha_8\right)\right) + 2\cos(\alpha - \phi)\left(-3c_{\Phi,2}\beta_3c_{\Phi,3}\beta_3c_\phi^2\alpha_3^2 + 3b_{\Phi,2}\beta_2c_{\Phi,3}\beta_3a_\phi\alpha_1c_\phi\alpha_3\right. \\
 & \left.\left.+ 3b_{\Phi,2}\beta_2c_{\Phi,1}\beta_3b_\phi\alpha_2c_\phi\alpha_3 + 2\sqrt{3}a_{\Phi,1}\beta_1c_{\Phi,1}\beta_3h_\phi\alpha_8c_\phi\alpha_3 - 2\sqrt{3}a_{\Phi,2}\beta_1c_{\Phi,3}\beta_3h_\phi\alpha_8c_\phi\alpha_3\right.\right. \\
 & \left.\left.- 3c_{\Phi,2}\beta_3c_{\Phi,3}\beta_3d_\phi^2\alpha_4^2 - 3c_{\Phi,2}\beta_3c_{\Phi,3}\beta_3e_\phi^2\alpha_5^2 - 3c_{\Phi,2}\beta_3c_{\Phi,3}\beta_3f_\phi^2\alpha_6^2 - 4c_{\Phi,2}\beta_3c_{\Phi,3}\beta_3h_\phi^2\alpha_8^2\right.\right. \\
 & \left.\left.- 3b_{\Phi,2}\beta_2c_{\Phi,1}\beta_3a_\phi\alpha_1d_\phi\alpha_4 + 3b_{\Phi,2}\beta_2c_{\Phi,3}\beta_3b_\phi\alpha_2d_\phi\alpha_4 - 6b_{\Phi,2}\beta_2c_{\Phi,1}\beta_3e_\phi\alpha_5\right.\right. \\
 & \left.\left.+ 6a_{\Phi,2}\beta_1c_{\Phi,1}\beta_3a_\phi\alpha_1e_\phi\alpha_5 + 6a_{\Phi,1}\beta_1c_{\Phi,3}\beta_3a_\phi\alpha_1e_\phi\alpha_5 - 6a_{\Phi,1}\beta_1c_{\Phi,1}\beta_3b_\phi\alpha_2e_\phi\alpha_5\right.\right. \\
 & \left.\left.+ 6a_{\Phi,2}\beta_1c_{\Phi,3}\beta_3b_\phi\alpha_2e_\phi\alpha_5 - 6b_{\Phi,2}\beta_2c_{\Phi,3}\beta_3f_\phi\alpha_6 - 6a_{\Phi,1}\beta_1c_{\Phi,1}\beta_3a_\phi\alpha_1f_\phi\alpha_6\right.\right. \\
 & \left.\left.+ 6a_{\Phi,2}\beta_1c_{\Phi,3}\beta_3a_\phi\alpha_1f_\phi\alpha_6 - 6a_{\Phi,2}\beta_1c_{\Phi,1}\beta_3b_\phi\alpha_2f_\phi\alpha_6 - 6a_{\Phi,1}\beta_1c_{\Phi,3}\beta_3b_\phi\alpha_2f_\phi\alpha_6\right.\right. \\
 & \left.\left.- 3(a_{\Phi,2}\beta_1(2c_{\Phi,1}\beta_3d_\phi\alpha_4 - 2c_{\Phi,3}\beta_3c_\phi\alpha_3) + 2a_{\Phi,1}\beta_1(c_{\Phi,1}\beta_3c_\phi\alpha_3 + c_{\Phi,3}\beta_3d_\phi\alpha_4) + \right.\right. \\
 & \left.\left.b_{\Phi,2}\beta_2(c_{\Phi,1}\beta_3e_\phi\alpha_5 + c_{\Phi,3}\beta_3f_\phi\alpha_6))g_\phi\alpha_7 + 4\sqrt{3}c_{\Phi,2}\beta_3c_{\Phi,3}\beta_3h_\phi\alpha_8 + 2\sqrt{3}a_{\Phi,2}\beta_1c_{\Phi,1}\beta_3d_\phi\alpha_4h_\phi\alpha_8\right.\right.
 \end{aligned}$$

$$\begin{aligned}
 & + 2\sqrt{3}a_{\Phi,1}\beta_1c_{\Phi,3}\beta_3d_{\phi}\alpha_4h_{\phi}\alpha_8 - \sqrt{3}b_{\Phi,2}\beta_2c_{\Phi,1}\beta_3e_{\phi}\alpha_5h_{\phi}\alpha_8 - \sqrt{3}b_{\Phi,2}\beta_2c_{\Phi,3}\beta_3f_{\phi}\alpha_6h_{\phi}\alpha_8 \\
 & + b_{\Phi,1}\beta_2\left(6(a_{\Phi,1}\beta_1d_{\phi}\alpha_4 - a_{\Phi,2}\beta_1c_{\phi}\alpha_3)e_{\phi}\alpha_5 - 6(a_{\Phi,1}\beta_1c_{\phi}\alpha_3 + a_{\Phi,2}\beta_1d_{\phi}\alpha_4)f_{\phi}\alpha_6\right. \\
 & \quad \left.- 4\sqrt{3}(a_{\Phi,1}\beta_1a_{\phi}\alpha_1 + a_{\Phi,2}\beta_1b_{\phi}\alpha_2)h_{\phi}\alpha_8 + b_{\Phi,3}\beta_2\left(3a_{\phi}^2\alpha_1^2 + 3b_{\phi}^2\alpha_2^2 + 3e_{\phi}^2\alpha_5^2 + 3f_{\phi}^2\alpha_6^2\right.\right. \\
 & \quad \left.+ h_{\phi}^2\alpha_8^2 + 3g_{\phi}\alpha_7(g_{\phi}\alpha_7 + 2) - 2\sqrt{3}(g_{\phi}\alpha_7 + 1)h_{\phi}\alpha_8\right) + c_{\Phi,2}\beta_3\left(3b_{\phi}\alpha_2c_{\phi}\alpha_3 - 3a_{\phi}\alpha_1d_{\phi}\alpha_4\right. \\
 & \quad \left.- e_{\phi}\alpha_5\left(3g_{\phi}\alpha_7 + \sqrt{3}h_{\phi}\alpha_8 - 6\right)\right) + b_{\Phi,3}\beta_2\left(c_{\Phi,3}\beta_3\left(-3b_{\phi}\alpha_2c_{\phi}\alpha_3 + 3a_{\phi}\alpha_1d_{\phi}\alpha_4\right.\right. \\
 & \quad \left.+ e_{\phi}\alpha_5\left(3g_{\phi}\alpha_7 + \sqrt{3}h_{\phi}\alpha_8 + 6\right)\right) + c_{\Phi,1}\beta_3\left(3a_{\phi}\alpha_1c_{\phi}\alpha_3 + 3b_{\phi}\alpha_2d_{\phi}\alpha_4 - f_{\phi}\alpha_6\left(3g_{\phi}\alpha_7\right.\right. \\
 & \quad \left.\left.+ \sqrt{3}h_{\phi}\alpha_8 + 6\right)\right) - 2\left(3c_{\Phi,1}\beta_3c_{\Phi,2}\beta_3c_{\phi}^2\alpha_3^2 + 3b_{\Phi,3}\beta_2c_{\Phi,3}\beta_3a_{\phi}\alpha_1c_{\phi}\alpha_3\right. \\
 & \quad \left.+ 3b_{\Phi,3}\beta_2c_{\Phi,1}\beta_3b_{\phi}\alpha_2c_{\phi}\alpha_3 + 2\sqrt{3}a_{\Phi,2}\beta_1c_{\Phi,1}\beta_3h_{\phi}\alpha_8c_{\phi}\alpha_3 + 2\sqrt{3}a_{\Phi,1}\beta_1c_{\Phi,3}\beta_3h_{\phi}\alpha_8c_{\phi}\alpha_3\right. \\
 & \quad \left.+ 3c_{\Phi,1}\beta_3c_{\Phi,2}\beta_3d_{\phi}^2\alpha_4^2 + 3c_{\Phi,1}\beta_3c_{\Phi,2}\beta_3e_{\phi}^2\alpha_5^2 + 3c_{\Phi,1}\beta_3c_{\Phi,2}\beta_3f_{\phi}^2\alpha_6^2 + 4c_{\Phi,1}\beta_3c_{\Phi,2}\beta_3h_{\phi}^2\alpha_8^2\right. \\
 & \quad \left.- 3b_{\Phi,3}\beta_2c_{\Phi,1}\beta_3a_{\phi}\alpha_1d_{\phi}\alpha_4 + 3b_{\Phi,3}\beta_2c_{\Phi,3}\beta_3b_{\phi}\alpha_2d_{\phi}\alpha_4 - 6b_{\Phi,3}\beta_2c_{\Phi,1}\beta_3e_{\phi}\alpha_5\right. \\
 & \quad \left.- 6a_{\Phi,1}\beta_1c_{\Phi,1}\beta_3a_{\phi}\alpha_1e_{\phi}\alpha_5 + 6a_{\Phi,2}\beta_1c_{\Phi,3}\beta_3a_{\phi}\alpha_1e_{\phi}\alpha_5 - 6a_{\Phi,2}\beta_1c_{\Phi,1}\beta_3b_{\phi}\alpha_2e_{\phi}\alpha_5\right. \\
 & \quad \left.- 6a_{\Phi,1}\beta_1c_{\Phi,3}\beta_3b_{\phi}\alpha_2e_{\phi}\alpha_5 - 6b_{\Phi,3}\beta_2c_{\Phi,3}\beta_3f_{\phi}\alpha_6 - 6a_{\Phi,2}\beta_1c_{\Phi,1}\beta_3a_{\phi}\alpha_1f_{\phi}\alpha_6\right. \\
 & \quad \left.- 6a_{\Phi,1}\beta_1c_{\Phi,3}\beta_3a_{\phi}\alpha_1f_{\phi}\alpha_6 + 6a_{\Phi,1}\beta_1c_{\Phi,1}\beta_3b_{\phi}\alpha_2f_{\phi}\alpha_6 - 6a_{\Phi,2}\beta_1c_{\Phi,3}\beta_3b_{\phi}\alpha_2f_{\phi}\alpha_6\right. \\
 & \quad \left.- 3(2a_{\Phi,1}\beta_1(c_{\Phi,3}\beta_3c_{\phi}\alpha_3 - c_{\Phi,1}\beta_3d_{\phi}\alpha_4) + 2a_{\Phi,2}\beta_1(c_{\Phi,1}\beta_3c_{\phi}\alpha_3 + c_{\Phi,3}\beta_3d_{\phi}\alpha_4)\right. \\
 & \quad \left.+ b_{\Phi,3}\beta_2(c_{\Phi,1}\beta_3e_{\phi}\alpha_5 + c_{\Phi,3}\beta_3f_{\phi}\alpha_6))g_{\phi}\alpha_7 - 4\sqrt{3}c_{\Phi,1}\beta_3c_{\Phi,2}\beta_3h_{\phi}\alpha_8\right. \\
 & \quad \left.- 2\sqrt{3}a_{\Phi,1}\beta_1c_{\Phi,1}\beta_3d_{\phi}\alpha_4h_{\phi}\alpha_8 + 2\sqrt{3}a_{\Phi,2}\beta_1c_{\Phi,3}\beta_3d_{\phi}\alpha_4h_{\phi}\alpha_8 - \sqrt{3}b_{\Phi,3}\beta_2c_{\Phi,1}\beta_3e_{\phi}\alpha_5h_{\phi}\alpha_8\right. \\
 & \quad \left.- \sqrt{3}b_{\Phi,3}\beta_2c_{\Phi,3}\beta_3f_{\phi}\alpha_6h_{\phi}\alpha_8 + b_{\Phi,1}\beta_2\left(-6a_{\Phi,1}\beta_1c_{\phi}\alpha_3e_{\phi}\alpha_5 - 6a_{\Phi,2}\beta_1d_{\phi}\alpha_4e_{\phi}\alpha_5\right.\right. \\
 & \quad \left.+ 6a_{\Phi,2}\beta_1c_{\phi}\alpha_3f_{\phi}\alpha_6 - 6a_{\Phi,1}\beta_1d_{\phi}\alpha_4f_{\phi}\alpha_6 + 4\sqrt{3}a_{\Phi,2}\beta_1a_{\phi}\alpha_1h_{\phi}\alpha_8 - 4\sqrt{3}a_{\Phi,1}\beta_1b_{\phi}\alpha_2h_{\phi}\alpha_8\right. \\
 & \quad \left.+ b_{\Phi,2}\beta_2\left(3a_{\phi}^2\alpha_1^2 + 3b_{\phi}^2\alpha_2^2 + 3e_{\phi}^2\alpha_5^2 + 3f_{\phi}^2\alpha_6^2 + h_{\phi}^2\alpha_8^2 + 3g_{\phi}\alpha_7(g_{\phi}\alpha_7 + 2) - 2\sqrt{3}(g_{\phi}\alpha_7 + 1)h_{\phi}\alpha_8\right)\right. \\
 & \quad \left.+ c_{\Phi,2}\beta_3\left(-3a_{\phi}\alpha_1c_{\phi}\alpha_3 - 3b_{\phi}\alpha_2d_{\phi}\alpha_4 + f_{\phi}\alpha_6\left(3g_{\phi}\alpha_7 + \sqrt{3}h_{\phi}\alpha_8 - 6\right)\right)\right) \\
 & \quad \left.- b_{\Phi,2}\beta_2\left(c_{\Phi,3}\beta_3\left(-3b_{\phi}\alpha_2c_{\phi}\alpha_3 + 3a_{\phi}\alpha_1d_{\phi}\alpha_4 + e_{\phi}\alpha_5\left(3g_{\phi}\alpha_7 + \sqrt{3}h_{\phi}\alpha_8 + 6\right)\right)\right)\right. \\
 & \quad \left.+ c_{\Phi,1}\beta_3\left(3a_{\phi}\alpha_1c_{\phi}\alpha_3 + 3b_{\phi}\alpha_2d_{\phi}\alpha_4 - f_{\phi}\alpha_6\left(3g_{\phi}\alpha_7 + \sqrt{3}h_{\phi}\alpha_8 + 6\right)\right)\right)\sin(\alpha - \phi)\right. \\
 & \quad \left.- 2b_{\Phi,1}\beta_2\left(c_{\Phi,1}\beta_3\left(3b_{\phi}\alpha_2c_{\phi}\alpha_3 - 3a_{\phi}\alpha_1d_{\phi}\alpha_4 - e_{\phi}\alpha_5\left(3g_{\phi}\alpha_7 + \sqrt{3}h_{\phi}\alpha_8\right)\right)\right)\right)
 \end{aligned}$$

$$+ c_{\Phi,3} \beta_3 \left( 3a_\phi \alpha_1 c_\phi \alpha_3 + 3b_\phi \alpha_2 d_\phi \alpha_4 - f_\phi \alpha_6 \left( 3g_\phi \alpha_7 + \sqrt{3} h_\phi \alpha_8 \right) \right) \sin(2(\alpha - \phi)) \Big\} \quad (\text{B.18})$$

$$\begin{aligned} \hat{e}_{Hpot} = & \frac{\lambda v^4}{64} \left\{ -2 \sin(\alpha - \phi) \left( b_{\Phi,1} b_{\Phi,2} \beta_2^2 + c_{\Phi,1} c_{\Phi,2} \beta_3^2 \right) + 2 \cos(\alpha - \phi) \left( b_{\Phi,1} b_{\Phi,3} \beta_2^2 - c_{\Phi,2} c_{\Phi,3} \beta_3^2 \right) \right. \\ & \left. + 4 \beta_1^2 \left( a_{\Phi,1}^2 + a_{\Phi,2}^2 \right) + \beta_2^2 \left( b_{\Phi,1}^2 + b_{\Phi,2}^2 + b_{\Phi,3}^2 \right) + \beta_3^2 \left( c_{\Phi,1}^2 + c_{\Phi,2}^2 + c_{\Phi,3}^2 \right) - 4 \right\}^2 \end{aligned} \quad (\text{B.19})$$

## C Simulated annealing base source code (C++)

What follows is a simplified version of the Simulated Annealing (SA) program, that has been written for the application in chapter 5. The source code of the final programs is too extensive to be included here, it is however included on the enclosed CD.

```

2  * SA_base.cpp -- program to minimize multivariate functions. *
3  *
4  * Author:    Pascal Nagel
5  *
6  * Purpose:   Minimizing a multivariate function.
7  *
8  * Usage:     Adjust the following parameters to best suit
9  *             your problem:
10 *
11 *
12 *           steps: number of proposal cycles before temperature
13 *                  is lowered
14 *           ns: number of proposal cycles before step length
15 *                  is adjusted
16 *           NX: dimension of parameter space
17 *           initemp: starting temperature
18 *           endtemp: temperature after which the algorithm halts
19 *           tempdecr: temperature reduction factor
20 *           inistep: initial step length
21 *           cstep: adjustment factor for step length changes
22 *                  (needs to be >1.0)
23 *           lratio: lower boundary for step length adjustments
24 *           uratio: upper boundary for step length adjustments
25 *           fct(x): insert your function here
26 */
27
28 #include <iostream>
29 #include <math.h>
30 #include <cstdlib>
31 #include "include/nr3.h" //numerical recipes lib for rng
32 #include "include/ran.h" //numerical recipes lib for rng
33
34 using namespace std;
35
36 //METROPOLIS
37 int accept_proposal(double current, double proposal, double temperature,
38                     double rand)
39 {
40     double prob;
41     if (proposal < current)
42 
```



```

    step [ i]=inistep ;
    lowestx [ i]=x [ i ] ;
}
88

90 //INITIAL FUNCTION EVALUATION
f = fct (x);
lowest = f;

94 //START TEMPERATURE LOOP
for ( double temp = initemp ;temp>=endtemp ;temp*=tempdecr )
{
    //RESET COUNTER FOR ACCEPTED STEPS
    for ( int i=0;i<NX; i++){
        stepsup [ i]=0;
    }
100

102 //START STEP LOOP
for ( int i=1;i<=steps ;i++)
{
    //RESET PROPOSALS
    for ( int j=0;j<NX; j++){
        xp [ j]=x [ j ] ;
    }
    for ( int j=0;j<NX; j++){
        //GENERATE NEW PARAMETER IN STEPLENGTH RANGE
        xp [ j ] += ( ran1 .doub () *2.0 -1.0 ) * step [ j ];
        //CHECK PROPOSAL
        prop = fct (xp);
        if ( accept_proposal (f , prop , temp , ran1 .doub ())){
            f = prop ;
            x [ j ] = xp [ j ] ;
            stepsup [ j]++;
            //CHECK FOR NEW MINIMUM
            if ( f < lowest ){
                lowest = f ;
                for ( int k=0;k<NX; k++){
                    lowestx [ k]=x [ k ] ;
                }
            }
        }
        else {
            xp [ j]=x [ j ] ;
        }
        //ADJUST STEPLENGTH VECTOR
        step [ j]=adjstep (stepsup [ j ] , i , ns , lratio , uratio , cstep ,
                           step [ j ]) ;
    }
}
130

```

```

132         }
133     }
134 //OUTPUT RESULTS
135     cout << "Lowest Value: " << lowest << endl << endl;
136     cout << "Corr. Parameters x[0]...x[NX]: " << endl;
137     for (int i=0;i<NX;i++){
138         cout << lowestx[i] << endl;
139     }
140     return 0;
}

```

## D Coefficients of the $\hat{S}_{approx}$ Ansatz

These parameters generate profile functions (5.2) and (5.3), approximating the minimum of the  $\hat{S}_{approx}$  energy functional.

Coefficient	Value	Coefficient	Value
$a_0$	1.044004	$b_0$	0.822425
$a_2$	-0.478237	$b_2$	-0.158065
$a_4$	1.433294	$b_4$	0.702794
$a_6$	-1.164826	$b_6$	-0.574269
$a_8$	0.281641	$b_8$	0.421543
$a_{10}$	-0.181782	$b_{10}$	-0.387924
$a_{12}$	-0.0966991	$b_{12}$	0.289111
$a_{14}$	0.174073	$b_{14}$	-0.180986
$a_{16}$	0.0780239	$b_{16}$	0.0921646
$a_{18}$	-0.219206	$b_{18}$	-0.0111742
$a_{20}$	0.256833	$b_{20}$	-0.0343903
$a_{22}$	-0.131366	$b_{22}$	0.0383913
$a_{24}$	-0.0239561	$b_{24}$	-0.0196208
$a_{26}$	0.0358777		
$a_{28}$	-0.0762262		
$a_{30}$	0.122090		
$a_{32}$	-0.0941909		
$a_{34}$	0.0406536		

Table D.1:  $\hat{S}_{approx}$  Ansatz coefficients

## E Figures and coefficients of the generalized $\hat{S}$ Ansatz

The following figures show the profile functions, as well as the energy densities of the configurations of lowest energy obtained from the SA programs at each order of angular expansion.

Expansion coefficients associated with approximations  $N = 0, 1, 2$  are listed as well. All expansion coefficients are included on the enclosed CD.

### E.1 $N = 0$ Legendre expansion

Coefficient	Value	Coefficient	Value	Coefficient	Value
$a_{1,0}$	0.556067	$a_{2,0}$	1.043733	$a_{3,0}$	0.436071
$a_{1,2}$	0.424028	$a_{2,2}$	0.0992037	$a_{3,2}$	0.491228
$a_{1,4}$	0.452151	$a_{2,4}$	0.502999	$a_{3,4}$	0.585042
$a_{1,6}$	-0.196171	$a_{2,6}$	-0.541655	$a_{3,6}$	-0.287261
$a_{1,8}$	-0.210094	$a_{2,8}$	-0.365586	$a_{3,8}$	-0.221628
$a_{1,10}$	-0.0331486	$a_{2,10}$	0.339779	$a_{3,10}$	0.000570390
$a_{1,12}$	-0.130845	$a_{2,12}$	-0.428739	$a_{3,12}$	-0.162076
$a_{1,14}$	0.165267	$a_{2,14}$	0.647585	$a_{3,14}$	0.207937
$a_{1,16}$	-0.105956	$a_{2,16}$	-0.542978	$a_{3,16}$	-0.0877929
$a_{1,18}$	0.161556	$a_{2,18}$	0.535555	$a_{3,18}$	0.0572194
$a_{1,20}$	-0.148091	$a_{2,20}$	-0.510324	$a_{3,20}$	-0.00448562
$a_{1,22}$	0.158418	$a_{2,22}$	0.442020	$a_{3,22}$	-0.0248459
$a_{1,24}$	-0.176860	$a_{2,24}$	-0.417013	$a_{3,24}$	0.00958338
$a_{1,26}$	0.165246	$a_{2,26}$	0.364581	$a_{3,26}$	0.0158518
$a_{1,28}$	-0.165019	$a_{2,28}$	-0.314805	$a_{3,28}$	-0.0546127
$a_{1,30}$	0.126173	$a_{2,30}$	0.233551	$a_{3,30}$	0.0646954
$a_{1,32}$	-0.0917124	$a_{2,32}$	-0.163036	$a_{3,32}$	-0.0700975
$a_{1,34}$	0.0489926	$a_{2,34}$	0.0751309	$a_{3,34}$	0.0446016
$a_{4,0}$	0.581364	$a_{5,0}$	0.923877	$b_{1,0}$	0.456372
$a_{4,2}$	0.0566448	$a_{5,2}$	0.475071	$b_{1,2}$	0.632028
$a_{4,4}$	0.981488	$a_{5,4}$	0.178995	$b_{1,4}$	-0.145331
$a_{4,6}$	-0.694843	$a_{5,6}$	-0.688394	$b_{1,6}$	0.274933
$a_{4,8}$	0.522680	$a_{5,8}$	0.233717	$b_{1,8}$	-0.406255
$a_{4,10}$	-0.757501	$a_{5,10}$	-0.707571	$b_{1,10}$	0.356691
$a_{4,12}$	0.550825	$a_{5,12}$	1.051904	$b_{1,12}$	-0.327821
$a_{4,14}$	-0.527570	$a_{5,14}$	-0.982187	$b_{1,14}$	0.297029
$a_{4,16}$	0.468401	$a_{5,16}$	1.090118	$b_{1,16}$	-0.232754
$a_{4,18}$	-0.342129	$a_{5,18}$	-0.987887	$b_{1,18}$	0.169800

$a_{4,20}$	0.263774	$a_{5,20}$	0.743588	$b_{1,20}$	-0.113115
$a_{4,22}$	-0.159501	$a_{5,22}$	-0.539076	$b_{1,22}$	0.0594534
$a_{4,24}$	0.0738188	$a_{5,24}$	0.284864	$b_{1,24}$	-0.0210310
$a_{4,26}$	-0.0140776	$a_{5,26}$	-0.0759311		
$a_{4,28}$	-0.0341055	$a_{5,28}$	-0.0579462		
$a_{4,30}$	0.0444465	$a_{5,30}$	0.114454		
$a_{4,32}$	-0.0422806	$a_{5,32}$	-0.122482		
$a_{4,34}$	0.0285655	$a_{5,34}$	0.0648855		
$b_{2,0}$	0.350192	$b_{3,0}$	0.920200		
$b_{2,2}$	0.385718	$b_{3,2}$	-0.327175		
$b_{2,4}$	0.542089	$b_{3,4}$	0.888671		
$b_{2,6}$	-0.322702	$b_{3,6}$	-0.842369		
$b_{2,8}$	0.218083	$b_{3,8}$	0.718652		
$b_{2,10}$	-0.297826	$b_{3,10}$	-0.676122		
$b_{2,12}$	0.201873	$b_{3,12}$	0.561800		
$b_{2,14}$	-0.132540	$b_{3,14}$	-0.409230		
$b_{2,16}$	0.0849788	$b_{3,16}$	0.270805		
$b_{2,18}$	-0.0309151	$b_{3,18}$	-0.143291		
$b_{2,20}$	-0.00220750	$b_{3,20}$	0.0484467		
$b_{2,22}$	0.0127066	$b_{3,22}$	0.00119808		
$b_{2,24}$	-0.00945516	$b_{3,24}$	-0.0115856		

Table E.1:  $N = 0$  expansion coefficients.

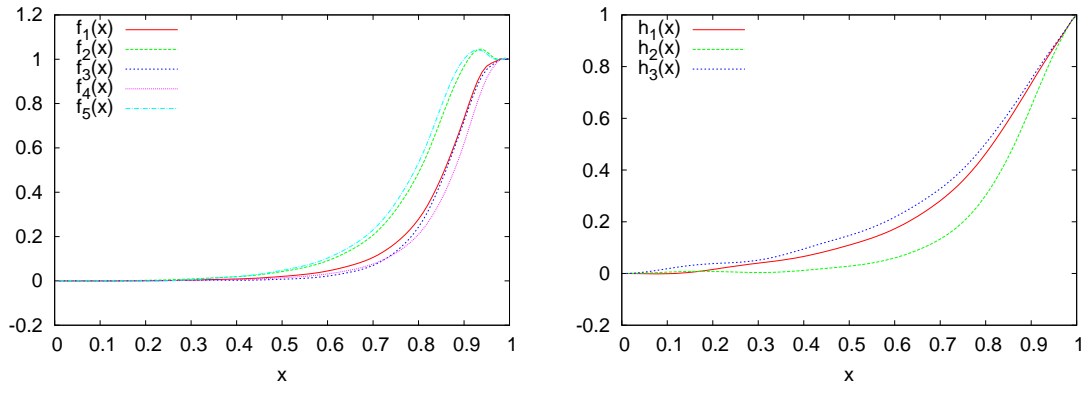


Figure E.1:  $N = 0$  plots

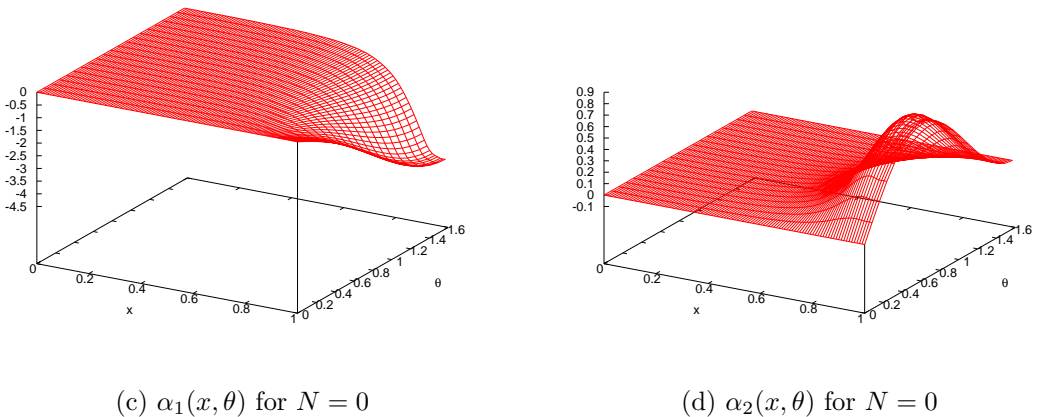


Figure E.1:  $N = 0$  plots (cont.)

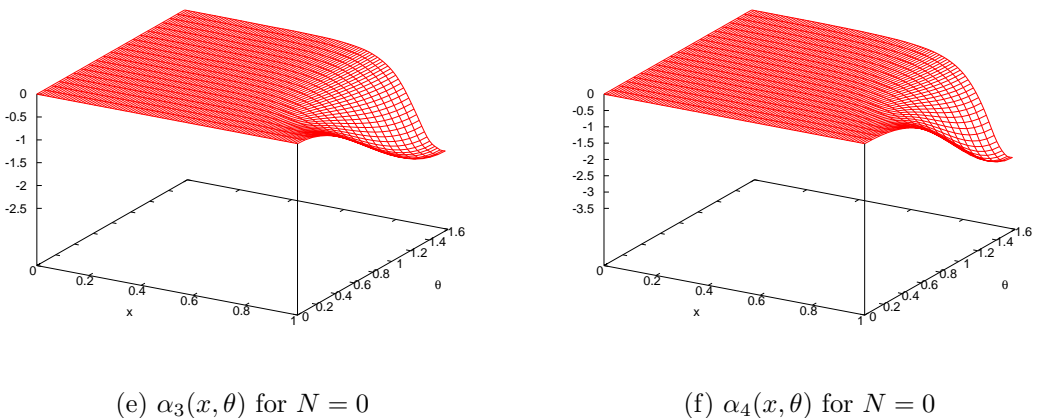


Figure E.1:  $N = 0$  plots (cont.)

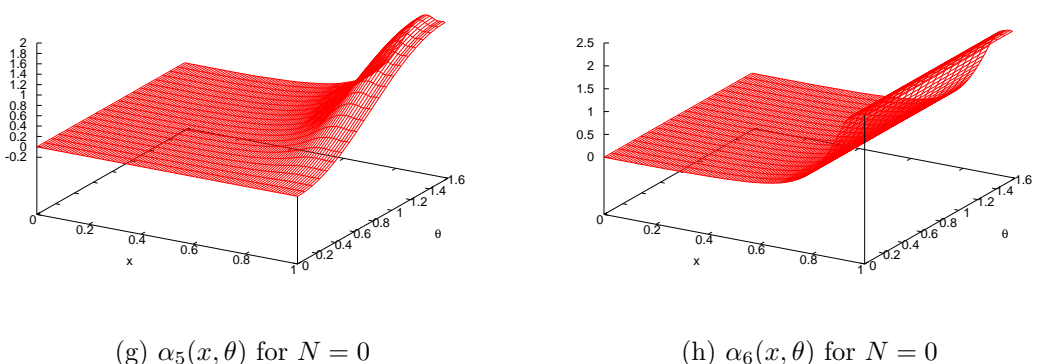


Figure E.1:  $N = 0$  plots (cont.)

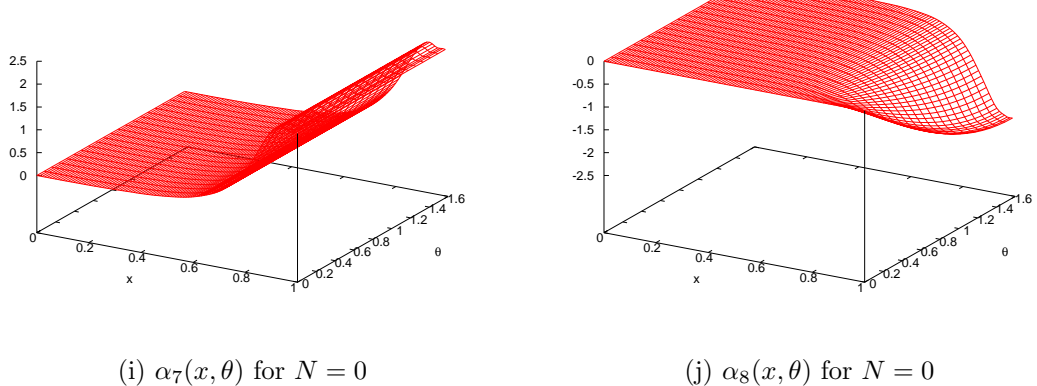


Figure E.1:  $N = 0$  plots (cont.)

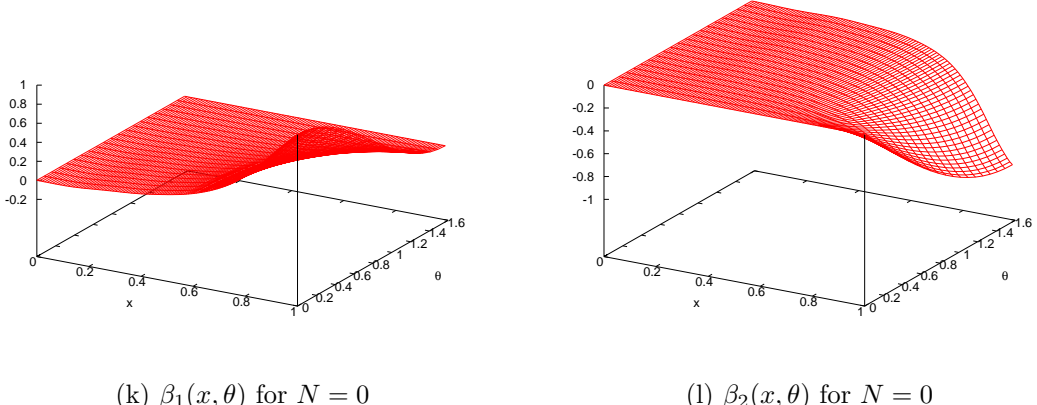


Figure E.1:  $N = 0$  plots (cont.)

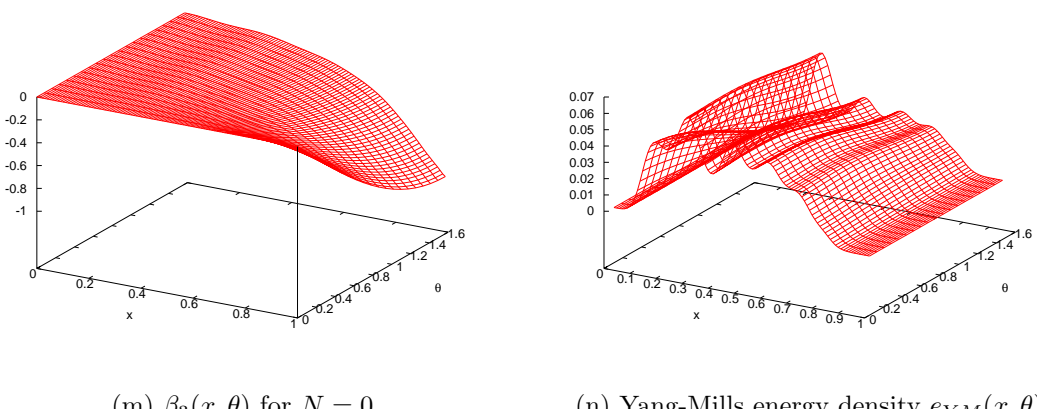
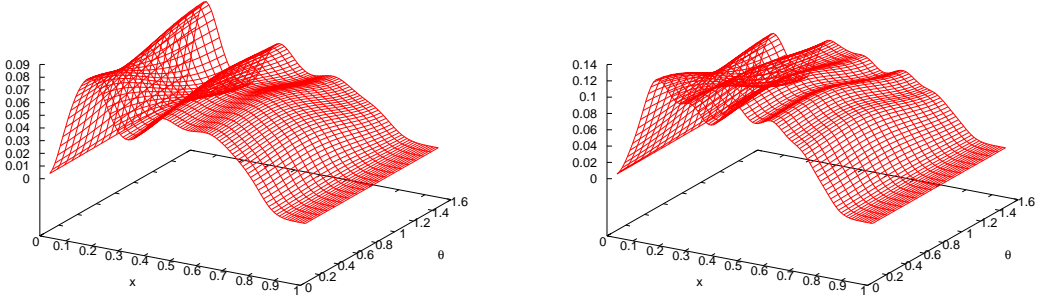


Figure E.1:  $N = 0$  plots (cont.)



(o) Kinetic Higgs energy density  $e_{H\text{kin}}(x, \theta)$

(p) Total energy density  $e_{\text{tot}}(x, \theta)$

Figure E.1:  $N = 0$  plots (cont.)

## E.2 $N = 1$ Legendre expansion

The coefficients and figures given below are related to the  $N = 1$  run of lowest energy ( $N_S = 13000$ ,  $E_{\hat{S}}/E_S = 1.038$ ), as discussed in chapter 5.2.1.

Coefficient	Value	Coefficient	Value	Coefficient	Value
$a_{1,0}$	0.9537741216	$a_{2,0}$	3.89899226	$a_{3,0}$	-0.5426186734
$a_{1,2}$	0.7939067557	$a_{2,2}$	-4.498476065	$a_{3,2}$	3.507642123
$a_{1,4}$	-1.989679542	$a_{2,4}$	2.932981239	$a_{3,4}$	-4.562498062
$a_{1,6}$	2.711065211	$a_{2,6}$	-1.622137053	$a_{3,6}$	3.787383642
$a_{1,8}$	-2.710790059	$a_{2,8}$	-0.0756505785	$a_{3,8}$	-2.889367431
$a_{1,10}$	2.233212025	$a_{2,10}$	0.827789476	$a_{3,10}$	2.02077785
$a_{1,12}$	-1.524469418	$a_{2,12}$	-1.021900406	$a_{3,12}$	-0.9548532262
$a_{1,14}$	0.6381560807	$a_{2,14}$	0.9033224166	$a_{3,14}$	0.643944019
$a_{1,16}$	0.06386599493	$a_{2,16}$	-0.5115259855	$a_{3,16}$	-0.07593460411
$a_{1,18}$	-0.4760053067	$a_{2,18}$	0.1573563972	$a_{3,18}$	0.2117440667
$a_{1,20}$	0.5497207558	$a_{2,20}$	0.1089643776	$a_{3,20}$	-0.1243454496
$a_{1,22}$	-0.331517536	$a_{2,22}$	-0.2176422576	$a_{3,22}$	0.2540334454
$a_{1,24}$	0.03585825261	$a_{2,24}$	0.2354394188	$a_{3,24}$	-0.1417756052
$a_{1,26}$	0.2098990799	$a_{2,26}$	-0.1849599794	$a_{3,26}$	-0.05869072579
$a_{1,28}$	-0.2986465331	$a_{2,28}$	0.1187608928	$a_{3,28}$	0.1458685019
$a_{1,30}$	0.2497021373	$a_{2,30}$	-0.06832142337	$a_{3,30}$	-0.1840499661
$a_{1,32}$	-0.140124174	$a_{2,32}$	0.01719739425	$a_{3,32}$	0.01596688752
$a_{1,34}$	0.03207215506	$a_{2,34}$	-0.0001901246786	$a_{3,34}$	-0.05322679197
$a_{4,0}$	1.955661533	$a_{5,0}$	2.0521452	$b_{1,0}$	4.840293639
$a_{4,2}$	-4.262907361	$a_{5,2}$	-1.027682832	$b_{1,2}$	-7.875246388
$a_{4,4}$	6.661725657	$a_{5,4}$	1.962915139	$b_{1,4}$	7.217382079

$a_{4,6}$	-5.61423456	$a_{5,6}$	-2.137669963	$b_{1,6}$	-5.466826572
$a_{4,8}$	5.23568502	$a_{5,8}$	1.641695322	$b_{1,8}$	3.772288858
$a_{4,10}$	-3.73970287	$a_{5,10}$	-1.85918302	$b_{1,10}$	-2.38883479
$a_{4,12}$	1.803643817	$a_{5,12}$	1.507767986	$b_{1,12}$	1.433051674
$a_{4,14}$	-0.9809125967	$a_{5,14}$	-1.52219536	$b_{1,14}$	-0.8323957953
$a_{4,16}$	-0.08605407415	$a_{5,16}$	0.8728512029	$b_{1,16}$	0.5012096043
$a_{4,18}$	0.1114315136	$a_{5,18}$	-0.6864216567	$b_{1,18}$	-0.3108215709
$a_{4,20}$	-0.2106977229	$a_{5,20}$	0.08206660094	$b_{1,20}$	0.1733663347
$a_{4,22}$	-0.1827321238	$a_{5,22}$	-0.0642202889	$b_{1,22}$	-0.06556367422
$a_{4,24}$	0.5608708139	$a_{5,24}$	0.01532106716	$b_{1,24}$	0.002096602117
$a_{4,26}$	-0.8630740671	$a_{5,26}$	-0.1605029793		
$a_{4,28}$	0.4012482491	$a_{5,28}$	0.1535427206		
$a_{4,30}$	0.3380578488	$a_{5,30}$	0.04544287419		
$a_{4,32}$	-0.2006981077	$a_{5,32}$	-0.02720133742		
$a_{4,34}$	0.07268903059	$a_{5,34}$	0.1513293245		
$b_{2,0}$	0.4540155784	$b_{3,0}$	1.840124323	$d_{1,0,0}$	-11.87513522
$b_{2,2}$	0.4906195409	$b_{3,2}$	-1.697723796	$d_{1,0,2}$	2.83296657
$b_{2,4}$	0.02261700235	$b_{3,4}$	1.944764915	$d_{1,0,4}$	-35.88457513
$b_{2,6}$	0.1201230446	$b_{3,6}$	-1.918914146	$d_{1,0,6}$	8.272620372
$b_{2,8}$	-0.1198169941	$b_{3,8}$	1.522133922	$d_{1,0,8}$	-42.09824444
$b_{2,10}$	0.109765908	$b_{3,10}$	-1.188851373	$d_{1,0,10}$	27.94701221
$b_{2,12}$	-0.1268088185	$b_{3,12}$	0.7882760793	$d_{1,0,12}$	-38.3545422
$b_{2,14}$	0.0713716179	$b_{3,14}$	-0.4342835216	$d_{1,0,14}$	46.06945289
$b_{2,16}$	-0.01556452497	$b_{3,16}$	0.1706028536	$d_{1,0,16}$	-32.44417622
$b_{2,18}$	-0.01816836179	$b_{3,18}$	-0.009797901313	$d_{1,0,18}$	49.45049102
$b_{2,20}$	0.009914329798	$b_{3,20}$	-0.03943502099	$d_{1,0,20}$	-23.09273535
$b_{2,22}$	0.06351499935	$b_{3,22}$	0.03253901091	$d_{1,0,22}$	37.31423233
$b_{2,24}$	-0.06158332202	$b_{3,24}$	-0.009435343573	$d_{1,0,24}$	-11.9314511
				$d_{1,0,26}$	20.40908836
				$d_{1,0,28}$	-4.856936363
				$d_{1,0,30}$	8.658228812
				$d_{1,0,32}$	-2.384488233
				$d_{1,0,34}$	2.821911298
				$d_{1,0,36}$	-0.9657542702
				$d_{1,0,38}$	0.1120346363
$d_{2,0,0}$	-27.65534393	$d_{3,0,0}$	22.26474322	$d_{4,0,0}$	-4.12796071
$d_{2,0,2}$	54.5645621	$d_{3,0,2}$	-73.07171535	$d_{4,0,2}$	-27.53965349
$d_{2,0,4}$	-59.40076295	$d_{3,0,4}$	71.01479963	$d_{4,0,4}$	-24.98089163
$d_{2,0,6}$	58.98750431	$d_{3,0,6}$	-95.96436163	$d_{4,0,6}$	-39.32341203

$d_{2,0,8}$	-48.45185655	$d_{3,0,8}$	94.70362265	$d_{4,0,8}$	-2.940491716
$d_{2,0,10}$	40.97573575	$d_{3,0,10}$	-96.55242715	$d_{4,0,10}$	-29.41793011
$d_{2,0,12}$	-30.02659172	$d_{3,0,12}$	98.69724676	$d_{4,0,12}$	29.78859663
$d_{2,0,14}$	22.01733562	$d_{3,0,14}$	-89.00418173	$d_{4,0,14}$	-18.39240158
$d_{2,0,16}$	-13.92624224	$d_{3,0,16}$	89.09209993	$d_{4,0,16}$	43.69357599
$d_{2,0,18}$	7.902767763	$d_{3,0,18}$	-74.88627644	$d_{4,0,18}$	-9.114039962
$d_{2,0,20}$	-3.776178334	$d_{3,0,20}$	72.11027396	$d_{4,0,20}$	39.59978961
$d_{2,0,22}$	0.1105442296	$d_{3,0,22}$	-56.01828973	$d_{4,0,22}$	-2.032902778
$d_{2,0,24}$	0.8884759922	$d_{3,0,24}$	50.73283806	$d_{4,0,24}$	26.36558841
$d_{2,0,26}$	-2.512527843	$d_{3,0,26}$	-34.55838349	$d_{4,0,26}$	2.865058741
$d_{2,0,28}$	1.936663985	$d_{3,0,28}$	28.97979872	$d_{4,0,28}$	13.8262029
$d_{2,0,30}$	-2.21098719	$d_{3,0,30}$	-17.09960512	$d_{4,0,30}$	-3.960672971
$d_{2,0,32}$	1.319852126	$d_{3,0,32}$	13.56320621	$d_{4,0,32}$	6.033254153
$d_{2,0,34}$	-1.00726424	$d_{3,0,34}$	-6.317350111	$d_{4,0,34}$	-1.31238373
$d_{2,0,36}$	0.4555711473	$d_{3,0,36}$	3.661293818	$d_{4,0,36}$	1.297991194
$d_{2,0,38}$	-0.1912580432	$d_{3,0,38}$	-1.347332198	$d_{4,0,38}$	-0.3273169116
$d_{5,0,0}$	21.02348374	$d_{6,0,0}$	13.89948992	$d_{7,0,0}$	-67.96057628
$d_{5,0,2}$	-36.73167934	$d_{6,0,2}$	9.961292792	$d_{7,0,2}$	144.7753154
$d_{5,0,4}$	71.57854064	$d_{6,0,4}$	16.70285264	$d_{7,0,4}$	-204.0910381
$d_{5,0,6}$	-61.44846786	$d_{6,0,6}$	3.079048955	$d_{7,0,6}$	184.7962676
$d_{5,0,8}$	83.10183898	$d_{6,0,8}$	4.246143099	$d_{7,0,8}$	-189.5432885
$d_{5,0,10}$	-75.15258283	$d_{6,0,10}$	-5.463936273	$d_{7,0,10}$	167.8215813
$d_{5,0,12}$	77.6303188	$d_{6,0,12}$	-3.934992511	$d_{7,0,12}$	-142.4903778
$d_{5,0,14}$	-76.43171007	$d_{6,0,14}$	-8.666181781	$d_{7,0,14}$	126.9972692
$d_{5,0,16}$	62.56221918	$d_{6,0,16}$	-5.882720396	$d_{7,0,16}$	-91.97665598
$d_{5,0,18}$	-65.55114972	$d_{6,0,18}$	-7.603383815	$d_{7,0,18}$	82.87241408
$d_{5,0,20}$	44.17610623	$d_{6,0,20}$	-4.613717688	$d_{7,0,20}$	-51.12796343
$d_{5,0,22}$	-48.19538111	$d_{6,0,22}$	-4.80762737	$d_{7,0,22}$	46.03603597
$d_{5,0,24}$	28.38406501	$d_{6,0,24}$	-2.626762967	$d_{7,0,24}$	-23.74226155
$d_{5,0,26}$	-30.67175624	$d_{6,0,26}$	-2.233213583	$d_{7,0,26}$	20.63271211
$d_{5,0,28}$	16.2209821	$d_{6,0,28}$	-1.055594159	$d_{7,0,28}$	-8.505335416
$d_{5,0,30}$	-14.59072794	$d_{6,0,30}$	-0.6776526572	$d_{7,0,30}$	6.465058665
$d_{5,0,32}$	7.177353822	$d_{6,0,32}$	-0.2352267636	$d_{7,0,32}$	-1.866768853
$d_{5,0,34}$	-4.449917268	$d_{6,0,34}$	-0.08781744612	$d_{7,0,34}$	0.9076116296
$d_{5,0,36}$	2.153847174				
$d_{5,0,38}$	-0.7853832822				
$d_{8,0,0}$	2.852767144	$e_{1,0,0}$	-6.805193418	$e_{2,0,0}$	-0.1373094076
$d_{8,0,2}$	-10.65145423	$e_{1,0,2}$	11.46583614	$e_{2,0,2}$	-2.195069547
$d_{8,0,4}$	26.19293362	$e_{1,0,4}$	-11.69446267	$e_{2,0,4}$	0.2301560799

$d_{8,0,6}$	-5.354092927	$e_{1,0,6}$	10.75691463	$e_{2,0,6}$	-1.216958711
$d_{8,0,8}$	20.05560485	$e_{1,0,8}$	-8.585802158	$e_{2,0,8}$	1.75237816
$d_{8,0,10}$	-5.109068207	$e_{1,0,10}$	6.997056487	$e_{2,0,10}$	-0.749867429
$d_{8,0,12}$	7.418372401	$e_{1,0,12}$	-4.898914935	$e_{2,0,12}$	1.909763816
$d_{8,0,14}$	-6.203010819	$e_{1,0,14}$	3.642031181	$e_{2,0,14}$	-0.7095149755
$d_{8,0,16}$	-1.69978979	$e_{1,0,16}$	-2.067845265	$e_{2,0,16}$	1.25895469
$d_{8,0,18}$	-6.21003006	$e_{1,0,18}$	1.370335581	$e_{2,0,18}$	-0.5770044893
$d_{8,0,20}$	-5.112379281	$e_{1,0,20}$	-0.4888774351	$e_{2,0,20}$	0.6107783983
$d_{8,0,22}$	-4.793088839	$e_{1,0,22}$	0.2816321598	$e_{2,0,22}$	-0.5407206737
$d_{8,0,24}$	-4.588116426	$e_{1,0,24}$	0.027289697	$e_{2,0,24}$	0.3644140889
$d_{8,0,26}$	-2.615473688				
$d_{8,0,28}$	-2.571571149				
$d_{8,0,30}$	-0.8347358836				
$d_{8,0,32}$	-0.7320475221				
$d_{8,0,34}$	-0.04481918915				
$e_{3,0,0}$	-0.2388972782				
$e_{3,0,2}$	-0.3045137619				
$e_{3,0,4}$	-0.405489122				
$e_{3,0,6}$	0.3524822757				
$e_{3,0,8}$	-0.1123723019				
$e_{3,0,10}$	0.1823456291				
$e_{3,0,12}$	0.2889092789				
$e_{3,0,14}$	-0.2430828303				
$e_{3,0,16}$	0.5336131922				
$e_{3,0,18}$	-0.3916154975				
$e_{3,0,20}$	0.3948915562				
$e_{3,0,22}$	-0.1663073455				
$e_{3,0,24}$	0.1100362052				

 Table E.2:  $N = 1$  expansion coefficients

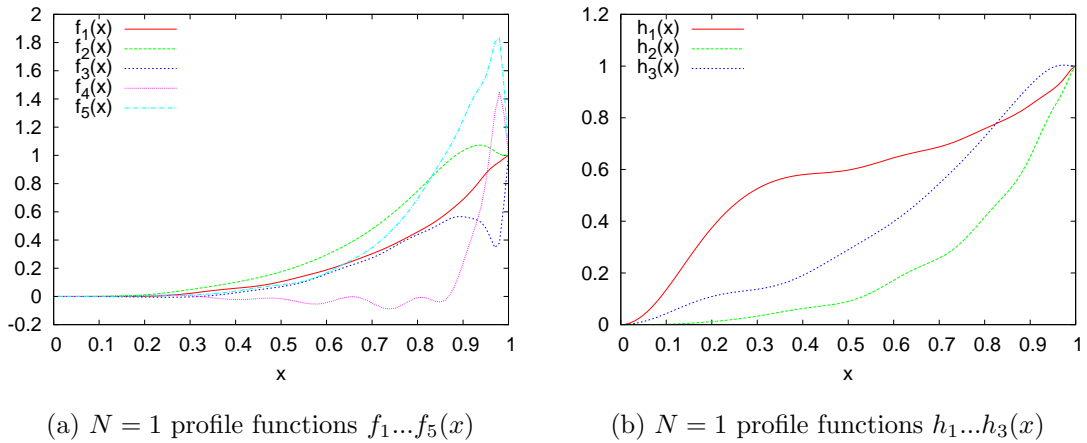


Figure E.2:  $N = 1$  plots

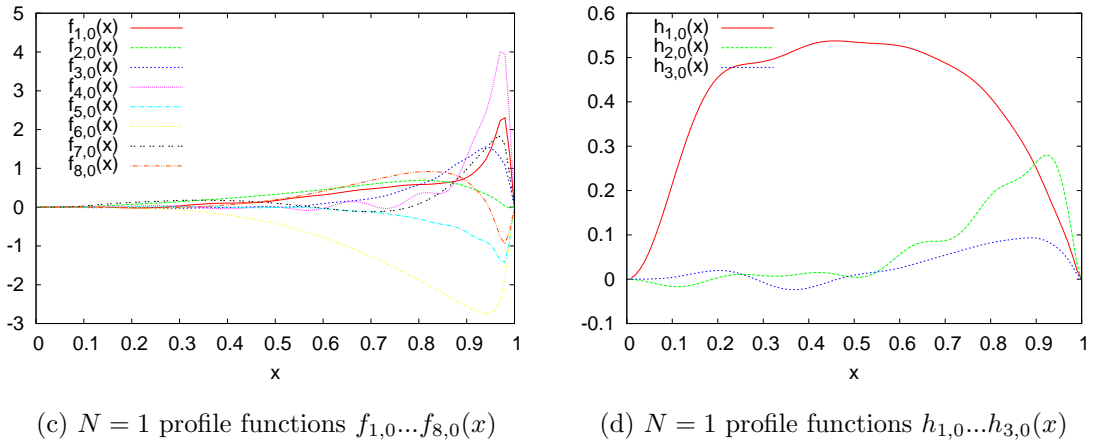


Figure E.2:  $N = 1$  plots (cont.)

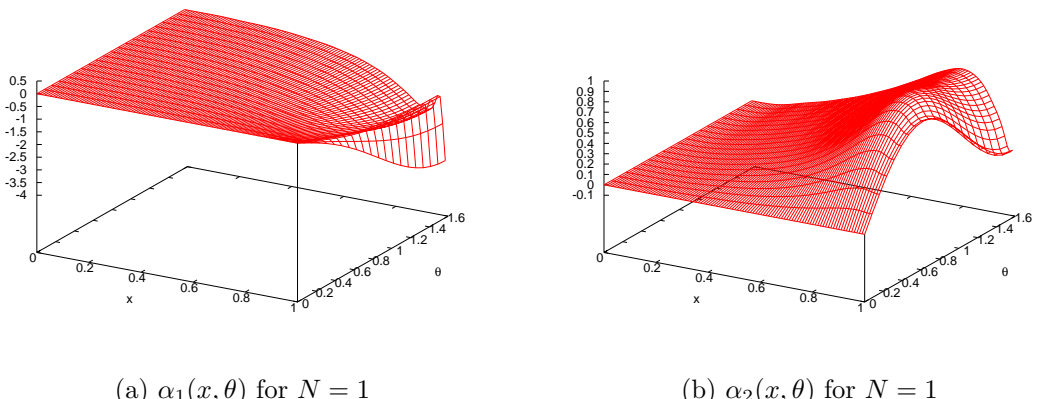
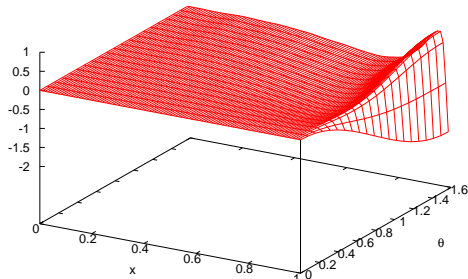
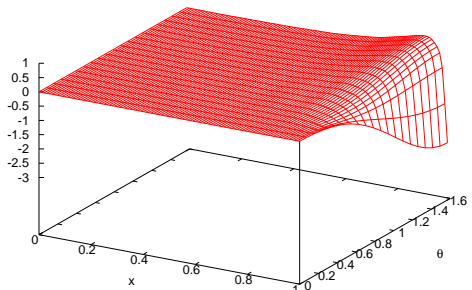


Figure E.3:  $N = 1$  plots (cont.)

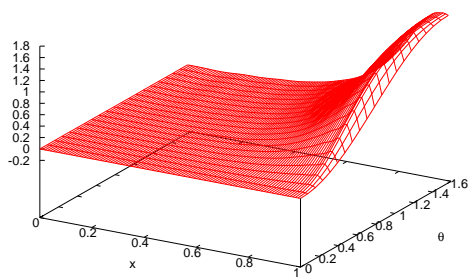


(c)  $\alpha_3(x, \theta)$  for  $N = 1$

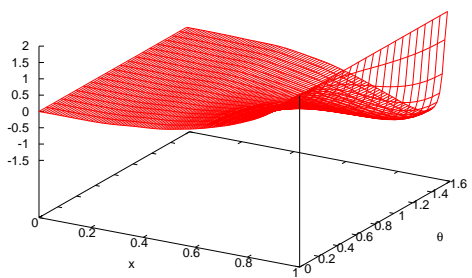


(d)  $\alpha_4(x, \theta)$  for  $N = 1$

Figure E.3:  $N = 1$  plots (cont.)

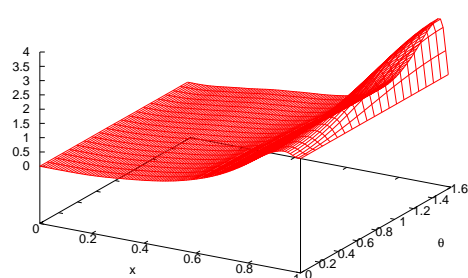


(e)  $\alpha_5(x, \theta)$  for  $N = 1$

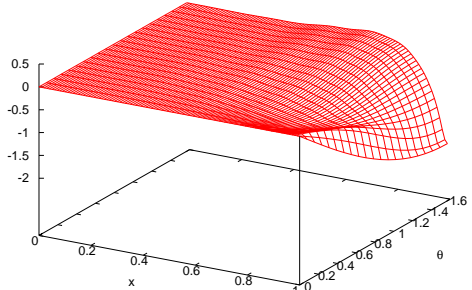


(f)  $\alpha_6(x, \theta)$  for  $N = 1$

Figure E.3:  $N = 1$  plots (cont.)

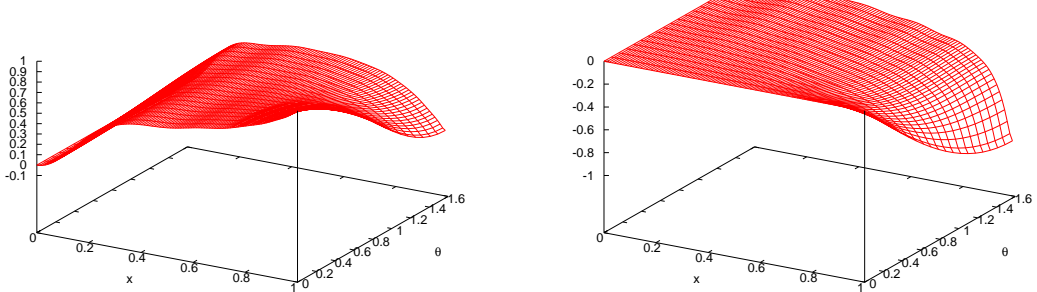


(g)  $\alpha_7(x, \theta)$  for  $N = 1$



(h)  $\alpha_8(x, \theta)$  for  $N = 1$

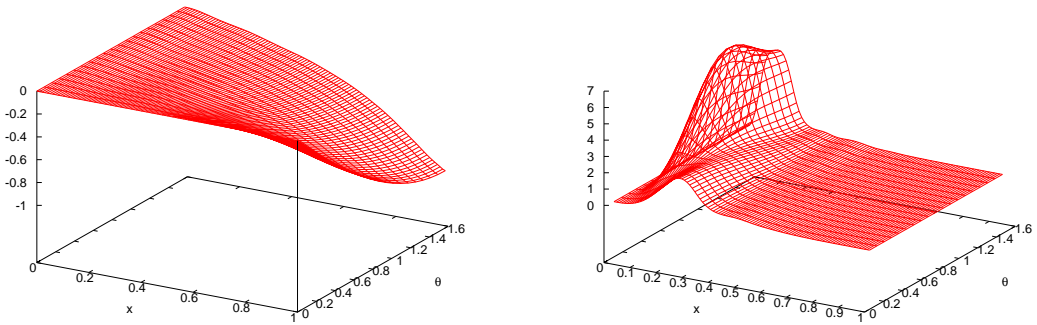
Figure E.3:  $N = 1$  plots (cont.)



(i)  $\beta_1(x, \theta)$  for  $N = 1$

(j)  $\beta_2(x, \theta)$  for  $N = 1$

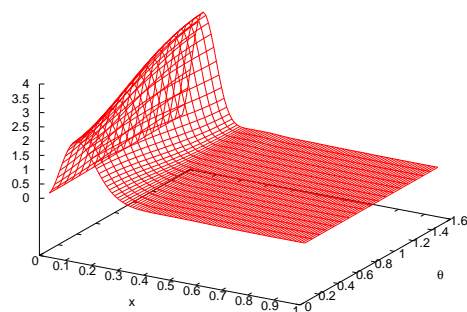
Figure E.3:  $N = 1$  plots (cont.)



(k)  $\beta_3(x, \theta)$  for  $N = 1$

(l) Yang-Mills energy density  $e_{YM}(x, \theta)$

Figure E.3:  $N = 1$  plots (cont.)



(m) Kinetic Higgs energy density  $e_{Hkin}(x, \theta)$

Figure E.3:  $N = 1$  plots (cont.)

### E.3 $N = 2$ Legendre expansion

The coefficients and figures given below are related to the  $N = 2$  run of lowest energy ( $N_S = 1200$ ,  $E_{\hat{S}}/E_S = 0.888$ ), as discussed in chapter 5.2.2.

Coefficient	Value	Coefficient	Value	Coefficient	Value
$a_{1,0}$	2.423700085	$a_{2,0}$	4.422727995	$a_{3,0}$	-0.2118777497
$a_{1,2}$	-3.029390858	$a_{2,2}$	-6.074925143	$a_{3,2}$	-0.5133676731
$a_{1,4}$	2.778456991	$a_{2,4}$	4.82471548	$a_{3,4}$	0.6401477401
$a_{1,6}$	-1.595715997	$a_{2,6}$	-3.083345574	$a_{3,6}$	0.2361958228
$a_{1,8}$	0.5775281321	$a_{2,8}$	1.057928928	$a_{3,8}$	-0.5166643552
$a_{1,10}$	-0.1258571117	$a_{2,10}$	0.01465071622	$a_{3,10}$	1.337006891
$a_{1,12}$	-0.06372425607	$a_{2,12}$	-0.4768977113	$a_{3,12}$	-0.3237975858
$a_{1,14}$	-0.08892149285	$a_{2,14}$	0.6125544385	$a_{3,14}$	0.01863958765
$a_{1,16}$	0.2929091429	$a_{2,16}$	-0.4699307418	$a_{3,16}$	0.948279181
$a_{1,18}$	-0.1957612101	$a_{2,18}$	0.3342203856	$a_{3,18}$	-0.5002421511
$a_{1,20}$	-0.1079298023	$a_{2,20}$	-0.2873903583	$a_{3,20}$	0.2423276373
$a_{1,22}$	0.3831713862	$a_{2,22}$	0.2150052405	$a_{3,22}$	0.07578206801
$a_{1,24}$	-0.2742053363	$a_{2,24}$	-0.1752633551	$a_{3,24}$	-0.07622284835
$a_{1,26}$	-0.05662235185	$a_{2,26}$	0.1085068762	$a_{3,26}$	-0.1640045115
$a_{1,28}$	0.1464863526	$a_{2,28}$	-0.1344240858	$a_{3,28}$	-0.2224032533
$a_{1,30}$	-0.1466007924	$a_{2,30}$	0.1782027679	$a_{3,30}$	0.05778675575
$a_{1,32}$	0.1138431732	$a_{2,32}$	-0.04635548495	$a_{3,32}$	-0.01980001983
$a_{1,34}$	-0.03136605505	$a_{2,34}$	-0.01998037404	$a_{3,34}$	-0.007785535763
$a_{4,0}$	-1.231700701	$a_{5,0}$	3.37060488	$b_{1,0}$	4.294602459
$a_{4,2}$	2.483463877	$a_{5,2}$	-4.814670145	$b_{1,2}$	-6.502184357
$a_{4,4}$	-0.6223668702	$a_{5,4}$	5.709780237	$b_{1,4}$	5.595900594
$a_{4,6}$	0.04717380874	$a_{5,6}$	-5.629542459	$b_{1,6}$	-3.925668604
$a_{4,8}$	1.595866548	$a_{5,8}$	4.088173091	$b_{1,8}$	2.433775405
$a_{4,10}$	-1.771097898	$a_{5,10}$	-2.833455815	$b_{1,10}$	-1.356860402
$a_{4,12}$	0.5314861913	$a_{5,12}$	1.238179141	$b_{1,12}$	0.6816371424
$a_{4,14}$	-0.5660695448	$a_{5,14}$	-0.02427586314	$b_{1,14}$	-0.3102566411
$a_{4,16}$	0.2910620946	$a_{5,16}$	-0.4920153002	$b_{1,16}$	0.1446255748
$a_{4,18}$	0.3609807415	$a_{5,18}$	0.5841150834	$b_{1,18}$	-0.1047320908
$a_{4,20}$	-0.4934871599	$a_{5,20}$	-0.3958927885	$b_{1,20}$	0.1120411423
$a_{4,22}$	0.4190332752	$a_{5,22}$	0.1997893831	$b_{1,22}$	-0.08474003881
$a_{4,24}$	0.5064175983	$a_{5,24}$	-0.07064875233	$b_{1,24}$	0.02185981612
$a_{4,26}$	-0.1500049851	$a_{5,26}$	0.1282147197		
$a_{4,28}$	-0.1534488294	$a_{5,28}$	0.008947613008		
$a_{4,30}$	-0.4498438248	$a_{5,30}$	0.1053799396		

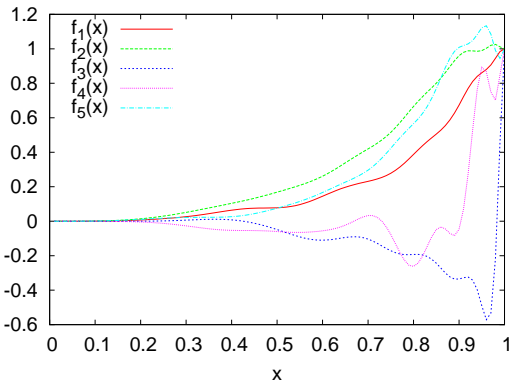
$a_{4,32}$	0.004130243912	$a_{5,32}$	-0.1810123011		
$a_{4,34}$	0.1984054337	$a_{5,34}$	0.008329336753		
$b_{2,0}$	-0.009600231179	$b_{3,0}$	1.630150597	$d_{1,0,0}$	8.826466945
$b_{2,2}$	1.517454558	$b_{3,2}$	-1.301567805	$d_{1,0,2}$	-51.00045948
$b_{2,4}$	-1.254508592	$b_{3,4}$	1.313426947	$d_{1,0,4}$	32.79356493
$b_{2,6}$	1.572259738	$b_{3,6}$	-0.9361372074	$d_{1,0,6}$	-67.04774802
$b_{2,8}$	-1.464202498	$b_{3,8}$	0.3040005411	$d_{1,0,8}$	46.50785125
$b_{2,10}$	1.01410577	$b_{3,10}$	0.2490525113	$d_{1,0,10}$	-55.17806626
$b_{2,12}$	-0.3954942227	$b_{3,12}$	-0.6594226441	$d_{1,0,12}$	43.51235445
$b_{2,14}$	-0.1641749731	$b_{3,14}$	0.7709428119	$d_{1,0,14}$	-32.97472223
$b_{2,16}$	0.3044047044	$b_{3,16}$	-0.5075601787	$d_{1,0,16}$	30.25307923
$b_{2,18}$	-0.1216277418	$b_{3,18}$	0.09553216179	$d_{1,0,18}$	-14.13357369
$b_{2,20}$	0.1136942015	$b_{3,20}$	0.2251646939	$d_{1,0,20}$	22.33695617
$b_{2,22}$	-0.1534978214	$b_{3,22}$	-0.3139511952	$d_{1,0,22}$	-5.726141217
$b_{2,24}$	0.04118710805	$b_{3,24}$	0.1303687667	$d_{1,0,24}$	15.20141079
				$d_{1,0,26}$	5.185815148
				$d_{1,0,28}$	6.457804041
				$d_{1,0,30}$	6.433516004
				$d_{1,0,32}$	2.141988182
				$d_{1,0,34}$	4.004483526
				$d_{1,0,36}$	0.7646621201
				$d_{1,0,38}$	1.640758111
$d_{2,0,0}$	-28.81166724	$d_{3,0,0}$	-44.83554198	$d_{4,0,0}$	2.656645712
$d_{2,0,2}$	48.96390082	$d_{3,0,2}$	102.7538258	$d_{4,0,2}$	-35.1733726
$d_{2,0,4}$	-59.7439777	$d_{3,0,4}$	-135.0669598	$d_{4,0,4}$	-10.37408871
$d_{2,0,6}$	47.95798025	$d_{3,0,6}$	134.4837064	$d_{4,0,6}$	-32.81035566
$d_{2,0,8}$	-40.59389074	$d_{3,0,8}$	-146.7134886	$d_{4,0,8}$	-4.210743137
$d_{2,0,10}$	27.10331229	$d_{3,0,10}$	129.626403	$d_{4,0,10}$	-5.731157993
$d_{2,0,12}$	-13.38246192	$d_{3,0,12}$	-136.6489448	$d_{4,0,12}$	19.45244819
$d_{2,0,14}$	6.612589837	$d_{3,0,14}$	116.5231087	$d_{4,0,14}$	4.133218639
$d_{2,0,16}$	6.502720504	$d_{3,0,16}$	-114.7845709	$d_{4,0,16}$	16.41556764
$d_{2,0,18}$	-6.847063576	$d_{3,0,18}$	93.73906963	$d_{4,0,18}$	2.332523586
$d_{2,0,20}$	14.70904405	$d_{3,0,20}$	-77.38116688	$d_{4,0,20}$	10.49194418
$d_{2,0,22}$	-11.75689112	$d_{3,0,22}$	67.16618287	$d_{4,0,22}$	0.79936951
$d_{2,0,24}$	14.3663871	$d_{3,0,24}$	-43.60970511	$d_{4,0,24}$	-1.670833174
$d_{2,0,26}$	-10.75756907	$d_{3,0,26}$	46.36540469	$d_{4,0,26}$	6.507437975
$d_{2,0,28}$	9.92877446	$d_{3,0,28}$	-18.51985435	$d_{4,0,28}$	6.132051598
$d_{2,0,30}$	-6.53198731	$d_{3,0,30}$	24.38532363	$d_{4,0,30}$	12.44266117
$d_{2,0,32}$	4.948320604	$d_{3,0,32}$	-7.196308314	$d_{4,0,32}$	4.15498661

$d_{2,0,34}$	-3.201271901	$d_{3,0,34}$	9.3542417	$d_{4,0,34}$	3.350955818
$d_{2,0,36}$	1.319831809	$d_{3,0,36}$	-1.609839111	$d_{4,0,36}$	0.1949562904
$d_{2,0,38}$	-0.7860811466	$d_{3,0,38}$	1.96911354	$d_{4,0,38}$	0.9057843529
$d_{5,0,0}$	-12.61471224	$d_{6,0,0}$	12.69651452	$d_{7,0,0}$	-53.49449537
$d_{5,0,2}$	22.60833747	$d_{6,0,2}$	13.98166469	$d_{7,0,2}$	90.07388583
$d_{5,0,4}$	-41.6459668	$d_{6,0,4}$	23.44846896	$d_{7,0,4}$	-149.2735531
$d_{5,0,6}$	32.10537623	$d_{6,0,6}$	17.14992096	$d_{7,0,6}$	115.303652
$d_{5,0,8}$	-47.38721005	$d_{6,0,8}$	5.633114056	$d_{7,0,8}$	-132.6846493
$d_{5,0,10}$	36.70832969	$d_{6,0,10}$	6.719565807	$d_{7,0,10}$	103.6862499
$d_{5,0,12}$	-42.71119589	$d_{6,0,12}$	-3.766565132	$d_{7,0,12}$	-87.03114874
$d_{5,0,14}$	35.98095804	$d_{6,0,14}$	-7.082273065	$d_{7,0,14}$	75.68332347
$d_{5,0,16}$	-29.09689142	$d_{6,0,16}$	-4.115607754	$d_{7,0,16}$	-44.35867943
$d_{5,0,18}$	25.84972409	$d_{6,0,18}$	-15.3473449	$d_{7,0,18}$	47.95953746
$d_{5,0,20}$	-12.29344375	$d_{6,0,20}$	-5.576899468	$d_{7,0,20}$	-17.35934339
$d_{5,0,22}$	14.34138626	$d_{6,0,22}$	-14.01056702	$d_{7,0,22}$	28.18206121
$d_{5,0,24}$	-0.3012631459	$d_{6,0,24}$	-5.086364179	$d_{7,0,24}$	-4.099930837
$d_{5,0,26}$	7.601000346	$d_{6,0,26}$	-13.3737655	$d_{7,0,26}$	15.23990003
$d_{5,0,28}$	4.37853726	$d_{6,0,28}$	-1.61427147	$d_{7,0,28}$	0.5704100109
$d_{5,0,30}$	2.884613714	$d_{6,0,30}$	-7.486180947	$d_{7,0,30}$	8.333955397
$d_{5,0,32}$	2.22196802	$d_{6,0,32}$	-0.04735003683	$d_{7,0,32}$	1.040845407
$d_{5,0,34}$	0.2088333351	$d_{6,0,34}$	-2.122059521	$d_{7,0,34}$	2.227979386
$d_{5,0,36}$	1.006664636				
$d_{5,0,38}$	0.1549542221				
$d_{8,0,0}$	0.2165886879	$d_{1,1,0}$	5.770431238	$d_{2,1,0}$	5.332239921
$d_{8,0,2}$	30.72243828	$d_{1,1,2}$	-18.50832348	$d_{2,1,2}$	-28.9312691
$d_{8,0,4}$	-0.5829319856	$d_{1,1,4}$	18.32089841	$d_{2,1,4}$	20.49596371
$d_{8,0,6}$	24.84981964	$d_{1,1,6}$	-23.96026874	$d_{2,1,6}$	-46.92413065
$d_{8,0,8}$	-8.910539262	$d_{1,1,8}$	28.68889908	$d_{2,1,8}$	45.3950102
$d_{8,0,10}$	7.045760501	$d_{1,1,10}$	-21.71252311	$d_{2,1,10}$	-57.12220905
$d_{8,0,12}$	-21.0318626	$d_{1,1,12}$	34.20256199	$d_{2,1,12}$	65.68302485
$d_{8,0,14}$	5.089984925	$d_{1,1,14}$	-20.45517581	$d_{2,1,14}$	-62.34969415
$d_{8,0,16}$	-29.6151165	$d_{1,1,16}$	32.31316824	$d_{2,1,16}$	71.30168197
$d_{8,0,18}$	6.150529174	$d_{1,1,18}$	-22.9598124	$d_{2,1,18}$	-58.80843063
$d_{8,0,20}$	-21.21459331	$d_{1,1,20}$	28.69051934	$d_{2,1,20}$	61.8467063
$d_{8,0,22}$	6.385803013	$d_{1,1,22}$	-27.97384519	$d_{2,1,22}$	-46.60795314
$d_{8,0,24}$	-11.11006916	$d_{1,1,24}$	21.22768624	$d_{2,1,24}$	44.3772014
$d_{8,0,26}$	9.342251572	$d_{1,1,26}$	-22.5541692	$d_{2,1,26}$	-31.10901182
$d_{8,0,28}$	-2.564845978	$d_{1,1,28}$	11.03189118	$d_{2,1,28}$	26.13635071
$d_{8,0,30}$	4.931473877	$d_{1,1,30}$	-16.43248137	$d_{2,1,30}$	-15.65083096

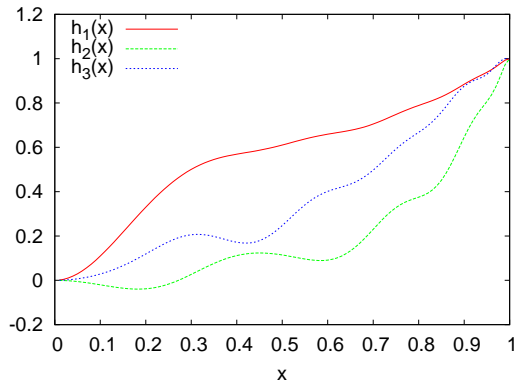
$d_{8,0,32}$	-0.9899101186	$d_{1,1,32}$	4.747050975	$d_{2,1,32}$	11.81934002
$d_{8,0,34}$	1.285219248	$d_{1,1,34}$	-9.159545073	$d_{2,1,34}$	-6.546042452
		$d_{1,1,36}$	1.521008279	$d_{2,1,36}$	2.966702734
		$d_{1,1,38}$	-2.797970594	$d_{2,1,38}$	-1.304649864
$d_{3,1,0}$	-46.14360439	$d_{4,1,0}$	11.39957733	$d_{5,1,0}$	-18.67164909
$d_{3,1,2}$	125.1282177	$d_{4,1,2}$	-26.97787047	$d_{5,1,2}$	28.33604893
$d_{3,1,4}$	-143.9737185	$d_{4,1,4}$	36.79618056	$d_{5,1,4}$	-63.683327
$d_{3,1,6}$	185.5594336	$d_{4,1,6}$	-32.17947712	$d_{5,1,6}$	42.47883521
$d_{3,1,8}$	-181.9956279	$d_{4,1,8}$	44.17606596	$d_{5,1,8}$	-65.28008168
$d_{3,1,10}$	197.297622	$d_{4,1,10}$	-27.05006886	$d_{5,1,10}$	48.20259533
$d_{3,1,12}$	-193.3115854	$d_{4,1,12}$	44.11763226	$d_{5,1,12}$	-50.58588768
$d_{3,1,14}$	184.4836588	$d_{4,1,14}$	-23.60472727	$d_{5,1,14}$	42.3187897
$d_{3,1,16}$	-179.9256191	$d_{4,1,16}$	29.33975683	$d_{5,1,16}$	-27.17781158
$d_{3,1,18}$	151.5486359	$d_{4,1,18}$	-21.51280607	$d_{5,1,18}$	25.86007258
$d_{3,1,20}$	-141.2609536	$d_{4,1,20}$	13.436693	$d_{5,1,20}$	-3.806195266
$d_{3,1,22}$	109.1048852	$d_{4,1,22}$	-18.12703438	$d_{5,1,22}$	9.613373217
$d_{3,1,24}$	-96.80402072	$d_{4,1,24}$	-0.6490581355	$d_{5,1,24}$	10.47996092
$d_{3,1,26}$	70.95225177	$d_{4,1,26}$	-11.89854115	$d_{5,1,26}$	1.059347305
$d_{3,1,28}$	-54.89440238	$d_{4,1,28}$	-1.926787803	$d_{5,1,28}$	13.61435772
$d_{3,1,30}$	34.90885792	$d_{4,1,30}$	-5.420395076	$d_{5,1,30}$	-2.037652617
$d_{3,1,32}$	-25.98639482	$d_{4,1,32}$	-2.186469589	$d_{5,1,32}$	8.079515677
$d_{3,1,34}$	11.40625927	$d_{4,1,34}$	-4.528987806	$d_{5,1,34}$	-1.74974038
$d_{3,1,36}$	-7.36933706	$d_{4,1,36}$	-1.386878664	$d_{5,1,36}$	3.034144918
$d_{3,1,38}$	1.275441658	$d_{4,1,38}$	-1.816803548	$d_{5,1,38}$	-0.08469620985
$d_{6,1,0}$	-30.33688013	$d_{7,1,0}$	-141.5348898	$d_{8,1,0}$	-69.75044647
$d_{6,1,2}$	68.00783212	$d_{7,1,2}$	347.9689191	$d_{8,1,2}$	162.8403106
$d_{6,1,4}$	-89.77477823	$d_{7,1,4}$	-430.895143	$d_{8,1,4}$	-207.9301583
$d_{6,1,6}$	83.55073981	$d_{7,1,6}$	480.1130427	$d_{8,1,6}$	216.2125223
$d_{6,1,8}$	-88.23182285	$d_{7,1,8}$	-474.3063429	$d_{8,1,8}$	-227.3766425
$d_{6,1,10}$	66.99412464	$d_{7,1,10}$	461.6657552	$d_{8,1,10}$	211.6735688
$d_{6,1,12}$	-60.89436929	$d_{7,1,12}$	-412.3309642	$d_{8,1,12}$	-212.8427452
$d_{6,1,14}$	40.96530883	$d_{7,1,14}$	366.5277564	$d_{8,1,14}$	190.442949
$d_{6,1,16}$	-27.91861711	$d_{7,1,16}$	-307.3346808	$d_{8,1,16}$	-179.1059967
$d_{6,1,18}$	20.99580709	$d_{7,1,18}$	248.2928329	$d_{8,1,18}$	152.5367475
$d_{6,1,20}$	-8.684444248	$d_{7,1,20}$	-200.585556	$d_{8,1,20}$	-124.8844177
$d_{6,1,22}$	12.32014856	$d_{7,1,22}$	142.8214876	$d_{8,1,22}$	105.3329747
$d_{6,1,24}$	-0.09858864866	$d_{7,1,24}$	-110.7323638	$d_{8,1,24}$	-72.35392391
$d_{6,1,26}$	4.101912743	$d_{7,1,26}$	65.09352118	$d_{8,1,26}$	63.05336577
$d_{6,1,28}$	3.362544142	$d_{7,1,28}$	-47.02740151	$d_{8,1,28}$	-30.90700281

$d_{6,1,30}$	2.272974874	$d_{7,1,30}$	21.743051	$d_{8,1,30}$	26.1287588
$d_{6,1,32}$	1.982937163	$d_{7,1,32}$	-11.57300238	$d_{8,1,32}$	-8.782232905
$d_{6,1,34}$	1.385170554	$d_{7,1,34}$	2.093978419	$d_{8,1,34}$	5.712368916
$e_{1,0,0}$	-5.812296944	$e_{2,0,0}$	0.1225785243	$e_{3,0,0}$	0.2321731781
$e_{1,0,2}$	9.343709082	$e_{2,0,2}$	0.0009564796491	$e_{3,0,2}$	-0.6806900729
$e_{1,0,4}$	-8.769838832	$e_{2,0,4}$	0.2266215129	$e_{3,0,4}$	0.5698985158
$e_{1,0,6}$	7.69430468	$e_{2,0,6}$	-0.09278162734	$e_{3,0,6}$	-1.152544332
$e_{1,0,8}$	-5.484590032	$e_{2,0,8}$	0.1070250523	$e_{3,0,8}$	1.510454673
$e_{1,0,10}$	4.002873782	$e_{2,0,10}$	0.4344648239	$e_{3,0,10}$	-2.185341137
$e_{1,0,12}$	-2.283315113	$e_{2,0,12}$	-1.257416597	$e_{3,0,12}$	2.355808671
$e_{1,0,14}$	1.363577864	$e_{2,0,14}$	1.736316027	$e_{3,0,14}$	-2.347887454
$e_{1,0,16}$	-0.3758926847	$e_{2,0,16}$	-1.73127609	$e_{3,0,16}$	1.450625049
$e_{1,0,18}$	0.1040643551	$e_{2,0,18}$	0.282928451	$e_{3,0,18}$	-0.4295379898
$e_{1,0,20}$	0.2736392687	$e_{2,0,20}$	-0.4273667787	$e_{3,0,20}$	-0.09654307276
$e_{1,0,22}$	-0.1611338208	$e_{2,0,22}$	0.3875955644	$e_{3,0,22}$	0.7090790578
$e_{1,0,24}$	0.1048983933	$e_{2,0,24}$	0.2103546581	$e_{3,0,24}$	0.06450491506
$e_{1,1,0}$	0.631447536	$e_{2,1,0}$	-0.3724021349	$e_{3,1,0}$	0.1044050312
$e_{1,1,2}$	-1.657287648	$e_{2,1,2}$	0.9124277066	$e_{3,1,2}$	-0.3490571066
$e_{1,1,4}$	2.260812981	$e_{2,1,4}$	-1.020870838	$e_{3,1,4}$	0.361322621
$e_{1,1,6}$	-2.626900049	$e_{2,1,6}$	1.187439705	$e_{3,1,6}$	-0.7317047802
$e_{1,1,8}$	3.068030318	$e_{2,1,8}$	-1.191595267	$e_{3,1,8}$	0.926756224
$e_{1,1,10}$	-3.228219813	$e_{2,1,10}$	1.456979745	$e_{3,1,10}$	-1.422051914
$e_{1,1,12}$	3.315344446	$e_{2,1,12}$	-2.229413592	$e_{3,1,12}$	1.539971409
$e_{1,1,14}$	-3.062544026	$e_{2,1,14}$	2.323449008	$e_{3,1,14}$	-1.48261686
$e_{1,1,16}$	2.630828206	$e_{2,1,16}$	-2.061544471	$e_{3,1,16}$	0.8217700259
$e_{1,1,18}$	-2.048086794	$e_{2,1,18}$	0.3641661783	$e_{3,1,18}$	-0.04841593029
$e_{1,1,20}$	1.402086469	$e_{2,1,20}$	-0.224502187	$e_{3,1,20}$	-0.341095186
$e_{1,1,22}$	-0.8148166357	$e_{2,1,22}$	0.3462909506	$e_{3,1,22}$	0.7013313185
$e_{1,1,24}$	0.1293050093	$e_{2,1,24}$	0.5095751972	$e_{3,1,24}$	-0.08061485265

 Table E.3:  $N = 2$  expansion coefficients

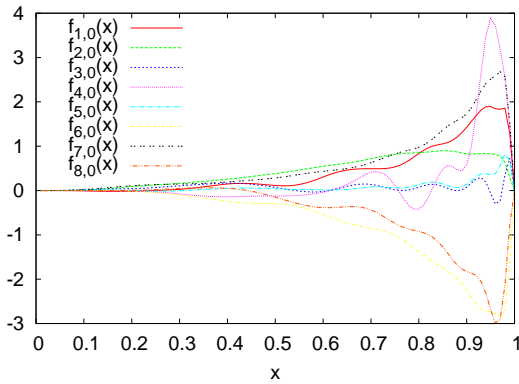


(a)  $N = 2$  profile functions  $f_1 \dots f_5(x)$

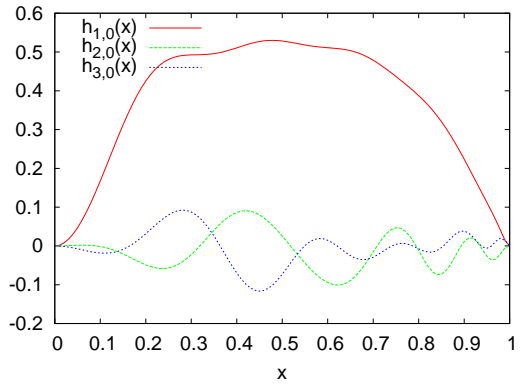


(b)  $N = 2$  profile functions  $h_1 \dots h_3(x)$

Figure E.4:  $N = 2$  plots

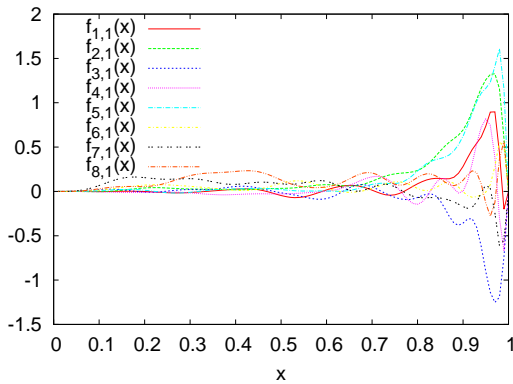


(c)  $N = 2$  profile functions  $f_{1,0} \dots f_{8,0}(x)$

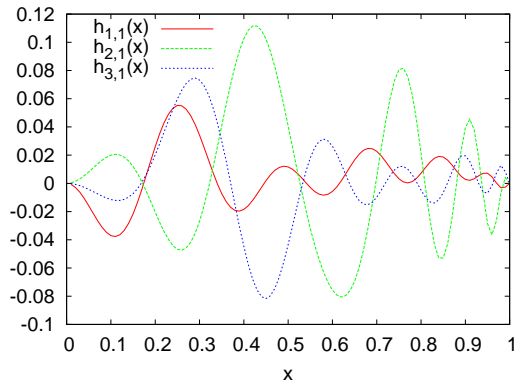


(d)  $N = 2$  profile functions  $h_{1,0} \dots h_{3,0}(x)$

Figure E.4:  $N = 2$  plots (cont.)

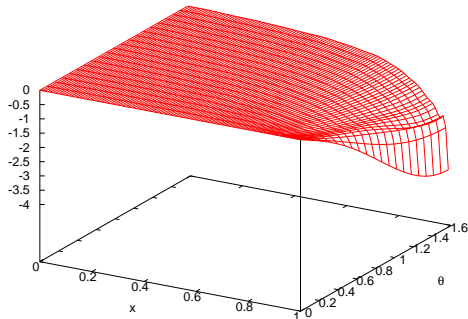


(e)  $N = 2$  profile functions  $f_{1,1} \dots f_{8,1}(x)$

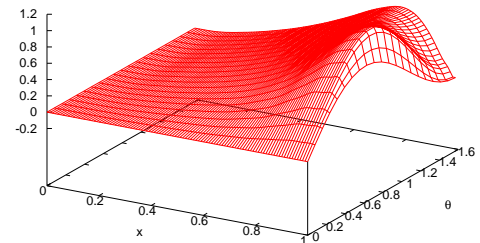


(f)  $N = 2$  profile functions  $h_{1,1} \dots h_{3,1}(x)$

Figure E.4:  $N = 2$  plots (cont.)

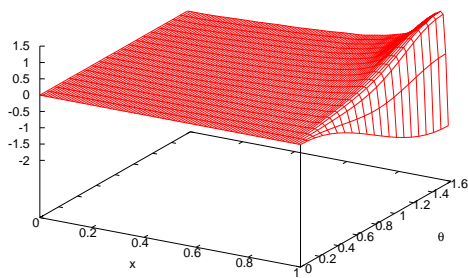


(a)  $\alpha_1(x, \theta)$  for  $N = 2$

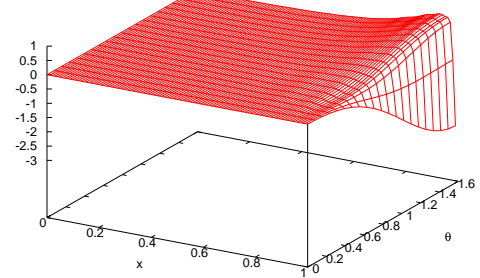


(b)  $\alpha_2(x, \theta)$  for  $N = 2$

Figure E.5:  $N = 2$  plots

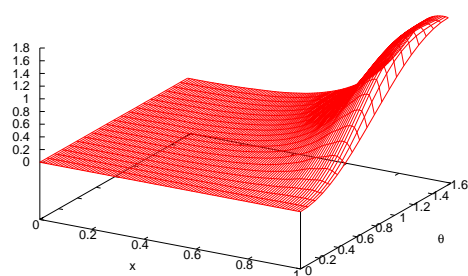


(c)  $\alpha_3(x, \theta)$  for  $N = 2$

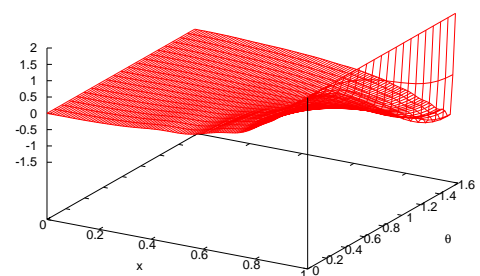


(d)  $\alpha_4(x, \theta)$  for  $N = 2$

Figure E.5:  $N = 2$  plots (cont.)

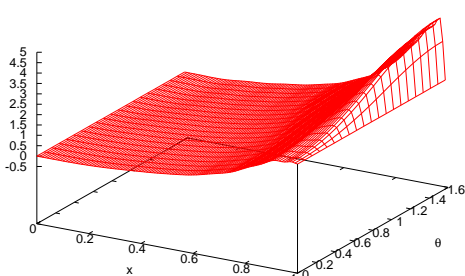


(e)  $\alpha_5(x, \theta)$  for  $N = 2$

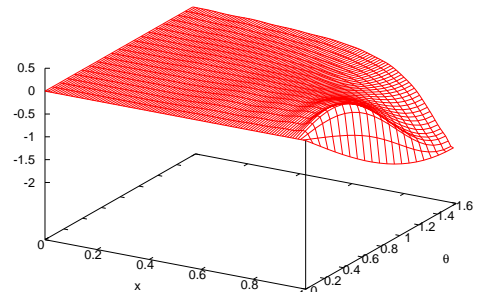


(f)  $\alpha_6(x, \theta)$  for  $N = 2$

Figure E.5:  $N = 2$  plots (cont.)

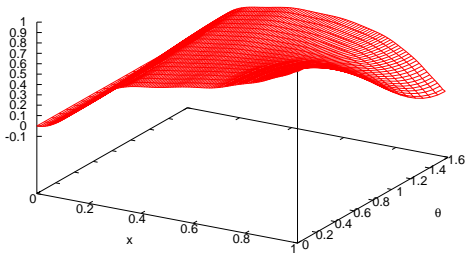


(g)  $\alpha_7(x, \theta)$  for  $N = 2$

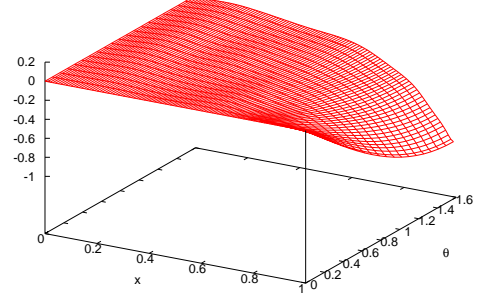


(h)  $\alpha_8(x, \theta)$  for  $N = 2$

Figure E.5:  $N = 2$  plots (cont.)

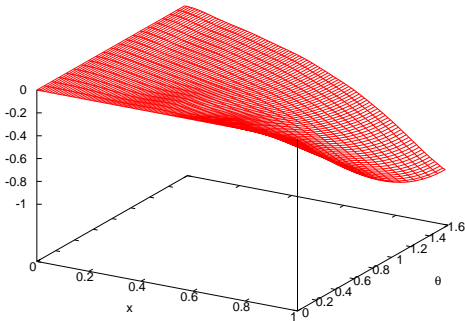


(i)  $\beta_1(x, \theta)$  for  $N = 2$

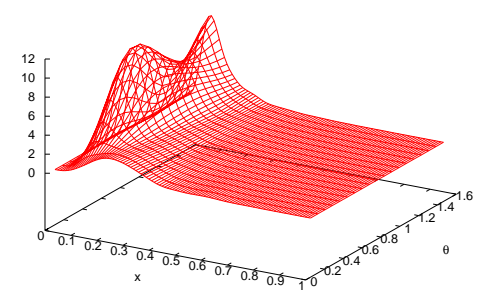


(j)  $\beta_2(x, \theta)$  for  $N = 2$

Figure E.5:  $N = 2$  plots (cont.)

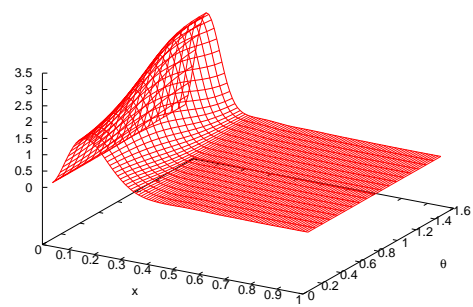


(k)  $\beta_3(x, \theta)$  for  $N = 2$



(l) Yang-Mills energy density  $e_{YM}(x, \theta)$

Figure E.5:  $N = 2$  plots (cont.)



(m) Kinetic Higgs energy density  $e_{Hkin}(x, \theta)$

Figure E.5:  $N = 2$  plots (cont.)

#### E.4 $N = 3$ Legendre expansion

The figures given below are related to the  $N = 3$  run of lowest energy ( $N_S = 800$ ,  $E_{\hat{S}}/E_S = 0.906$ ), as discussed in chapter 5.2.3.

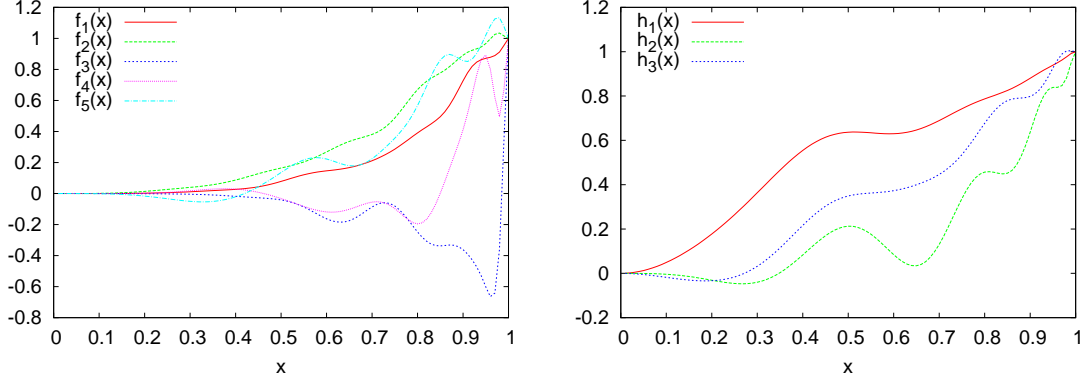


Figure E.6:  $N = 3$  zeroth order profile functions  $f_1 \dots f_5(x)$  and  $h_1 \dots h_3(x)$

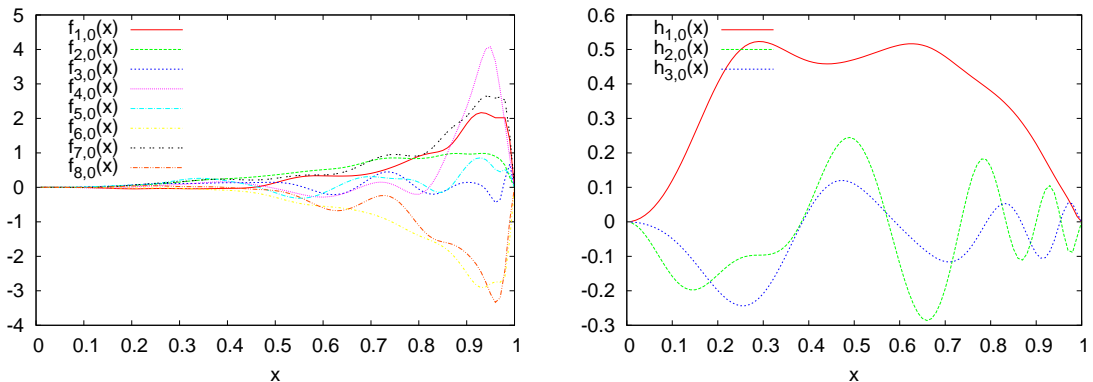


Figure E.7:  $N = 3$  first order profile functions  $f_{1,0} \dots f_{8,0}(x)$  and  $h_{1,0} \dots h_{3,0}(x)$

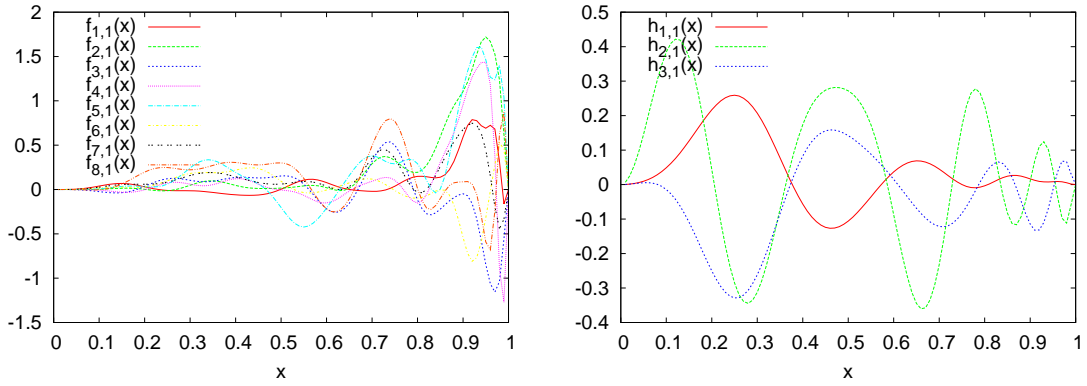


Figure E.8:  $N = 3$  second order profile functions  $f_{1,1} \dots f_{8,1}(x)$  and  $h_{1,1} \dots h_{3,1}(x)$

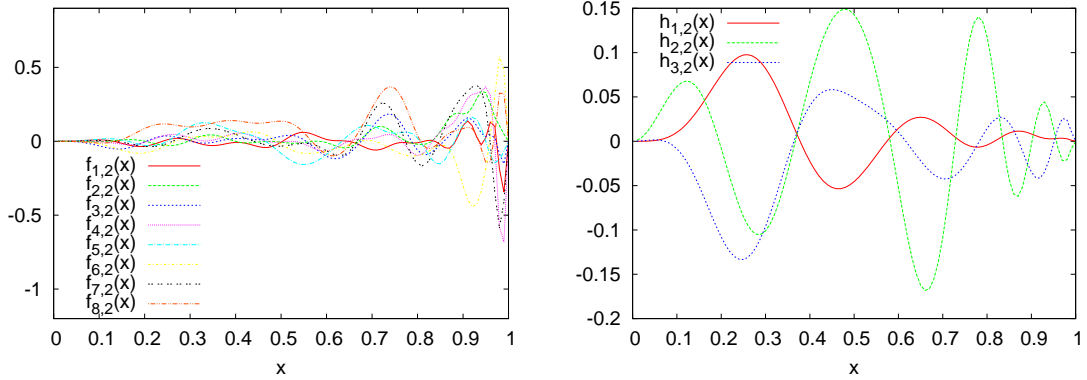
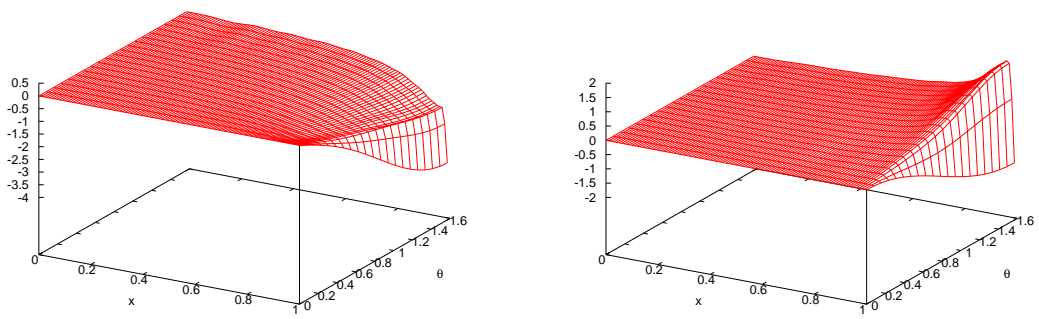


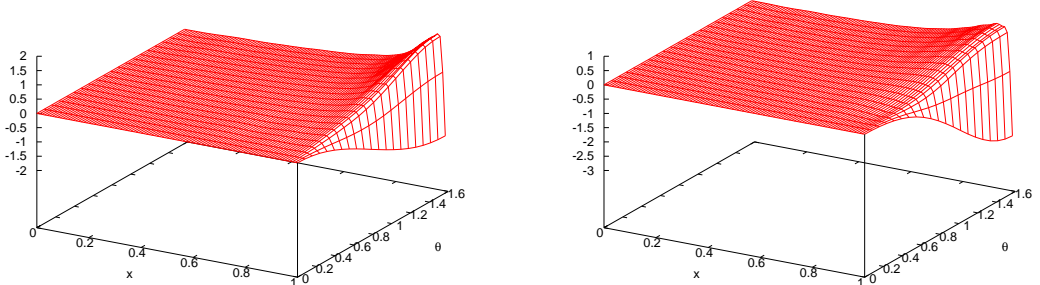
Figure E.9:  $N = 3$  third order profile functions  $f_{1,2} \dots f_{8,2}(x)$  and  $h_{1,2} \dots h_{3,2}(x)$



(a)  $\alpha_1(x, \theta)$  for  $N = 3$

(b)  $\alpha_2(x, \theta)$  for  $N = 3$

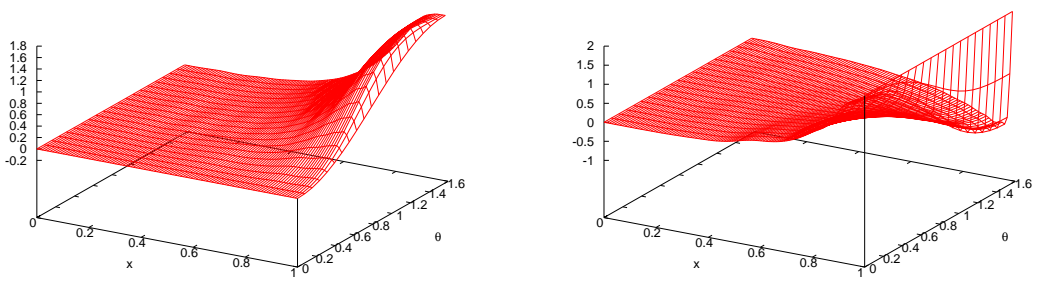
Figure E.10:  $N = 3$  plots



(c)  $\alpha_3(x, \theta)$  for  $N = 3$

(d)  $\alpha_4(x, \theta)$  for  $N = 3$

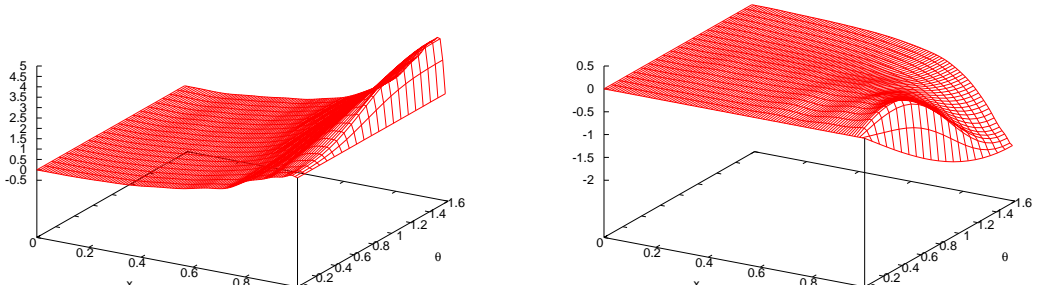
Figure E.10:  $N = 3$  plots (cont.)



(e)  $\alpha_5(x, \theta)$  for  $N = 3$

(f)  $\alpha_6(x, \theta)$  for  $N = 3$

Figure E.10:  $N = 3$  plots (cont.)



(g)  $\alpha_7(x, \theta)$  for  $N = 3$

(h)  $\alpha_8(x, \theta)$  for  $N = 3$

Figure E.10:  $N = 3$  plots (cont.)

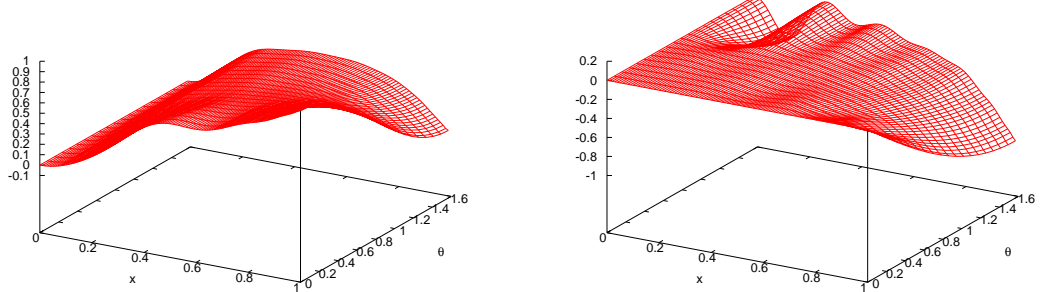


Figure E.10:  $N = 3$  plots (cont.)

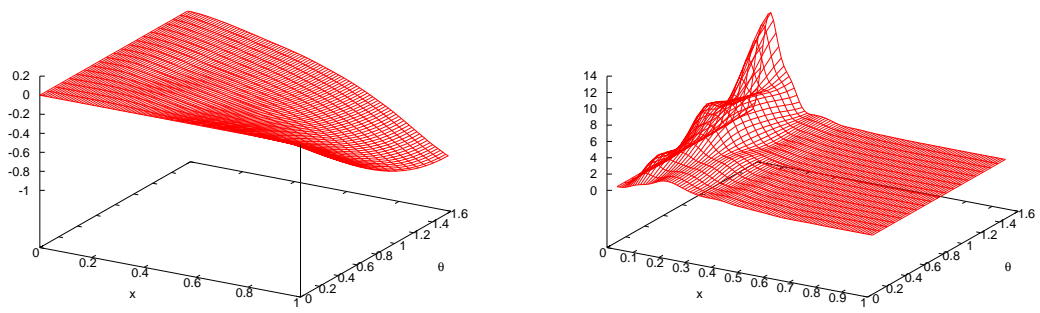
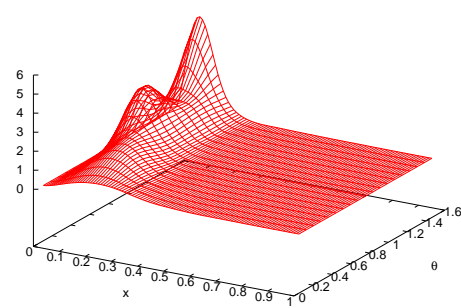


Figure E.10:  $N = 3$  plots (cont.)



(m) Kinetic Higgs energy density  $e_{Hkin}(x, \theta)$

Figure E.10:  $N = 3$  plots (cont.)

## F Coefficients of the regular $S$ Ansatz

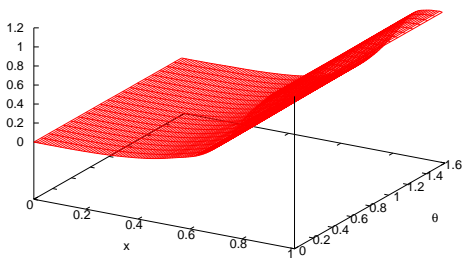
The profile functions generated by the following expansion coefficients approximate the minimum of the  $S$  sphaleron energy functional (6.6).

Coefficient	Value	Coefficient	Value
$a_0$	3.487839	$b_0$	1.739477
$a_2$	-5.000355	$b_2$	-1.845219
$a_4$	5.732301	$b_4$	2.411635
$a_6$	-5.688814	$b_6$	-2.471319
$a_8$	4.073117	$b_8$	2.160709
$a_{10}$	-2.665080	$b_{10}$	-1.799734
$a_{12}$	1.478312	$b_{12}$	1.390072
$a_{14}$	-0.429207	$b_{14}$	-0.956726
$a_{16}$	-0.115868	$b_{16}$	0.578793
$a_{18}$	0.294847	$b_{18}$	-0.294568
$a_{20}$	-0.294325	$b_{20}$	0.111839
$a_{22}$	0.245020	$b_{22}$	-0.0221282
$a_{24}$	-0.239994	$b_{24}$	-0.00283016
$a_{26}$	0.201420		
$a_{28}$	-0.0901584		
$a_{30}$	-0.0931849		
$a_{32}$	0.156959		
$a_{34}$	-0.0528279		

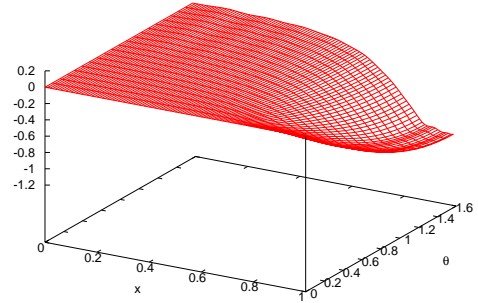
Table F.1:  $S$  Ansatz coefficients

## G Figures of the generalized S Ansatz

The following figures correspond to profile functions (6.2) and (6.3), which serve to further demonstrate, that the regular *S Ansatz* can minimize  $E_S$ .

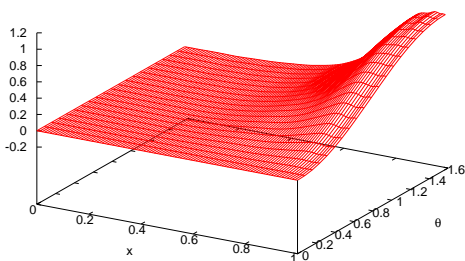


(a)  $\alpha_1(x, \theta)$

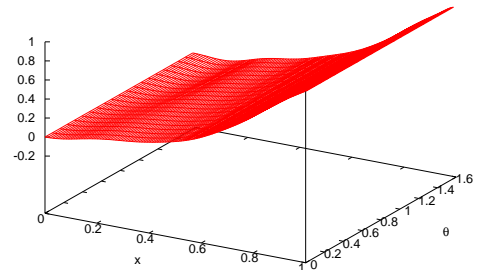


(b)  $\alpha_2(x, \theta)$

Figure G.1: Generalized S Ansatz plots

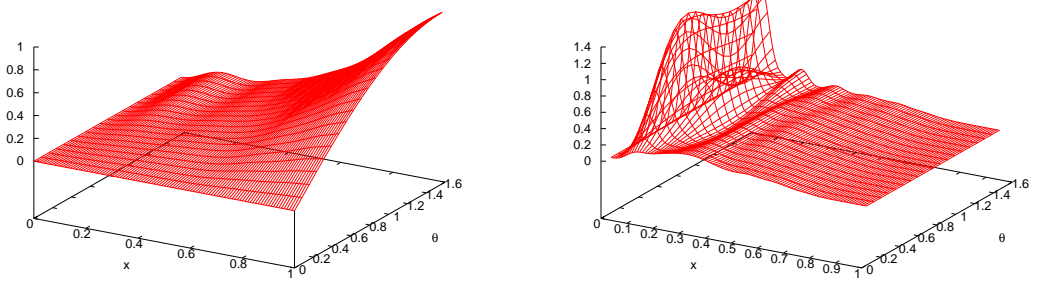


(c)  $\alpha_3(x, \theta)$



(d)  $\beta_1(x, \theta)$

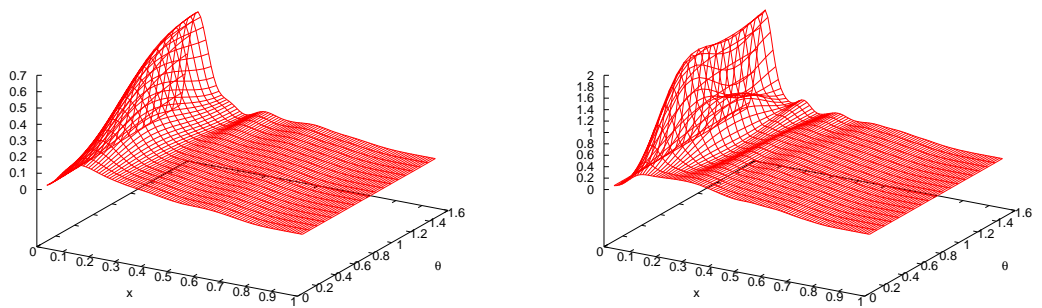
Figure G.1: Generalized S Ansatz plots (cont.)



(e)  $\beta_2(x, \theta)$

(f) Yang-Mills energy density  $e_{YM}(x, \theta)$

Figure G.1: Generalized S Ansatz plots (cont.)



(g) Kinetic Higgs energy density  $e_{Hkin}(x, \theta)$

(h) Total energy density  $e_{tot}(x, \theta)$

Figure G.1: Generalized S Ansatz plots (cont.)